INSTITUT FÜR
ENERGIETECHNIK
UND THERMODYNAMIK
Institute of Energy Systems and Thermodynamics

Master's Thesis

Wind Tunnel Design for Wind Turbines

under the supervision of

Assistant Prof. Dipl.-Ing. Bernhard Semlitsch (PhD)
E302 - Institute of Energy Systems and Thermodynamics

submitted to the Faculty of Mechanical and Industrial Engineering
of Technische Universität Wien
for the degree of Diplom-Ingenieur (Dipl.-Ing.)

by

Bernhard Kunitzky, BSc
Matr.Nr. 00826806
[redacted]

Die approbierte gedruckte Originalversion dieser Diplomarbeit ist an der TU Wien Bibliothek verfügbar
The approved original version of this thesis is available in print at TU Wien Bibliothek.
TU Bibliothek WIEN Your knowledge hub

Statutory Declaration

This thesis is the result of my own work and includes nothing that is the outcome of work done in collaboration except as specified in the text.

It is not substantially the same as any that I have submitted, or, is being concurrently submitted for a degree or diploma or other qualification at Technische Universität Wien or any other University or similar institution except as specified in the text. I further state that no substantial part of my thesis has already been submitted, or, is being concurrently submitted for any such degree, diploma or other qualification at Technische Universität Wien or any other University or similar institution except as specified in the text.

Wien, September 2021

(Bernhard Kunitzky, BSc)

Die approbierte gedruckte Originalversion dieser Diplomarbeit ist an der TU Wien Bibliothek verfügbar
The approved original version of this thesis is available in print at TU Wien Bibliothek.
TU Bibliothek WIEN Your knowledge hub

Acknowledgements

I wish to express my sincere appreciation to my supervisor, Assistant Prof. Dipl.-Ing. PhD. Bernhard Semlitsch, for the excellent support, for the time he devoted for me, for the debates on an equal footing and his patience. I do not take that for granted!

Furthermore I would like to thank all the people, that supported and accompanied me during my studies, especially my dear friends Simon and Tom.

I must express my very profound gratitude to my parents Eveline and Berthold as well as my sister Carina for providing me with endless support and continuous encouragement throughout my years of study. Thank you for always being there for me.

I would like to thank my girlfriend Olivia for all the love, support and patience. Thank you for always standing by my side and for the sacrifices you have made in order for me to pursue a Master´s degree.

This accomplishment would not have been possible without them.

Die approbierte gedruckte Originalversion dieser Diplomarbeit ist an der TU Wien Bibliothek verfügbar
The approved original version of this thesis is available in print at TU Wien Bibliothek.
TU Bibliothek WIEN Your knowledge hub

Abstract

The ever-increasing volume of wind power plants all around the globe has increased the run on the further development of wind turbines. Nevertheless, even with today´s simulation methods like CFD (Computational Fluid Dynamics), it is mandatory to predetermine the behaviour of the evolved turbine with experimental results. Wind tunnel systems are the best way to test down-scaled models of wind turbines with similar dimensions and parameters as the full-scale application. Besides, this test facility is beneficial for education at universities. A wide variety of aerodynamic experiments are possible, and complex flow profiles can be visualized, enabling a better understanding of the matter. Hence, a wind tunnel was developed for the Institute of Energy Systems and Thermodynamics at the Vienna University of Technology. The study presented also provides a detailed insight into the fundamentals of energy generation through wind power and the modelling of wind turbines. However, the focus is on the computation and technical design of each component of the wind tunnel and the selection of the best compatible outsourced parts. Since commercially available wind tunnel facilities are comparatively expensive on the market, the goal was to keep the costs for materials and construction as low as possible but ensuring maximum efficiency. For that reason, several performance checks have been carried out with the help of the CFD-Software Ansys-Fluent until nearly no flow separation occurred inside the wind tunnel, and the flow quality, as well as velocity inside the test chamber, was satisfying. Furthermore, quotations of all parts have been requested to evaluate the economic competitiveness of independently building a wind tunnel facility or buying the whole system from a well-known manufacturer.

Die approbierte gedruckte Originalversion dieser Diplomarbeit ist an der TU Wien Bibliothek verfügbar
The approved original version of this thesis is available in print at TU Wien Bibliothek.
TU Bibliothek WIEN Your knowledge hub

Kurzfassung

Die weltweit steigende Anzahl an Windkraftwerken beschert der Weiterentwicklung an Windturbinen ebenfalls einen großen Aufschwung. Obwohl computerunterstützte Simulationsmethoden wie CFD (Computational Fluid Dynamics) einen wichtigen Beitrag zur Erprobung von Windturbinen leisten, sind experimentell bestimmte Ergebnisse in diesem Bereich unerlässlich. Windtunnelanlagen eignen sich für solche Untersuchungen hervorragend, da es möglich ist, maßstabsgetreue und geometrisch ähnliche Modelle von Windturbinen unter realistischen Bedingungen auf deren Effizienz zu testen. Abgesehen davon stellt solch eine Anlage in der Lehre einen erheblichen Mehrwert dar, da mit dieser äußerst komplexe Strömungsexperimente durchgeführt werden können. Ein leichteres Verständnis wird dem/der Studierenden durch die Visualisierung ermöglicht. Deshalb wurde ein Windkanal für das Institut für Energietechnik und Thermodynamik an der Technischen Universität Wien entwickelt. In dieser Diplomarbeit werden die Grundlagen der Energiegewinnung durch Windkraftwerke und Modellierung von Windturbinen durchgearbeitet, wobei der Fokus dieser Arbeit auf der Entwicklung des Windtunnels liegt. Dabei wird auf die Berechnung, Auslegung und technische Konstruktion jedes Einzelteils der Anlage eingegangen und die bestmöglichen Zukaufteile ausgewählt. Da komplette, jedoch teure Windtunnelanlagen auf dem Markt erwerblich sind, wurde ein niedriger Preis bei der Entwicklung dieser Anlage stets angestrebt. Die Effizienz der Anlage durfte jedoch nicht unter dieser Vorgabe leiden, weshalb eine Strömungssimulation mit Hilfe der Simulationssoftware Ansys Fluent durchgeführt wurde. Erst nach Erreichen zufriedenstellender Ergebnisse wurden Kostenvoranschläge für Materialien und die Herstellung der finalen Bauteile eingeholt. Dadurch war es erst möglich, eine Entscheidung treffen zu können, ob sich der Eigenbau einer solchen Anlage rentiert.

Die approbierte gedruckte Originalversion dieser Diplomarbeit ist an der TU Wien Bibliothek verfügbar
The approved original version of this thesis is available in print at TU Wien Bibliothek.
TU Bibliothek WIEN Your knowledge hub

Contents

1 Introduction **1**

1.1 Motivation 1

1.2 Scope of Work 2

2 Fundamentals of Energy Generation through Wind Power **3**

2.1 Basics of Wind Energy Converters 3

2.1.1 Vertical Axis Rotors 4

2.1.2 Horizontal Axis Rotors 4

2.2 Physical Basics of Wind Energy Conversion 5

2.3 Betz´s Elementary Momentum Theory 7

3 Modelling of Wind Turbines **9**

3.1 Introduction 9

3.2 Parameters of Similarity 10

3.3 Estimation of Similarities 11

4 Creation and Design Methodology for a Low-Cost Wind Tunnel **16**

4.1 Introduction 16

4.1.1 Types of Wind Tunnels 17

4.2 Wind Tunnel for the Vienna University of Technology 19

4.3 Components of the Wind Tunnel 20

4.3.1 Test Chamber 21

Die approbierte gedruckte Originalversion dieser Diplomarbeit ist an der TU Wien Bibliothek verfügbar
The approved original version of this thesis is available in print at TU Wien Bibliothek.
TU Bibliothek WIEN Your knowledge hub

4.3.2 Contraction Cone 27
4.3.3 Settling Chamber 30
4.3.4 Suction Unit 34
4.3.5 Diffuser 38
4.4 CFD Simulation of the Wind Tunnel 41
4.4.1 Introduction 41
4.4.2 Modelling the Wind Tunnel 41
4.4.3 Meshing / Pre-processing 42
4.4.4 Setup, Boundary Conditions and Turbulence Model 43
4.4.5 Numerical Calculation 44
4.4.6 Interpretation / Post-processing 44

5 Statement of Costs **51**
5.1 Introduction 51
5.2 Wind Tunnel by TecQuipment 51
5.3 Costs of the Developed Wind Tunnel 53
5.3.1 Power Plant / Suction Unit 53
5.3.2 Components to be Manufactured 54
5.3.3 Prefabricated Parts 58
5.3.4 Costs for Assembly 62
5.3.5 Costs of the complete Wind Tunnel 62

6 Conclusions and Outlook **63**

Bibliography **65**

A Tables and diagrams **69**
A.1 Function Points, Bell and Mehta 69

B Drawings **74**
B.1 Designed Wind Tunnel 74

Die approbierte gedruckte Originalversion dieser Diplomarbeit ist an der TU Wien Bibliothek verfügbar
The approved original version of this thesis is available in print at TU Wien Bibliothek.
TU Bibliothek WIEN Your knowledge hub

C Quotations **96**

C.1 Quotation of the Wind Tunnel by TecQuipment 96

C.2 Quotation of the Suction Unit 101

C.3 Quotation of the Manufactured Components 116

C.4 Quotation of the Prefabricated Components 121

Die approbierte gedruckte Originalversion dieser Diplomarbeit ist an der TU Wien Bibliothek verfügbar
The approved original version of this thesis is available in print at TU Wien Bibliothek.
TU Bibliothek WIEN Your knowledge hub

Nomenclature

Abbrevations

approx	Approximately
C	Contraction ratio
CAD	Computer Aided Design
CFD	Computational Fluid Dynamics
cm	Centimeter
Eq	Equation
etc	Et cetera
FFG	Forschungsförderungsgesellschaft
FVM	Finite Volume Method
GBP	Great Britain Pound
HAWT	Horizontal Axis Wind Turbine
i.e.	id est – meaning „that is to say“
LDA	Laser Doppler Anemometry
m/s	Meter per second
MDF	Mitteldichte Holzfaserplatte
mm	Millimeter
No	Number
NREL	National Renewable Energy Laboratory
PIV	Particle Image Velocimetry
SST	Shear-Stress Transport
VAWT	Vertical Axis Wind Turbine
vs	Versus
WEC	Wind Energy Converters

Physical Constants

π	Pi	1

Die approbierte gedruckte Originalversion dieser Diplomarbeit ist an der TU Wien Bibliothek verfügbar
The approved original version of this thesis is available in print at TU Wien Bibliothek.
TU Bibliothek WIEN Your knowledge hub

g	Gravitational acceleration	m/s^2

Latin Symbols

$\dot{m}$	Mass flow	kg/s
$\dot{V}$	Volume flow	m^3/s
A	Cross sectional area	m^2
a	Acceleration	m/s^2
c_∞	Flow velocity of full scale turbine	m/s
c_m	Flow velocity of turbine model	m/s
C_p	Power coefficient of the turbine	W
d	Width	mm
E	Kinetic Energy	N m
E_{ex}	Extracted Energy	N m
F_T	Inertial force	N
F_τ	Viscous force	N
F_p	Pressure force	N
H_i	Height at inlet of contraction cone	mm
H_o	Height at outlet of contraction cone	mm
K_L	Loss coefficient	1
m	Mass	kg
p	Pressure	N/m^2
p_{dyn}	Dynamic pressure	N/m^2
P_{ex}	Extracted Power	W
P_e	Electrical power produced by the wind turbine	W
P_m	Mechanical power output of the turbine	W
p_{stat}	Static pressure	N/m^2
P_t	Output of the transmission system of wind turbine	W
P_w	Power in the wind	W
r	Radius	mm
rpm	revolutions per minute	min^{-1}
u	circumferential speed	min^{-1}
V	Volume	m^3
v	Velocity	m/s
CR	Contraction Ratio	1
L	Length of contraction cone	mm
M	Mach number	1

Die approbierte gedruckte Originalversion dieser Diplomarbeit ist an der TU Wien Bibliothek verfügbar
The approved original version of this thesis is available in print at TU Wien Bibliothek.
TU Bibliothek WIEN Your knowledge hub

Re	Reynolds number	1

Greek Symbols

α	Angle of velocity	rad
η	Dynamic viscosity	$\mathrm{N\,s/m^2}$
η_g	Generator efficiency	1
η_m	Transmission efficiency	1
ν	Kinematic viscosity	$\mathrm{m^2/s}$
ρ	Density	$\mathrm{kg/m^3}$
τ	Shear stress	$\mathrm{N/m^2}$
φ	Half opening angle	rad

Subscripts

max	Maximum
min	Minimum

Die approbierte gedruckte Originalversion dieser Diplomarbeit ist an der TU Wien Bibliothek verfügbar
The approved original version of this thesis is available in print at TU Wien Bibliothek.
TU Bibliothek WIEN Your knowledge hub

List of Figures

2.1 Types of vertical axis rotors [9] 4

2.2 Horizontal axis wind turbine [29] 5

2.3 Power stages of wind energy conversion system, inspired by [35] . . 6

2.4 Air flow through an ideal Betz wind turbine, [14] 8

3.1 Similarity of two profiles, [34] 10

3.2 Flow velocity for profile Reynolds number, inspired by www.wind-energie.de 13

4.1 Closed Circuit Wind Tunnel, [10] 18

4.2 Open-Circuit Wind Tunnel, [18] 19

4.3 Open-circuit wind tunnel 20

4.4 Test Section 1 23

4.5 Test Section 2 24

4.6 Test Section 3 25

4.7 Test Section 4, exploded view 25

4.8 Test section with and without offset 27

4.9 Contraction Cone 28

4.10 Contraction Cone Profile 30

4.11 Settling Chamber, exploded view 31

Die approbierte gedruckte Originalversion dieser Diplomarbeit ist an der TU Wien Bibliothek verfügbar
The approved original version of this thesis is available in print at TU Wien Bibliothek.
TU Bibliothek WIEN Your knowledge hub

4.12 Types of honeycomb, [3] 32
4.13 Radial Fan vs. Axial Fan, www.htk-vent.at 35
4.14 Radial Fan RS1120, www.gtg.at 36
4.15 Radial Fan Data Sheet, www.gtg.at 37
4.16 Diffuser with constant cross-section expansion, inspired by [27] . . . 38
4.17 Diffuser with sudden cross-section expansion, inspired by [27] 38
4.18 Diffuser with opening angle 2φ, inspired by [27] 39
4.19 Diffuser 40
4.20 Model of the wind tunnel in ICEM 41
4.21 Mesh of the wind tunnel in ICEM 42
4.22 Residuals, WT No.3 45
4.23 Velocity magnitude - wind tunnel No.1 46
4.24 Velocity magnitude - wind tunnel No.2 47
4.25 Change to the mesh from (a) to (b) 48
4.26 Velocity magnitude - wind tunnel No.3 48
4.27 Static Pressure - wind tunnel No.3 49
4.28 Velocity magnitude, yz-plane in test section - wind tunnel No.3 . . 49
4.29 Turbulence intensity, yz-plane in test section - wind tunnel No.3 . . 50

5.1 Wind Tunnel by TecQuipment, www.tecquipment.com 52
5.2 Quotation by TecQuipment 52
5.3 Quotation Suction Unit by GTG-Gebläsetechnik, www.gtg.at 54
5.4 Quotation Settling Chamber 55
5.5 Quotation Contraction Cone 56
5.6 Quotation Test Section 56
5.7 Quotation Diffuser 57

Die approbierte gedruckte Originalversion dieser Diplomarbeit ist an der TU Wien Bibliothek verfügbar
The approved original version of this thesis is available in print at TU Wien Bibliothek.
TU Bibliothek WIEN Your knowledge hub

5.8 Quotation Meshes 58

5.9 Quotation Honeycomb 59

A.1 Contraction Wall Profile 69

Die approbierte gedruckte Originalversion dieser Diplomarbeit ist an der TU Wien Bibliothek verfügbar
The approved original version of this thesis is available in print at TU Wien Bibliothek.
TU Bibliothek WIEN Your knowledge hub

List of Tables

3.1 NREL-5MW specifications, [20] 12
3.2 Comparison of rotor Reynolds number 12
3.3 Comparison of profile Reynolds number 14
3.4 Comparison of Mach number 14

4.1 Honeycomb loss coefficient, [3] 31
4.2 Boundary Conditions 43

5.1 Costs of the Manufactured Components 57
5.2 Costs of Acrylic-Glas 59
5.3 Costs of Small Part 60
5.4 Costs of the Prefabricated Parts 61
5.5 Costs of the complete Wind Tunnel 62

A.1 Contraction Cone Dimensions - Bell Mehta´s Polynomial 70

Die approbierte gedruckte Originalversion dieser Diplomarbeit ist an der TU Wien Bibliothek verfügbar
The approved original version of this thesis is available in print at TU Wien Bibliothek.
TU Bibliothek WIEN Your knowledge hub

Die approbierte gedruckte Originalversion dieser Diplomarbeit ist an der TU Wien Bibliothek verfügbar
The approved original version of this thesis is available in print at TU Wien Bibliothek.
TU Bibliothek WIEN Your knowledge hub

Chapter 1

Introduction

1.1 Motivation

The use of renewable energies and especially the use of wind power will become more and more important to cover the ever-increasing energy demand [7]. Only recently, Zabarjad -Shiraz et al.[38] investigated the potential of wind power generation of roof-mounted wind turbines and discovered their manifold deployment in cities with low building density. On the other side of the spectrum, huge wind parks on- and off-shore are installed at a progressive rate [21, 26]. The requirements for these different turbines vary widely, making the further development of the turbines even more diverse. The process of planning, engineering, computing and producing wind turbines is time and cost-intensive. Simulation methods that deliver meaningful results constitute a big advantage as they can be applied early in the design process [28, 31]. With the help of wind tunnel facilities, it is possible to investigate the performance, behaviour and interference of down-scaled models of wind turbines or even separate wings [4, 36]. Therefore also the Vienna University of Technology is interested in using a wind tunnel for educational reasons and research projects. Some companies sell whole wind tunnel systems, including instrumentation units for controlling and supervising the flow inside the tunnel, as well as data acquisition systems and even smoke generators. This comes at a cost. From the university´s point of view, some instruments and gimmicks are needless or some parts are already owned by the university and therefore unnecessary to purchase.

1.2 Scope of Work

The present contribution describes the computation, development, design and simulation of a compact, movable, inexpensive, but effective open-circuit wind tunnel to test down-scaled models of wind turbines, wings and other aerodynamically interesting bodies. This application will be developed for the department of fluid-flow machinery at the Vienna University of Technology to be used in the course of teaching events and research projects. When the application is completed, it should be used within a teaching event, where 3D-printed models of wind turbines can be tested. Also, the testing of the influence of superficial damage on the efficiency of a wing is desired. Besides, a wind tunnel is obviously a highly useful technical piece of equipment to teach students the fundamental principles of aerodynamics like lift, drag and pitching moments.

To better understand the matter, the fundamentals of energy generation through wind power and the modelling of wind turbines will be discovered. Betz´s elementary momentum theory and the theory of similarity will play a central role. When it comes to the technical layout of the wind tunnel, some guidelines will be compiled. Initially, it was striven to use the radial compressor PGW HL 100 / 50 / 00 already owned by the Technical University of Vienna, but as it turned out, the compressor could not generate the required flow velocity inside the test chamber. Therefore, different suction units will be taken into consideration. Besides the power plant, every other part of the wind tunnel will be designed individually, and different materials will also be considered. The main components of this wind tunnel are the settling chamber, the contraction cone, the test section, the diffuser and the suction. In every decision, the price of materials and construction will play a significant role, while the costs of every single component will be listed. However, the efficiency and usability of the wind tunnel come ahead of anything else. Therefore, simulation methods like CFD will be applied to the inner body of the wind tunnel, and the results will be analysed. Finally, it will be discussed whether it is worth building a wind tunnel facility independently or buying a whole system from a well-known manufacturer before conclusions will be drawn.

Die approbierte gedruckte Originalversion dieser Diplomarbeit ist an der TU Wien Bibliothek verfügbar
The approved original version of this thesis is available in print at TU Wien Bibliothek.
TU Bibliothek WIEN Your knowledge hub

Die approbierte gedruckte Originalversion dieser Diplomarbeit ist an der TU Wien Bibliothek verfügbar
The approved original version of this thesis is available in print at TU Wien Bibliothek.
TU Bibliothek WIEN Your knowledge hub

Chapter 2

Fundamentals of Energy Generation through Wind Power

Before digging into the development of wind tunnel systems, the basics of wind energy harvesting, wind turbine modelling, and non-dimensional numbers of wind turbines will be discussed in this chapter, as well as in chapter 3.

2.1 Basics of Wind Energy Converters

The purpose of wind turbines is to convert the wind´s kinetic energy into electrical energy for electrical feed. Wind energy converters (WEC) can be classified according to their [15]:

1. Aerodynamic function:
   - WEC get power exclusively from the aerodynamic drag of the air stream (drag-type rotors).
   - WEC utilise the aerodynamic lift created by the flow against suitably shaped surfaces (rotors which make use of the aerodynamic lift).
2. Constructional design:
   - Rotors with a vertical axis of rotation.
   - Rotors with a horizontal axis of rotation.

2.1.1 Vertical Axis Rotors

The main rotor shaft of a vertical axis wind turbine (VAWT) is placed transverse to the wind as seen in multiple designs in figure 2.1. The advantage of a vertical axis wind turbine (VAWT) over a horizontal axis wind turbine (HAWT) is the possibility of generating instant power independently of the wind direction. Thus, no yaw system for orientation is needed. Another advantage is their simple design and the fact that the mechanical housing, electrical components and gearbox, as well as the generator, can be placed at ground level. The simplicity has positive effects regarding maintenance, assembly and foundation construction. On the other hand, only low tip speed ratios are achievable and controlling the power output or speed by pitching the rotor blades is not possible. For these reasons, the VAWT is not a serious competitor to the horizontal axis wind turbine (HAWT), but it has been noted that the full potential of VAWT is not exhausted yet [15].

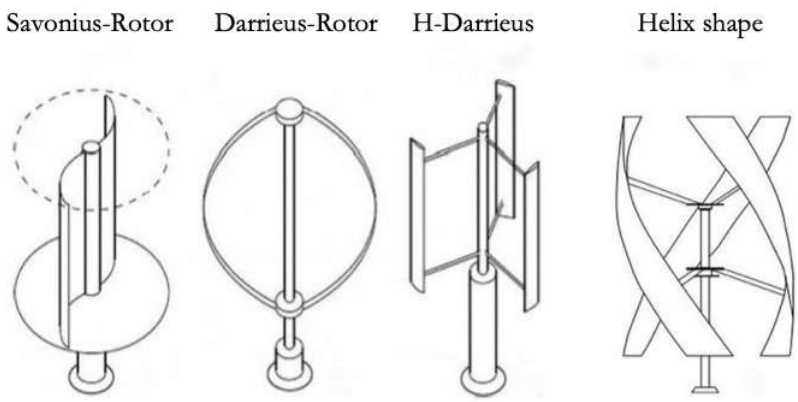

Figure 2.1: Types of vertical axis rotors [9]

2.1.2 Horizontal Axis Rotors

The main rotor shaft of a HAWT is placed parallel to the wind as seen in figure 2.2. This propeller-like concept is the most common design because of the following advantages [15]:

- Controlling the rotor speed and power output by pitching the rotor blades about their longitudinal axis.

Die approbierte gedruckte Originalversion dieser Diplomarbeit ist an der TU Wien Bibliothek verfügbar
The approved original version of this thesis is available in print at TU Wien Bibliothek.
TU Bibliothek WIEN Your knowledge hub

- Aerodynamic optimisation of the rotor blade shapes can be achieved if necessary and profitable.
- The technological lead in development of rotor design is a decisive factor.

The shape, size and manufacturing process of rotor blades are constantly evolving, and so are the simulation methods for wind turbine models. Therefore, wind tunnel facilities and their reasonable test capabilities are gaining more and more importance.

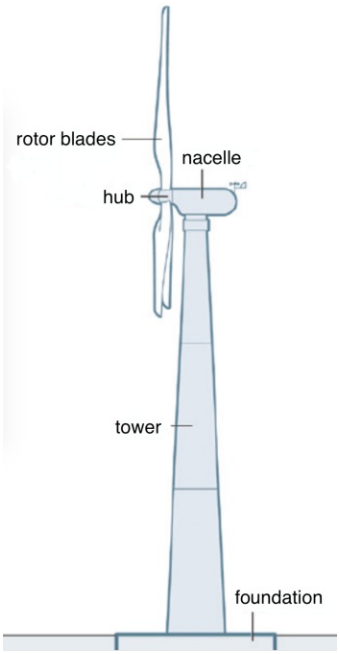

Figure 2.2: Horizontal axis wind turbine [29]

2.2 Physical Basics of Wind Energy Conversion

It is essential to understand the basics of wind energy conversion before modelling a wind turbine in wind tunnel environments. The segments of a wind energy conversion system can be seen in figure 2.3.

The key part of energy generation through wind power is the transformation of the kinetic wind energy into mechanical work and further into electrical power [16].

Die approbierte gedruckte Originalversion dieser Diplomarbeit ist an der TU Wien Bibliothek verfügbar
The approved original version of this thesis is available in print at TU Wien Bibliothek.
TU Bibliothek WIEN Your knowledge hub

Figure 2.3: Power stages of wind energy conversion system, inspired by [35]

The kinetic energy of an air mass m with a moving velocity v was expressed by Hau[15] as

$$E = \frac{1}{2}mv^2 \ . \tag{2.1}$$

Hau[15] also determined the mass flow rate $\dot{m}$ with the help of the air density ρ, a certain cross-sectional area A, and the velocity v expressed as $\dot{m} = \rho \cdot v \cdot A$.
This also applies to the volume flow rate $\dot{V}$ expressed as $\dot{V} = v \cdot A$.
The fact that power is energy divided by time, the correlation of $\dot{m}$ and $\dot{V}$ and with the help of equation (2.1), Thapar[35] derived the wind power as

$$P_w = \frac{1}{2}\rho A v^3 \ . \tag{2.2}$$

Figure 2.3 illustrates the link between the mechanical power P_m, the wind power P_w and the power coefficient C_p of the turbine as $P_m = P_w \cdot C_p$[35].

Since wind turbines turn at different rotational speeds, a transmission system is used in real wind power stations. In figure 2.3 one can see that the transmission power output P_t is dependant to the transmission efficiency η_m and Thapar[35] derived the relation as $P_t = P_m \cdot \eta_m$. Further, the generator output and, thus, the electrical power output can be determined by bringing in the efficiency of the generator η_g as: $P_e = P_t \cdot \eta_g$.

Thapar[35] expressed the final electrical output as

$$P_e = P_w \cdot \eta_g \cdot \eta_m \cdot C_p \ . \tag{2.3}$$

Die approbierte gedruckte Originalversion dieser Diplomarbeit ist an der TU Wien Bibliothek verfügbar
The approved original version of this thesis is available in print at TU Wien Bibliothek.
TU Bibliothek WIEN Your knowledge hub

2.3 Betz´s Elementary Momentum Theory

Albert Betz [6] was able to show by applying elementary physical laws that the energy extracted from an air stream passing through a given cross-sectional area is limited to a threshold proportion. Therefore, optimal power extraction can only be realised at a certain ratio of the airflow velocity in front of the energy converter and the flow velocity downstream of the converter. Because of the basic principles of the actuator theory, the exact nature of the energy converter is irrelevant, for which reason the flow around each wing is not mentioned[15].

Equation 2.2 showed that the wind power flowing through a control area, A, is given by $P_w = \frac{1}{2}\rho A v^3$. In section 2.3 one can see that a homogeneous air flow, v_1, hits the turbine while the slower velocity v_3 appears far downstream[14]. Betz[6] derived a stream tube with divergent streamlines due to the law of continuity

$$\rho \cdot v_1 \cdot A_1 = \rho \cdot v_2 \cdot A = \rho \cdot v_3 \cdot A_3 \ . \tag{2.4}$$

Betz [6] also assumed that the changes in air pressure are minimal, and the air density ρ remains constant. Further, the extracted energy E_{ex} can be computed as the upstream energy minus the downstream energy, resulting in the power P_{ex} extracted from the wind as show by

$$E_{ex} = \frac{1}{2} m (v_1^2 - v_3^2) \tag{2.5}$$

and

$$P_{ex} = \dot{E_{ex}} = \frac{1}{2} \dot{m} (v_1^2 - v_3^2) \ . \tag{2.6}$$

The velocity v_3 has to have a value between the incoming velocity v_1 and 0. Betz [6] explained that no power is extracted if v_3 is equal to v_1 and if $v_3 = 0$, the mass flow rate $\dot{m}$ becomes zero retarding the wind completely. Therefore, Betz assumed that $v_2 = \frac{v_1 + v_3}{2}$, while the mass flow rate will then be $\dot{m} = \rho \cdot A \cdot v_2$. With the help of these assumptions and equation (2.6), Betz [6] further derived

$$P_{ex} = \dot{E_{ex}} = \frac{1}{2} \rho A v_1^3 \left[\frac{1}{2} \cdot \left(1 + \frac{v_3}{v_1} \right) \cdot \left(1 - \left(\frac{v_3}{v_1} \right)^2 \right) \right] . \tag{2.7}$$

The expression inside the square brackets of equation (2.7) is called the power

Die approbierte gedruckte Originalversion dieser Diplomarbeit ist an der TU Wien Bibliothek verfügbar
The approved original version of this thesis is available in print at TU Wien Bibliothek.
TU Bibliothek WIEN Your knowledge hub

coefficient c_p, which depends on the ratio of v_3/v_1. If the first derivation of equation (2.7) is set to zero, the downstream velocity v_3 of figure 2.4 happens to be 1/3 of the upstream velocity v_1. This, in return, means that the maximum power of the wind is extracted if the velocity in the rotor plane is $\frac{2v_1}{3}$ [14]. This leads to a Betz-power coefficient [6] of

$$c_{p,Betz} = \frac{16}{27} = 0.59. \tag{2.8}$$

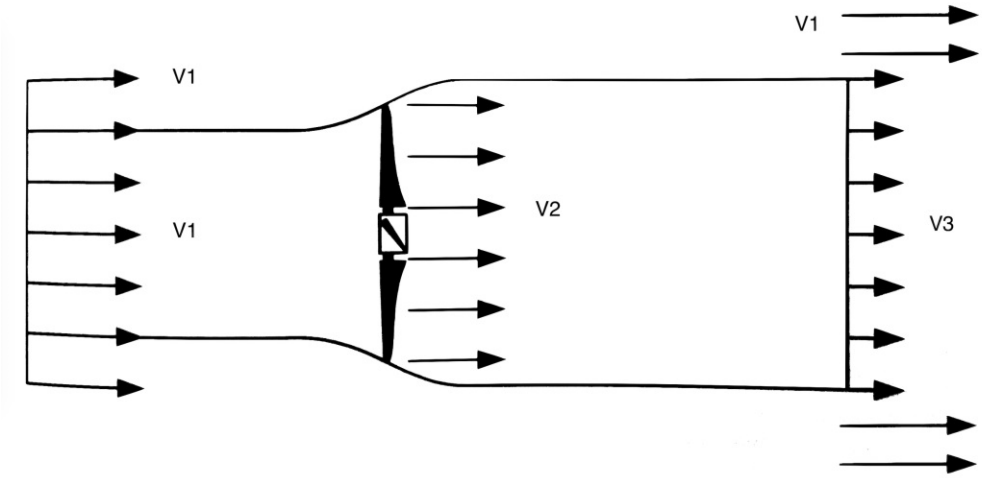

Figure 2.4: Air flow through an ideal Betz wind turbine, [14]

It should be mentioned that the Betz power coefficient has to be interpreted as a theoretical value since additional losses occur. However, depending on the wind velocity and the rotor diameter, modern wind turbines are capable of power coefficients up to $c_p = 0.5$ [14].

Die approbierte gedruckte Originalversion dieser Diplomarbeit ist an der TU Wien Bibliothek verfügbar
The approved original version of this thesis is available in print at TU Wien Bibliothek.
TU Bibliothek WIEN Your knowledge hub

Die approbierte gedruckte Originalversion dieser Diplomarbeit ist an der TU Wien Bibliothek verfügbar
The approved original version of this thesis is available in print at TU Wien Bibliothek.
TU Bibliothek Your knowledge hub WIEN

Chapter 3

Modelling of Wind Turbines

3.1 Introduction

The applications of the wind tunnel designed within the scope of this thesis project are wind turbine tests. To obtain reliable data with those tests, accurate models, including the full complexity of the real fluid flow, is mandatory. Thapar et al. [35] classified models predicting the behaviour of full-scale wind turbines into the following categories:

- Models based on the power curve concept of wind turbines.
- Models based on fundamental equations / theory of similarity.

When using the concept of power curves, either actual power curves supplied by the manufacturers are used, or models based on presumed shapes of power curves are utilised. The amount of electrical power that the given wind turbine generates at a specific wind speed can be directly found using power curves of the wind turbine [35]. The manufacturer usually provides these curves due to accurate tests of the final wind turbine. The wind tunnel developed within this thesis should be used for experiments of new shapes of wind turbine models. Therefore no power curves of these models can be provided for the time being. For that reason, the use of the concept of power curves is not sought and will not be discussed any further.

For the analysis of the power, torque and thrust characteristics of a planned larger system, down-scaled models are often tested in wind tunnel facilities [14].

Performance or efficiency statements can only be given with sufficient accuracy if the model is precise enough. Therefore, the theory of similarity is used, which determines in which manner the results of the tested down-scaled model can be transferred to the full-scale system [34].

3.2 Parameters of Similarity

Modern full-scale wind turbines with diameters of 125 meters cannot be tested easily in wind tunnel facilities. Therefore, down-scaled models are used. The model must have a similar geometry as the original full-scale turbine to ensure a meaningful transfer of the test results. Further, a similarity in the fluid's velocity, acceleration, forces, and kinematic viscosity shall be provided within a specific ratio. Even the forms of energy like kinematic energy, potential energy, and frictional energy have to be similar. Similar profiles as seen in figure 3.1 shall have a similar flow profile which means that both angels α of velocities have to be equal in a corresponding point. This implies that the velocities of the original turbine and the model shall be in the same ratio as $c/c_m, c_x/c_{xM}, c_y/c_{yM}$. Further, the inertial forces F_T as well as the viscous forces F_τ shall also be in the same ratio,

$$\frac{F_T}{F_\tau} = \frac{F_{TM}}{F_{\tau M}} \ . \tag{3.1}$$

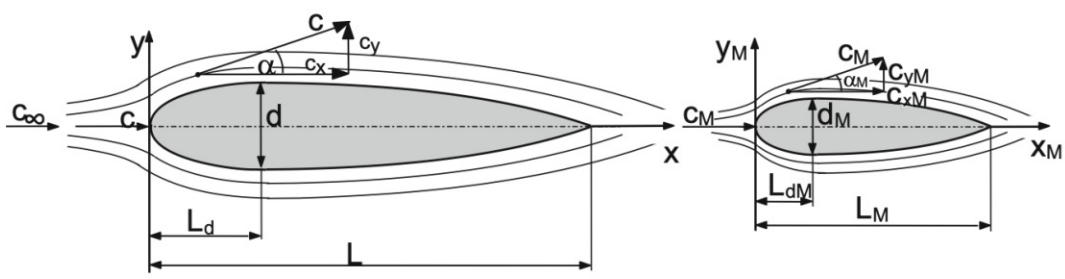

Figure 3.1: Similarity of two profiles, [34]

The parameters like flow velocity c_∞, c_M, the dimensions L, L_M, d, d_M as well as the density ρ and the kinematic viscosity ν of the fluid are crucial quantities. They cause the main forces acting on the system like the inertial force $F_T = m \cdot a$, the viscous force $F_\tau = \tau \cdot A$ and the pressure force $F_p = p \cdot A$ [34].

Die approbierte gedruckte Originalversion dieser Diplomarbeit ist an der TU Wien Bibliothek verfügbar
The approved original version of this thesis is available in print at TU Wien Bibliothek.
TU Bibliothek WIEN Your knowledge hub

When it comes to modelling a wind turbine, the Reynolds number and the Mach number are inevitable. If the down-scaled model has the same Reynolds and Mach numbers as the full-scale application, then the model and the full-scale flows will be dynamically similar [3].

The Reynolds number is the ratio of inertial force F_T and the viscous force F_τ

$$Re = \frac{F_T}{F_\tau} = \frac{m \cdot a}{\tau \cdot A} = \frac{\rho \pi d^2 L}{4\rho\nu \frac{dc}{dr} \pi d L} \frac{dc}{dt} = \frac{c \cdot d}{4\nu} \tag{3.2}$$

within a fluid and describes the impact of those two forces on the flow. If we assume a pipe flow, the dimensionless variable can be seen in equation (3.2), where the dynamic viscosity $\eta = \rho \cdot \nu$, the shear stress of a Newtonian fluid $\tau = \eta \frac{dc}{dr}$ and the surface of the pipe $A = \pi d L$ are included [34].

Equation 3.2 contains the Reynolds number with the geometric variable d, the kinematic variable c as well as the kinematic viscosity ν. According to Surek and Stempin [34], this dimensionless variable can be written as

$$\text{Reynolds number} = Re = \frac{c \cdot d}{\nu}. \tag{3.3}$$

The Mach number,

$$\text{Mach number} = M = \frac{c}{a} \tag{3.4}$$

is a dimensionless quantity describing the ratio of the local flow velocity, c, to the local speed of sound, a. It can be interpreted as the ratio of inertia force of the flow and the elasticity force of the fluid. Further, Surek and Stempin [34] claimed that air can be treated as being incompressible, if $M < 0.3$.

The Froude number should also be mentioned in this context, but since this quantity is used to indicate the influence of gravity on fluid motion, it plays a subordinated role in this application.

3.3 Estimation of Similarities

As mentioned before, the comparison of the Reynolds and Mach numbers of the down scaled wind turbine model and the full-scale application is important for the

Die approbierte gedruckte Originalversion dieser Diplomarbeit ist an der TU Wien Bibliothek verfügbar
The approved original version of this thesis is available in print at TU Wien Bibliothek.
TU Bibliothek WIEN Your knowledge hub

relevance of the experimental results. For an initial assessment a reference turbine was chosen and compared to a wind turbine model with assumed dimensions and flow velocity regarding to the wind tunnel designed in section 4.2. In the upcoming calculations the NREL-5MW turbine was used as the reference wind turbine and all essential data can be seen in table 3.1. In all calculations regarding the Reynolds number, the kinematic viscosity ν_{air} was set to $15.32 \cdot 10^{-6} m^2/s$.

Parameter	Value
Rotor diameter	126 m
Number of rotor blades	3
Rated aerodynamic power	5.3 MW
Rated wind speed	11.4 m/s
Rated rotational speed	12.1 rpm
Chord (at $r = 61.6\ m$)	1.419 m

Table 3.1: NREL-5MW specifications, [20]

At first, the rotor Reynolds number of both applications are computed, and the results can be seen in table 3.2. At the end of this chapter, all results are discussed in more detail. The rotor diameter of the down-scaled three-bladed wind turbine model was assumed to be 0.3 m to fit in the wind tunnel designed in section 4.2. Further, a relatively high flow velocity was assumed at 100 m/s. When calculating the rotor Reynolds number, the geometric variable d corresponds to the rotor diameter of the turbine.

Additionally, the profile Reynolds number of both applications are computed. Therefore, the geometric variable d of the Reynolds number corresponds to the blade's chord at a certain radius. According to Erich Hau [15], the profile Reynolds

Rotor-Reynolds number

Reference turbine NREL-5MW	Down-scaled wind turbine model
$Re_{ref} = \frac{D \cdot c}{\nu_{air}} = \frac{126 \cdot 11.4}{15.32 \cdot 10^{-6}}$	$Re_{mod} = \frac{D \cdot c}{\nu_{air}} = \frac{0{,}3 \cdot 100}{15.32 \cdot 10^{-6}}$
$Re_{ref} = 93759791.12$	$Re_{mod} = 1958224.54$

Table 3.2: Comparison of rotor Reynolds number

Die approbierte gedruckte Originalversion dieser Diplomarbeit ist an der TU Wien Bibliothek verfügbar
The approved original version of this thesis is available in print at TU Wien Bibliothek.
TU Bibliothek WIEN Your knowledge hub

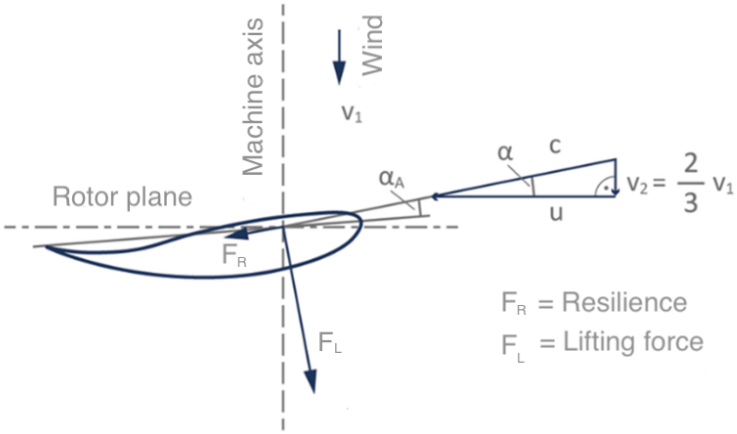

Figure 3.2: Flow velocity for profile Reynolds number, inspired by www.wind-energie.de

number near the tip of the blade of a modern wind turbine is in the range of $1 \cdot 10^6$ to $8 \cdot 10^6$. Therefore, the chord of the reference turbine was considered at radius $r = 61.6\ m$ and had a length of $1.419\ m$. These dimensions are given by the manufacturer and can be seen in table 3.1. The kinematic variable c of the profile Reynolds number should not be confused with the velocity of the wind. As indicated in figure 3.2 the flow velocity c acting on the profile is crucial for the calculation. It can be computed with the help of the velocity v_2 and the circumferential speed u of the turbine [14]. As mentioned in section 2.3 the velocity v_2 in the rotor plane is $\frac{2}{3}$ of the undisturbed wind velocity. The accurate calculation of the profile Reynolds number for both applications can be seen in table 3.3, while the results will be discussed at the end of this chapter.

Finally, the Mach number is computed for both cases. Therefore, the local flow velocity c in table 3.3 was considered to get the dimensionless Mach number near the tip of the rotor. The value for the local speed of sound within dry air was chosen to be 343.2 m/s at 20°C [1].

We can observe a considerable difference when comparing the Reynolds numbers of the down-scaled wind turbine model with the reference turbine. The Reynolds number of the model rotor is lower because of the small diameter of 0.3 m. Even if the velocity c reached unrealistic values, the difference in Reynolds numbers would be striking. Since the model's dimensions are dependent on the size of the wind tunnel, the countermeasures are limited. Moreover, the profile Reynolds numbers of the model is considerably lower than the one of the reference turbine. In this case,

Die approbierte gedruckte Originalversion dieser Diplomarbeit ist an der TU Wien Bibliothek verfügbar
The approved original version of this thesis is available in print at TU Wien Bibliothek.
TU Bibliothek WIEN Your knowledge hub

Profile-Reynolds number

Reference turbine NREL-5MW	Down-scaled wind turbine model
$v_2 = 11.4 \cdot \frac{2}{3} = 7.6\frac{m}{s}$	$v_2 = 100 \cdot \frac{2}{3} = 66.666\frac{m}{s}$
$u_{r=61.6m} = r \cdot 2\pi \cdot n = 61,6 \cdot 2\pi \cdot 12.1 = 4683.24\frac{m}{min} = 78.054\frac{m}{s}$	$u_{r=0.15m} = r \cdot 2\pi \cdot n = 0.15 \cdot 2\pi \cdot 1500 = 1413.72\frac{m}{min} = 23.56\frac{m}{s}$
$c = \sqrt{78.954^2 + 7.6^2} = 78.423\frac{m}{s}$	$c = \sqrt{23.56^2 + 66.666^2} = 70.71\frac{m}{s}$
$Re_{ref} = \frac{d \cdot c}{\nu_{air}} = \frac{1.419 \cdot 78.423}{15.32 \cdot 10^{-6}}$ $Re_{ref} = 7263853.59$	$Re_{mod} = \frac{D \cdot c}{\nu_{air}} = \frac{0.02 \cdot 70.71}{15.32 \cdot 10^{-6}}$ $Re_{mod} = 92310.705$

Table 3.3: Comparison of profile Reynolds number

Mach number

Reference turbine NREL-5MW	Down-scaled wind turbine model
$c = \sqrt{78.954^2 + 7,6^2} = 78.423\frac{m}{s}$	$c = \sqrt{23.56^2 + 66.666^2} = 70.71\frac{m}{s}$
$M_{ref} = \frac{c}{a} = \frac{78.423}{343.2}$ $M_{ref} = 0.2285$	$M_{mod} = \frac{c}{a} = \frac{70.71}{343.2}$ $M_{mod} = 0.206$

Table 3.4: Comparison of Mach number

the chord of the model causes the low Reynolds number. The Reynolds number depends on the rotor model dimension and implicitly on the size of the wind tunnel.

Barlow et al. [3] claimed that the reproduction of the full-scale Reynolds numbers is not necessary for many studies, but it must be of at a "reasonable value". A fundamental decision concerning the minimum acceptable value of the Reynolds number has to be made. Further, they claim that the lower boundary for testing airfoils and wings are Reynolds numbers in the range of 1000000 to 1500000 based on the chord.
Ann Hyvarinen et al. [19] corroborated these statements achieving a rotor Reynolds number of about $6 \cdot 10^4$ with their wind turbine model having a diameter of 11.2

Die approbierte gedruckte Originalversion dieser Diplomarbeit ist an der TU Wien Bibliothek verfügbar
The approved original version of this thesis is available in print at TU Wien Bibliothek.
TU Bibliothek WIEN Your knowledge hub

cm. Despite that, the Mach numbers in both cases are similar. Since the local flow velocities are almost equal in both cases, the Mach numbers are below 0.3, where air can be considered incompressible.

These results should be considered an initial assessment, and more accurate calculations can be done with the first down-scaled models, but these are not part of this work.

Die approbierte gedruckte Originalversion dieser Diplomarbeit ist an der TU Wien Bibliothek verfügbar
The approved original version of this thesis is available in print at TU Wien Bibliothek.
TU Bibliothek WIEN Your knowledge hub

Die approbierte gedruckte Originalversion dieser Diplomarbeit ist an der TU Wien Bibliothek verfügbar
The approved original version of this thesis is available in print at TU Wien Bibliothek.
TU Bibliothek WIEN Your knowledge hub

Chapter 4

Creation and Design Methodology for a Low-Cost Wind Tunnel

4.1 Introduction

A wind tunnel is an aerodynamic test facility, which is used to study flow patterns around bodies and measure aerodynamic forces [3]. Due to the limited size of the wind tunnel, the investigated models are usually down-scaled while keeping the properties similar to the original problem, including the complexity of actual fluid flow. Therefore, wind tunnel test results can be extrapolated to the actual velocity and body size using suitable scaling laws [33]. These tests can be carried out very early in the design process and repeated multiple times. Because of this economic advantage and a large amount of reliable and accurate data, wind tunnels are often the instrument of choice when it comes to aerodynamic tests and research [3].

Even with the possibility of today´s simulation methods like computational fluid dynamics (CFD), a wind tunnel is a highly useful technical piece of equipment. In university education, wind tunnels are used to teach students the fundamental principles of aerodynamics, like lift, drag, and pitching moments to more advanced phenomena such as boundary layers and pressure distributions around models or even wake investigations. A wide variety of aerodynamic experiments are possible, such as flow passing a wind turbine model with pressure and velocity observation and determination of the efficiency; flow passing bluff and streamlined bodies

with pressure and velocity observation in the wake; investigations into boundary layer developments; the influence of aspect ratio on aerofoil performance; pressure distribution around objects; study of the characteristics of models involving measurements of lift and drag forces and flow visualization, and the list of highly useful applications goes on [33].

4.1.1 Types of Wind Tunnels

A well-designed wind tunnel generates a uniform flow with a minimum turbulence intensity in the test section, where the model is investigated. The larger the wind tunnel, the larger the operating range at meaningful Reynolds numbers is possible. Further, more accurate and representative results are measurable, which leads to a better simulation [17]. The two basic types of wind tunnels are the open-, and the closed-circuit system [3]. Independently of the type of wind tunnel, every system consists of a settling section, a contraction section (also called effuser), a test section in which the model is kept, and a diffuser [33]. The closed-circuit wind tunnel consists of many more components, which are illustrated in figure 4.1.

Closed-Circuit Wind Tunnel

In a closed return wind tunnel, as shown in figure 4.1, the flowing air recirculates continuously with little or no air exchange with the exterior. The advantages and disadvantages of a closed-circuit wind tunnel are the following [3]:

Advantages

1. The flow quality can be controlled using turning vanes in each tunnel corner.
2. The required energy is less due to the closed circulation in comparison to open-circuit wind tunnel systems.
3. Relatively silent operation is possible.

Die approbierte gedruckte Originalversion dieser Diplomarbeit ist an der TU Wien Bibliothek verfügbar
The approved original version of this thesis is available in print at TU Wien Bibliothek.
TU Bibliothek WIEN Your knowledge hub

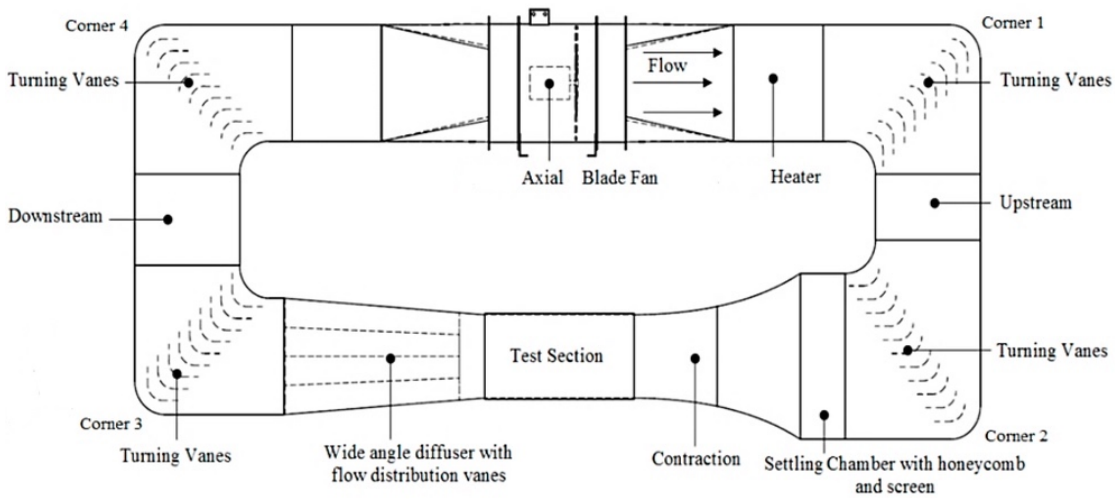

Figure 4.1: Closed Circuit Wind Tunnel, [10]

Disadvantages

1. Usually higher initial costs, due to the larger number and partially more expensive parts (like corners etc.).

2. When used for flow visualization or with internal combustion engines a way to purge the tunnel has to be implemented. That is justified by the fact that fumes and waste gas inside the closed circuit could disturb the experiment and falsify the results.

3. An air exchanger or some other method of cooling is needed when frequently used.

Open-Circuit Wind Tunnel

In an open-circuit wind tunnel, the air flows straight through the entrance, the settling chamber, the contraction cone into the test section, followed by the diffuser, the fan section, and the air exhaust. That means that open-circuit tunnels do not directly re-circulate the air. Instead, the air is drawn from the laboratory environment [3]. The benefits, as well as the drawbacks, are described below, and an example of the basic structure of such systems can be seen in figure 4.2.

Die approbierte gedruckte Originalversion dieser Diplomarbeit ist an der TU Wien Bibliothek verfügbar
The approved original version of this thesis is available in print at TU Wien Bibliothek.
TU Bibliothek WIEN Your knowledge hub

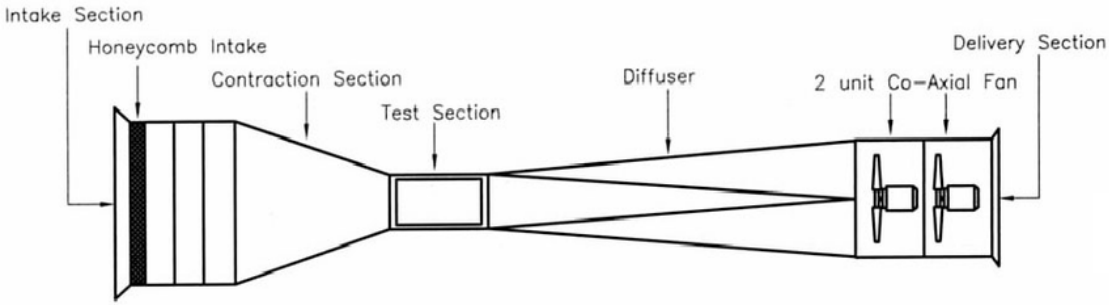

Figure 4.2: Open-Circuit Wind Tunnel, [18]

Advantages

1. The costs of an open-circuit wind tunnel are much lower compared to closed-circuit applications.
2. No purging is needed when flow visualization or internal combustion engines are used.

Disadvantages

1. The very long tunnel has to fit in the room or the weather conditions have to be considered when used outdoors.
2. Open-circuit wind tunnel systems are often very noisy.

4.2 Wind Tunnel for the Vienna University of Technology

Since this is a university research project, some guidelines which can be seen below must be satisfied. The cost factor must be taken into account since this project has to be financed.

Die approbierte gedruckte Originalversion dieser Diplomarbeit ist an der TU Wien Bibliothek verfügbar
The approved original version of this thesis is available in print at TU Wien Bibliothek.
TU Bibliothek WIEN Your knowledge hub

Requirements for this particular Wind Tunnel:

- The system has to be as cost-effective as possible, by having a solid functionality.
- For financial reasons and due to the local circumstances at the laboratory, an open-circuit wind tunnel is requested.
- Low turbulent flow inside test chamber shall be achieved.
- The wind tunnel has to be dismountable into movable components for better storage when not needed.
- A rectangular cross-section and visible walls of the test section is needed.
- A high level of safety is mandatory.
- The possibility to use the existing instruments like:
    1. Aerosol generator for flow visualization
    2. Laser Doppler Anemometry (LDA)
    3. Particle Image Velocimetry (PIV) is indispensable.

4.3 Components of the Wind Tunnel

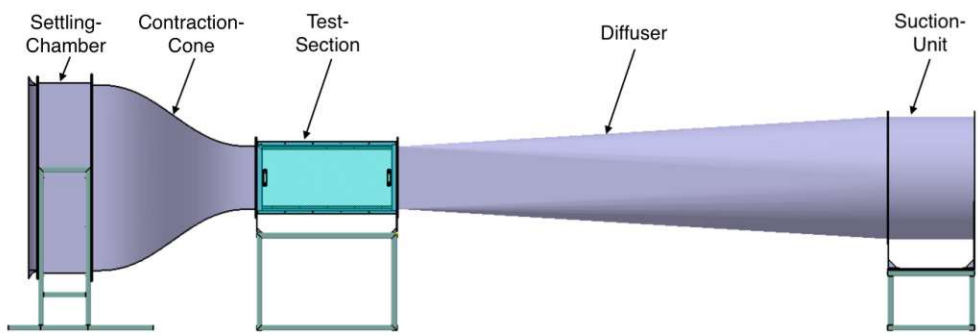

Figure 4.3: Open-circuit wind tunnel

The overall structure of the designed open-circuit wind tunnel can be seen in Figure figure 4.3. Air is drawn in from the laboratory environment through a honeycomb

Die approbierte gedruckte Originalversion dieser Diplomarbeit ist an der TU Wien Bibliothek verfügbar
The approved original version of this thesis is available in print at TU Wien Bibliothek.
TU Bibliothek WIEN Your knowledge hub

flow straightener and two meshes inside the settling chamber to make the flow velocity profile uniform. In the following, an aerodynamically designed contraction cone accelerates the air so that the velocity is as uniform as possible at the end of this effuser and the beginning of the subsequent test section. Through the transparent walls of the test chamber, one can observe the interaction of the airflow and a test model, like a wind turbine or a wing. Afterwards, the diffuser slows the airflow, which also serves as a shape adapter to match the round cross-sectional housing of the subsequent radial fan. In figure 4.3 the suction unit constitutes a simplified representation of the radial fan.

All parts are described in detail in the following sections.

4.3.1 Test Chamber

The design of a test section is dependent on the requirements of the individual experimenter [24].
Since the university has requirements on this part, this component of the wind tunnel was engineered with the highest care. The design and construction of the test section are based on the following guidelines:

- A rectangular cross-section is desired.
- Since a flow visualisation and measurement with PIV (Particle Image Velocimetry) is intended, walls made out of clear acrylic glass must be used.
- The needed measurement instruments for PIV must be placed below the test section.
- The possibility of a removable back wall for different models and measurements is desired.
- Instruments for pressure measurement must be placed inside the test section.
- The construction has to be resilient, since intense vibrations will occur.
- An easy accessibility to the tested model is requested.
- A mounting fixture for the models should be addable but the design of it is not part of this work.

Die approbierte gedruckte Originalversion dieser Diplomarbeit ist an der TU Wien Bibliothek verfügbar
The approved original version of this thesis is available in print at TU Wien Bibliothek.
TU Bibliothek WIEN Your knowledge hub

This particular wind tunnel aims to test small models of wind turbines with a diameter of approximately 20 to 30 *cm*. Individual wings of such a model and the effects of a damaged surface may also be tested. Therefore, a rectangular cross-section with a width of 550 to 600 *mm* is selected. Finding the ideal form and design of the needed test section was an iterative process with amendments of several factors. This process will be discussed in the following, whereby test chamber model 4 in chapter 4.3.1 was chosen for the final wind tunnel.

Test Chamber Model 1

The first two test section versions aimed to keep the costs low by having the highest ease of use and manufacturing. In figure 4.4 one can see that the welded flange of the test section 1 is made out of four mitre cut angled profiles for each flange. The holes for a screw connection on both sides ensure a solid attachment to the contraction cone and the diffuser on the other side. For the support of the acrylic glass along the sides, all three windows (displayed in turquoise in figure 4.4) are glued together in a longitudinal direction which saves material as well as production costs. Countersunk screws (not shown in figure 4.4) are used to connect the glass to the flange without creating turbulence. For ease of use, the door (displayed in blue in figure 4.4) is equipped with hinges and two gas struts mounted on the flanges. One of the requirements is a removable back wall. This can be realised only with the help of a cutout, whereby this is the first big disadvantage. The other one is the fact that glued joints might not hold well against strong vibrations due to the high flow velocity. Also, hinges could be unfavourable since they always have a certain freedom of movement, which could create cracks in the acrylic glass. Therefore, a decision was made against this model to use for the final wind tunnel.

Die approbierte gedruckte Originalversion dieser Diplomarbeit ist an der TU Wien Bibliothek verfügbar
The approved original version of this thesis is available in print at TU Wien Bibliothek.
TU Bibliothek WIEN Your knowledge hub

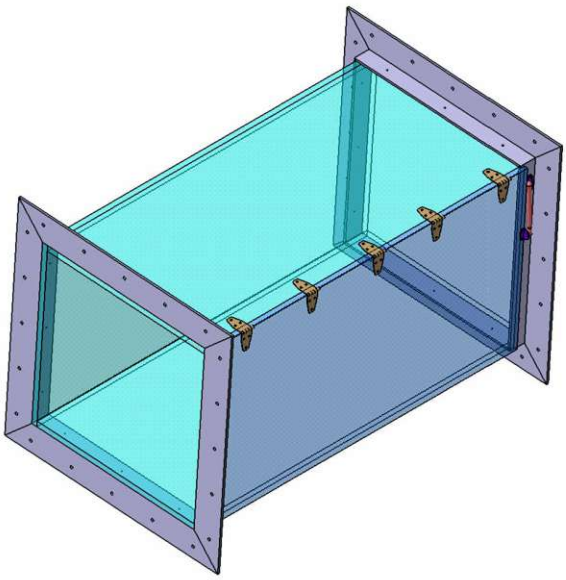

Figure 4.4: Test Section 1

Test Chamber Model 2

Figure 4.5 shows that the flange of test section 2 is cut out of a solid 5 mm steel plate to create a square with holes evenly spaced around the circumference. This model features four angled profiles with $35 \times 25 \times 5$ mm welded to the flange to support the longitudinal side of the glass through transit bolts with countersunk heads (not illustrated in Figure 4.5). Hinges are used for easy accessibility, while the access door of this model was cut out of the window compared to model 1. A groove along all four sides of the door creates a better fit inside the frame. In both models 1 and 2, the connection to the movable support frame (only illustrated in Figure 4.5) is realised by two angled profiles screwed to each flange.

The transverse sides of windows and the door frame are not connected to the flange, which is unfavourable with strong vibrations. Although the door of this model has a better fit to the frame compared to test section 1, the risk of wearing out due to the hinged door is increased. All components of this wind tunnel are designed for longevity, and for which reason, model 2 will also be discontinued.

Die approbierte gedruckte Originalversion dieser Diplomarbeit ist an der TU Wien Bibliothek verfügbar
The approved original version of this thesis is available in print at TU Wien Bibliothek.
TU Bibliothek WIEN Your knowledge hub

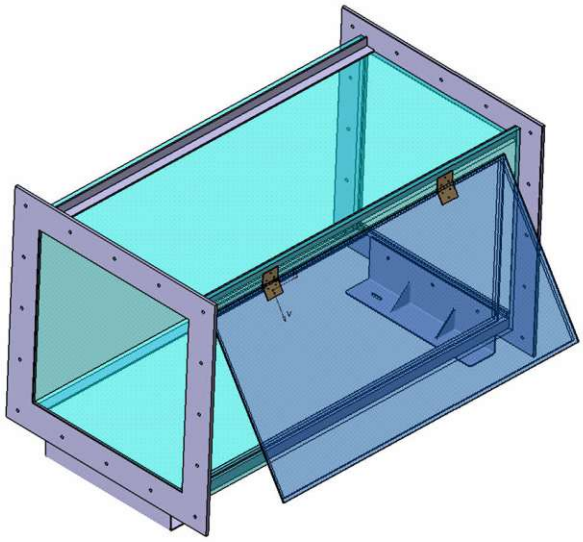

Figure 4.5: Test Section 2

Test Chamber Model 3

Figure 4.6 illustrates the third version of the test section, where the flange, which also acts as the connection to the movable frame, is cut out of solid 5 mm sheet metal. Holes evenly spaced around the circumference have also been made to connect strongly to the forward and subsequent parts. Due to economic reasons, the back surface is made out of 3 mm sheet metal and is screwed to the upper and lower window. These, in turn, are screwed to the flange with the help of angle brackets. Additionally, two steel profiles with a rectangular cross-section are welded to the flanges. The door (illustrated in blue) and the two windows (illustrated in turquoise) are screwed to these profiles. For convenient handling, two handles are attached to the door with countersunk screws.

The angle brackets are not the most elegant and sturdy solution for keeping the windows in place. Other disadvantages are the material offcuts and the manufacturing costs in order to produce the flanges. Therefore, a decision was made against this model.

Die approbierte gedruckte Originalversion dieser Diplomarbeit ist an der TU Wien Bibliothek verfügbar
The approved original version of this thesis is available in print at TU Wien Bibliothek.
TU Bibliothek WIEN Your knowledge hub

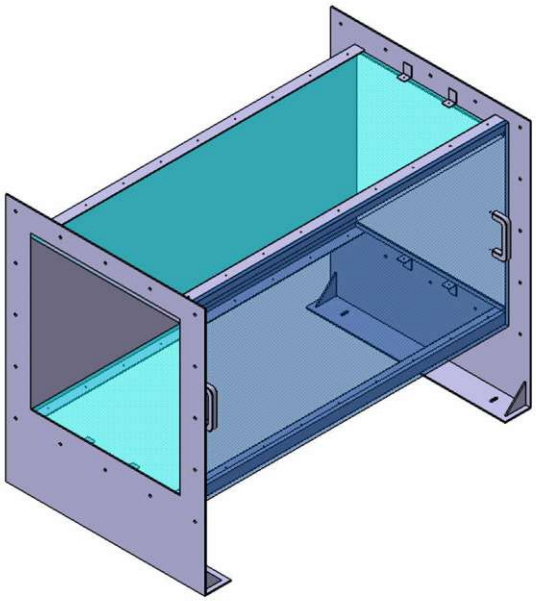

Figure 4.6: Test Section 3

Test Chamber Model 4

With the help of all the previous models and the knowledge acquired, model 4 includes most of the advantages of each version. The final inner dimensions of the test chamber are $570 \times 570 \times 1300\ mm$.

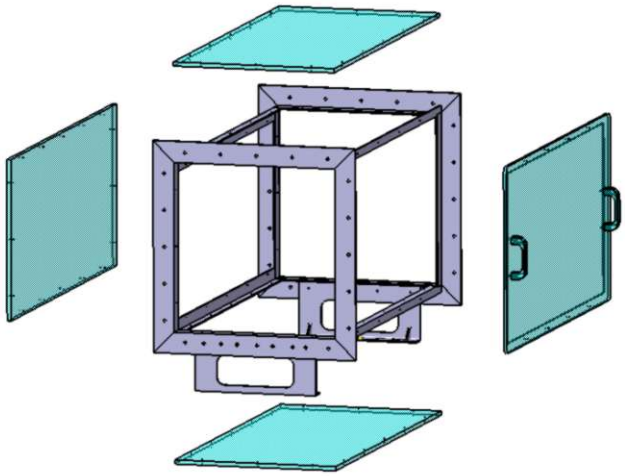

Figure 4.7: Test Section 4, exploded view

Die approbierte gedruckte Originalversion dieser Diplomarbeit ist an der TU Wien Bibliothek verfügbar
The approved original version of this thesis is available in print at TU Wien Bibliothek.
TU Bibliothek WIEN Your knowledge hub

As in model 1 and seen in figure 4.7, four mitre cut angle profiles have been welded together for each of the two flanges. This reduces material off-cuts and ensures a robust connection to the acrylic glass panels along the broadside since they can be screwed together with transit bolts with countersunk heads. On the longitudinal side of the metal frame, two different angle profiles have been used. At the backside of the frame, where the upper,- lower,- and back-glass panels with a thickness of 15 mm each come together, two angle profiles with the dimensions of $45 \times 30 \times 5$ mm have been used. Thereby, an exchange of the back wall for different mounting options can easily be realised. At the front of the frame, two angle profiles are attached so that the upper and lower window can be securely bolted to the frame from the inside and that the door can easily be mounted with knurled screws from the outside without interfering with the flow inside the test chamber. The door with the dimensions of $1280 \times 660 \times 15$ mm also has a milled recess on the entire periphery to ensure a good fit and generate less flow disturbance. As in model 3, two handles have been attached with countersunk screws for convenient usage. An angled and welded construction made out of 5 mm steel sheet with two reinforcement ribs connects the test section to a movable frame just like in model 2. This can be seen in the technical drawings in more detail within the appendix appendix B.1.

Model 4 with offset at the door For the first version of the test chamber model 4, a square flange was designed with four mitre cut angle profiles of the same length. The three windows with a thickness of 15 mm are mounted on the inside of the test chamber, while the door has to be mounted from the outside. This creates an offset of 15 mm at the transition to the contraction cone and to the diffuser. The offset can be seen on the right side of figure 4.8, where the diffuser is coloured in orange for better visibility. With the help of CFD simulation as seen in chapter 4.4.6 it was observed that this design creates a flow separation due to the offset of 15 mm at the door. Therefore another version of this model 4 without an offset was created, while the design remained the same.

Model 4 without offset at the door All three windows must be mounted from the inside to avoid the addressed turbulence inside the test section. The flanges' upper and lower angle profiles had to be shortened by 15 mm to get rid of

Die approbierte gedruckte Originalversion dieser Diplomarbeit ist an der TU Wien Bibliothek verfügbar
The approved original version of this thesis is available in print at TU Wien Bibliothek.
TU Bibliothek WIEN Your knowledge hub

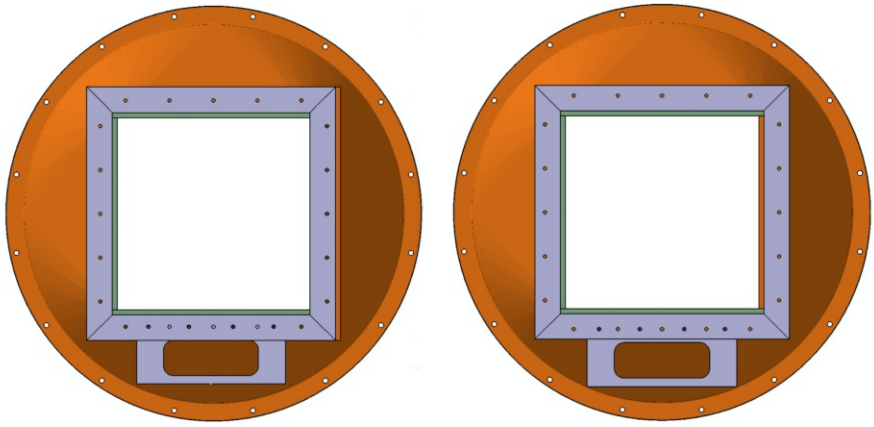

Figure 4.8: Test section with and without offset

the offset. Then the flanges are no longer squared, which can be seen on the left side of figure 4.8, but functionality is the major criteria. Therefore, a slightly higher price in production costs will be accepted to realise a much better flow quality inside the system. In chapter 4.4.6 and 4.4.6, the difference in performance from test section model 4 with and without the offset are discussed and the CFD-results can be seen in figure 4.24 and figure 4.26.

4.3.2 Contraction Cone

The contraction cone, a short nozzle, might be the crucial part of a wind tunnel since it is mainly responsible for avoiding flow separation, a uniform velocity field and an optimal flow quality inside the subsequent test section. Therefore, it was the second component in the design process.

The use of a well-designed contraction section causes an increase in the mean velocities of the flow at the test section inlet and moderate inconsistencies in the uniformity of the flow. The honeycomb and the screens reduce the turbulence level in the flow and are placed in a lower speed region, the settling chamber, for lower pressure losses and tunnel power factor. It is important to avoid flow separation by keeping the exit boundary layer thickness and the contraction length at a minimum. Therefore, the contraction ratio CR and the length l of the contraction has to be chosen wisely. The contraction ratio, CR, is the ratio of the cross-sectional area at the inlet, A_i, and the cross-sectional area at the outlet, A_o. It is possible to avoid flow separation by extending the contraction, but this increases cost and exit boundary layer thickness. Energy losses will be generated due to wall friction [24].

Die approbierte gedruckte Originalversion dieser Diplomarbeit ist an der TU Wien Bibliothek verfügbar
The approved original version of this thesis is available in print at TU Wien Bibliothek.
TU Bibliothek WIEN Your knowledge hub

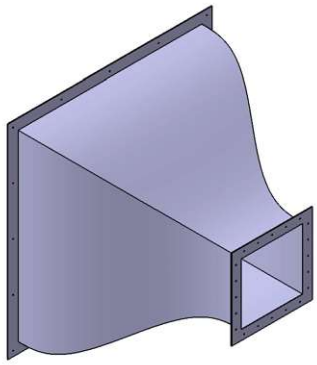

Figure 4.9: Contraction Cone

Based on the fundamentals of fluid dynamics, Barlow [3] derived the friction losses,

$$K_n = 0.32 \cdot f_{av} \cdot \frac{L}{D_{SC}} \ , \tag{4.1}$$

where f_{av} is the average friction coefficient, L is the length of the contraction and D_{SC} is the hydraulic diameter of the settling chamber.

Also, for short contraction sections, flow separation will occur with a high likelihood. Therefore, Bell and Mehta [24] recommend a contraction length in the range of $L/H_i = 0.7$ and $L/H_i = 1.4$, while L represents the contraction length, and H_i is the contraction wall height at the inlet respectively from the datum at the axis of symmetry [27]. The same conflict applies to the ratio, C, since a bigger contraction ratio leads to minimized flow non-uniformity and streamwise velocity fluctuations by increasing the construction and running costs, noise and separation near the cone end [11]. For smaller wind tunnels, contraction ratios between about 6 and 9 are recommended by Bell and Mehta [24]. When choosing the proper material, one must balance the flow quality and material and production costs. Some projects get by with a wooden solution because only simple flow tests are intended. As mentioned before, a well designed and, therefore a more advanced shape of the contraction cone is crucial for a high-quality flow inside the test chamber. Thus, a metal structure is indispensable for the wind tunnel. When it comes to the geometry of this part, axisymmetric contractions deliver the most uniform flow with low turbulence levels, although octagonal and rectangular designs are sometimes used because of the low manufacturing costs [8].

Die approbierte gedruckte Originalversion dieser Diplomarbeit ist an der TU Wien Bibliothek verfügbar
The approved original version of this thesis is available in print at TU Wien Bibliothek.
TU Bibliothek WIEN Your knowledge hub

There are several factors to consider when it comes to the optimum shape and length of a well-designed contraction cone with sufficient flow quality and low risk of separation. In the last 50 to 60 years, many studies and authors have dealt with this problem. The fact that the wall profile should have the first and second derivative equal to zero at the inlet and outlet was obvious. But in 1988, Bell and Mehta developed a fifth-order polynomial

$$h = [(-10\zeta^3 + 15\zeta^4 - 6\zeta^5) \cdot (H_i - H_o) + H_i] \qquad \text{where} \qquad \zeta = \frac{x}{L} \tag{4.2}$$

which is still widely used when it comes to designing a low-speed wind tunnel contraction profile. In this equation, H_i and H_o indicates the height at the inlet or outlet of the contraction wall measured from the axis of symmetry, while L represents the length of the contraction cone [33].

Bell and Mehta's fifth-order polynomial contraction profile should be applied at this particular wind tunnel. Since the test section was developed first, the inner height at the outlet of the nozzle is now defined by $H_o = 285\ mm$. The inner height at the inlet was set to be $H_i = 850\ mm$ to obtain as much air volume as possible contracted by the nozzle. This leads to a contraction ratio of $CR = A_i/A_o = 8.89$, which is within the range of 6 to 9, as Bell and Mehta recommend. The length of the contraction cone was chosen to be 1,5m which results in a ratio of $L/H_i = 1,76$. This might not be within the boundaries that Bell and Metha have predefined, but the main goal was a high contraction ratio by having a low possibility of flow separation. A variety of different contraction ratios and lengths have been considered, but every change implies an inevitable trade-off. A CFD simulation was also performed and is shown in section 4.4 to exclude a malfunction of the chosen profile of the contraction cone. With the variables, H_i, H_o, and L, and the help of equation (4.2) the contour of the contraction cone profile can be computed. In Matlab, all function points have been calculated and listed in the table A.1, while the equivalent illustration of the contour can be seen in figure 4.10.

After calculating the contraction cone profile in Matlab, all points have been passed to the CAD program CATIA using excel-files and macros. The profile line was designed by connecting all points, and the whole body was created with a thickness of 2 mm. An illustration of the final contraction cone can be seen in Figure 4.9 while the technical drawings can be seen in the appendix B.1.

Die approbierte gedruckte Originalversion dieser Diplomarbeit ist an der TU Wien Bibliothek verfügbar
The approved original version of this thesis is available in print at TU Wien Bibliothek.
TU Bibliothek WIEN Your knowledge hub

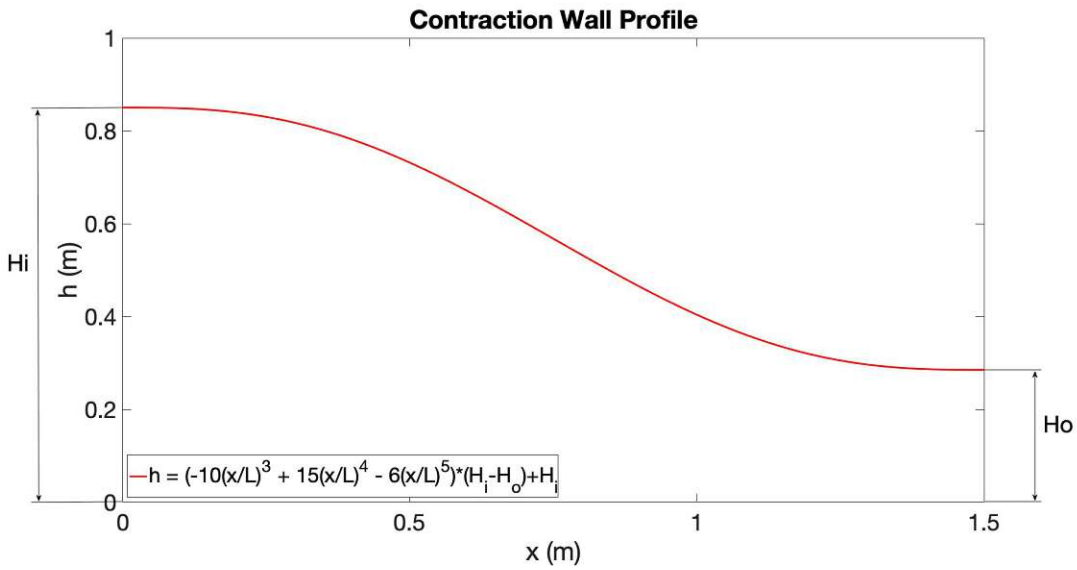

Figure 4.10: Contraction Cone Profile

4.3.3 Settling Chamber

A settling chamber is a flow conditioning section at the wind tunnel entrance, which has the purpose of reducing large-scale turbulence in the flow and removing eddies from the incoming air of the laboratory environment [37]. This is crucial for a predictable flow and repeatable testing. The most important parts of this section are the meshes and the honeycomb screen, while the complete structure is shown in figure 4.11.

Honeycomb

Usually, a honeycomb screen with cells aligned in the direction of the flow is used to reduce large-scale turbulence in the incoming low-velocity flow, especially the lateral components of turbulence. The honeycomb is positioned at the beginning of the settling chamber in a low-velocity region to generate a small pressure drop. Multiple shapes of honeycombs with different loss coefficients can be seen in figure 4.12, while the most effective and commonly used cross-sectional shape is hexagonal as seen in table 4.1. The loss coefficient K_l describes the ratio of the pressure loss in the wind tunnel section to the dynamic pressure at the entrance of the wind tunnel section [37]. When it comes to the right size of the honeycomb hexagons, Mehta and Bradshaw [24] claimed that the number of cells is proportional to the inlet

Die approbierte gedruckte Originalversion dieser Diplomarbeit ist an der TU Wien Bibliothek verfügbar
The approved original version of this thesis is available in print at TU Wien Bibliothek.
TU Bibliothek WIEN Your knowledge hub

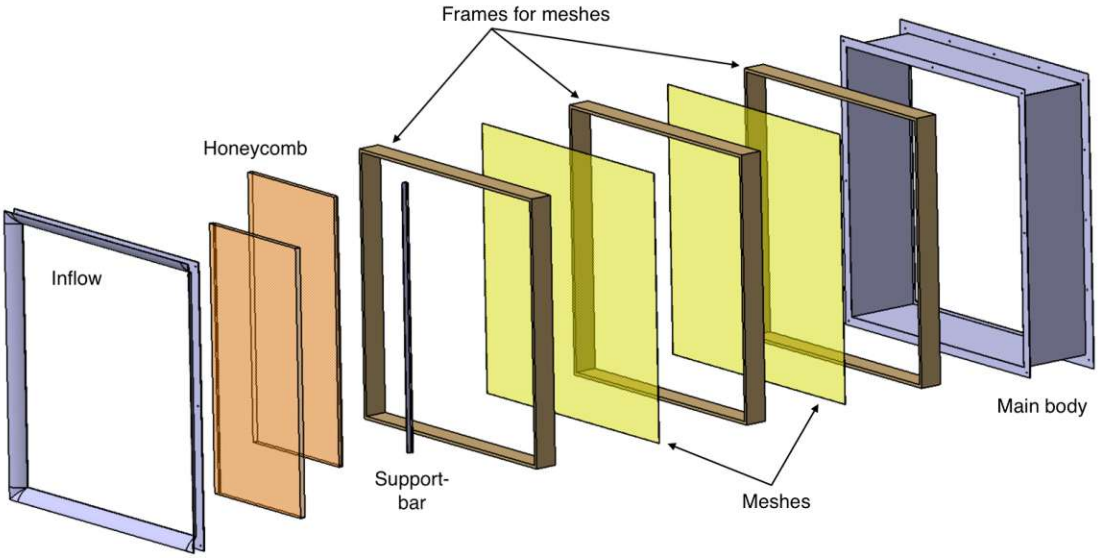

Figure 4.11: Settling Chamber, exploded view

diameter of the wind tunnel, whereby the number of recommended cells should be around 150 cells per settling chamber diameter. The length of each cell should be around 6-8 times the diameter of the hexagon for maximum overall benefit. Since the honeycomb itself induces small-scale turbulence in each cell, a certain settling distance is needed. Nevertheless, a honeycomb with long cells creates a higher pressure loss due to the growing boundary layer in each cell [37]. This particular settling chamber was chosen to use a honeycomb made out of aluminium with a 5 mm hexagonal width and an axial length of 35 mm. With a settling chamber width of 1.7 m, this results in roughly 270 cells per settling chamber diameter and a length of 7 times the cell diameter, which is both within the recommendations of Mehta and Bradshaw [24].

Honeycomb type	Loss coefficient K_l
a	0.3
b	0.22
c	0.2

Table 4.1: Honeycomb loss coefficient, [3]

Die approbierte gedruckte Originalversion dieser Diplomarbeit ist an der TU Wien Bibliothek verfügbar
The approved original version of this thesis is available in print at TU Wien Bibliothek.
TU Bibliothek WIEN Your knowledge hub

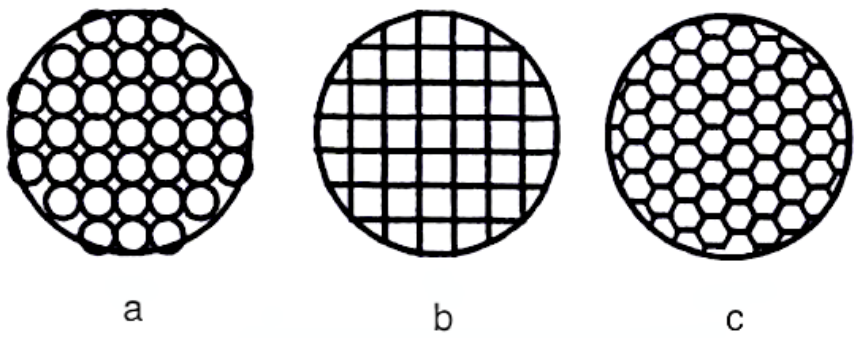

Figure 4.12: Types of honeycomb, [3]

Meshes

For an even better reduction of turbulence and more uniform flow velocity profiles, subsequent meshes or so-called screens should be implemented inside the settling chamber. As well as the honeycomb, they are placed in a low-velocity region of the chamber for lower pressure losses and, therefore, higher wind tunnel speeds [24]. The meshes are usually made out of metal wires interwoven to form a square cross-section and are tacked to the wooden frames, which can be seen in figure 4.11. Research for the best solution of honeycombs and meshes ranges from design principles based on experience to turbulence reduction studies. Regarding the statements of Scheiman and Brooks [30], it is impossible to predict the performance of different meshes consistently, but recommend a series of screens by going from a low to a high mesh size heading towards the contraction section. In addition, they also considered different variations like the use of two identical meshes, a honeycomb plus one screen and even three screens without any honeycomb. However, one honeycomb and two meshes gave the best results in their study, while it is noted that they did not study the use of even more meshes. Barlow [3] stated that the porosity of the screen has an even higher impact on the flow quality and is defined as the ratio between actual flow area and total flow area as

$$\beta_s = \frac{\Omega_{flow}}{\Omega_{tot}}. \tag{4.3}$$

Die approbierte gedruckte Originalversion dieser Diplomarbeit ist an der TU Wien Bibliothek verfügbar
The approved original version of this thesis is available in print at TU Wien Bibliothek.
TU Bibliothek WIEN Your knowledge hub

Mehta and Bradshaw [24] set the best range of porosity between $0.58 \leq \beta_s \leq 0.8$. The porosity can be determnined by,

$$\beta_s = \frac{L_{sc}^2 - 2n_w L_{sc} d_w + n_w^2 d_w^2}{L_{sc}^2} = 1 - 2n_w \frac{d_w}{L_{sc}} + \frac{n_w^2 d_w^2}{L_{sc}^2} = (1 - \frac{n_w d_w}{L_{sc}})^2 \tag{4.4}$$

where L_{sc} describes the width of the settling chamber, n_w the number of wires on one side of the chamber and d_w the thickness of one wire. The area covered by the wire is given by

$$n_w \cdot L_{sc} \cdot d_w + n_w \cdot L_{sc} \cdot d_w - n_w \cdot (n_w \cdot d_w^2) = 2 \cdot n_w \cdot L_{sc} \cdot d_w - n_w^2 \cdot d_w^2. \tag{4.5}$$

The opinions differ a lot for the determination of the distance between the screens. Mehta and Bradshaw [24] stated that the spacing between the meshes should be such that the static pressure is fully recovered from the interference with the respective mesh before reaching the next one. Therefore, they found that a space of about 0.2 times the settling chamber diameter between the meshes works fine. Regarding their study, also the distance from the last screen to the beginning of the contraction cone should be around 0.2 times the settling chamber diameter. Scheiman and Brooks [30] claimed a low impact of turbulence reduction due to higher distances between the screens. There is no question about the increasing boundary layer thickness with longer distance, and unnecessary space between the meshes should be avoided. However, a certain distance is mandatory, and the width of the frames was chosen to be 150 mm. Since three frames with two screens will be used, a distance of 150 mm from the last mesh to the beginning of the contraction section will be assembled. In case of insufficient flow quality, an upgrade with a second main body and, therefore, a settling chamber doubled in length is easily possible afterwards. Regarding all these aspects and the cost factor, two meshes have been chosen, while the first screen after the honeycomb has a 1.4 mm wire spacing, a wire thickness of 0.25 mm with a porosity of 0.72, and the second screen has a 0.8 mm wire spacing, a wire thickness of 0.22 mm, and a porosity of 0.61.

Assembly of the Settling Chamber

In figure 4.11 one can see the exploded view of the settling chamber. As mentioned before, the meshes are tacked to the wooden frames and then stacked on top of each other into the main body, while an edge on the main body prevents them from

Die approbierte gedruckte Originalversion dieser Diplomarbeit ist an der TU Wien Bibliothek verfügbar
The approved original version of this thesis is available in print at TU Wien Bibliothek.
TU Bibliothek WIEN Your knowledge hub

falling out. The frames are easily removable for maintenance or for experimenting with different meshes. Afterwards, two sheets of honeycomb can be push-fitted into the frame while a support bar is mounted in the middle of the third frame for more stability for the honeycomb. The inflow seen in figure 4.11 can then be screwed to the main body while bolting the stand of the settling chamber simultaneously to the main body.

4.3.4 Suction Unit

The suction unit is a necessary component of the wind tunnel to generate airflow inside the system. Different types of turbomachinery can be installed depending on the required flow velocity inside the test chamber and the cross-sectional area. Initially, the use of the radial compressor PGW HL 100 / 50 / 00 owned by the Technical University of Vienna was intended. Unfortunately, this power plant could not generate the required volume flow for a sufficient flow rate inside the test chamber. Therefore, another suction unit needed to be selected.

Axial fans are commonly employed in wind tunnel facilities. The axis of rotation of the propeller runs parallel to the generated airflow, and an example of such a power plant can be seen on the right side in Figure 4.13. With relatively small dimensions, a comparatively high volume flow rate can be generated with axial fans. The lower acquisition costs compared to radial fans is another reason for common use. However, the comparatively low flow velocity generated by axial fans limits this implementation. Such a power plant is also included within the compared wind tunnel by "TecQuipment" in section 5.2. After consultation with their technical department, it was found that their wind tunnel is only capable of wind speeds around 35 m/s inside the test section. A much higher flow velocity can be realised by using radial fans, while an example of such a power plant can be seen on the left side in Figure 4.13.

For the choice of a fan, the required volume flow rate and the pressure losses inside the wind tunnel has to be estimated to reach the desired velocity inside the test chamber. The aim was to reach a velocity inside the test chamber in the range of $50 - 60\ m/s$ in order to be able to test models of wind turbines in a meaningful way. With the help of the continuity equation,

$$\rho_1 \cdot v_1 \cdot A_1 = \rho_2 \cdot v_2 \cdot A_2 \ , \tag{4.6}$$

Die approbierte gedruckte Originalversion dieser Diplomarbeit ist an der TU Wien Bibliothek verfügbar
The approved original version of this thesis is available in print at TU Wien Bibliothek.
TU Bibliothek WIEN Your knowledge hub

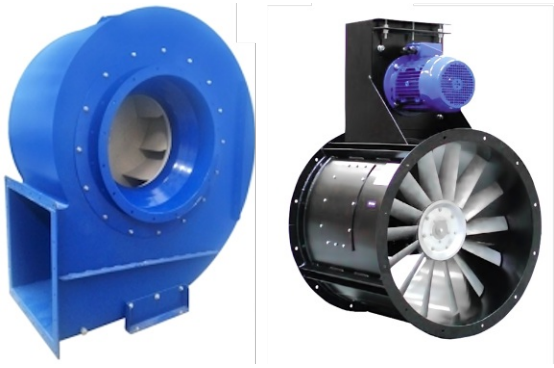

Figure 4.13: Radial Fan vs. Axial Fan, www.htk-vent.at

the required volume flow rate can be computed. In this particular case, index 1 references the variables to the conditions at the test section exit, and index 2 references the variables to the conditions at the diffuser end, which means the intake of the radial fan.

Eq.4.6 simplifies to $v_1 \cdot A_1 = v_2 \cdot A_2$ as we assume a constant density ρ, which be rewritten as $\dot{V}_1 = \dot{V}_2$. Because the cross-section of the test chamber is 0.3249 m^2 and the velocity is required to be between $50 - 60$ m/s, the volume flow rate is approximately $16 - 20$ m^3/s.

When choosing a suitable suction unit, the total pressure is another important factor and can be seen as the sum of $p_{dyn} + p_{stat}$, while p_{dyn} represents the dynamic pressure, and p_{stat} the static pressure. Every obstacle like meshes, the tested model inside the test section and the security grille inside the wind tunnel creates a pressure loss, which has to be overcome by the suction unit. Usually, such pressure losses are estimated, while their impact on the suction unit selection is discussed later. The dynamic pressure is determined by $p_{dyn} = 1/2 \cdot \rho \cdot v^2$, where v represents the flow velocity inside the narrowest cross-section of the system. In this case, this is the required velocity inside the test chamber of 60 m/s. Therefore, the dynamic pressure p_{dyn} is calculated as $1/2 \cdot 1.2 \cdot 60^2 = 2160$ Pa. Losses due to friction can be neglected due to their small contribution.

With the help of the required volume flow rate and total pressure, the selection of a suitable fan can be narrowed down. This is the case when it comes to designing the diffuser in the subsequent chapter 4.3.5 on page 38. There, it becomes clear that an efficient diffuser only allows a maximum wall inclination, which defines the maximum fan size.

Die approbierte gedruckte Originalversion dieser Diplomarbeit ist an der TU Wien Bibliothek verfügbar
The approved original version of this thesis is available in print at TU Wien Bibliothek.
TU Bibliothek WIEN Your knowledge hub

After gathering all this information, a selection of three different variants was made with the help of specialists of the manufacturer "GTG-Gebläsetechnik GmbH" in Vienna and can be seen in the appendix C.2. The final decision fell on the radial fan type $RS1120$ and can be seen in figure 4.14. According to the specification by the manufacturer "GTG-Gebläsetechnik GmbH", the casing is made out of a welded and galvanised sheet metal construction. The cast impeller is made out of cast aluminium, which promises to be highly wear-resistant. In figure 4.15 one can see that a required volume flow rate of $16 - 20\ m^3/s$ can easily be realised with this fan, where the volume flow rate is Q in the datasheet. The specialists at "GTG-Gebläsetechnik GmbH" consider a pressure loss of approximately 100 Pa per Mesh and security grille. With the two meshes and the honeycomb grille inside the settling chamber, a security grille before the suction unit, and the dynamic pressure of 2160 Pa, the fan has to be able to operate within a total pressure of around 2600 Pa. In figure 4.15 one can see that this can be achieved while still having considerable scope to rise.

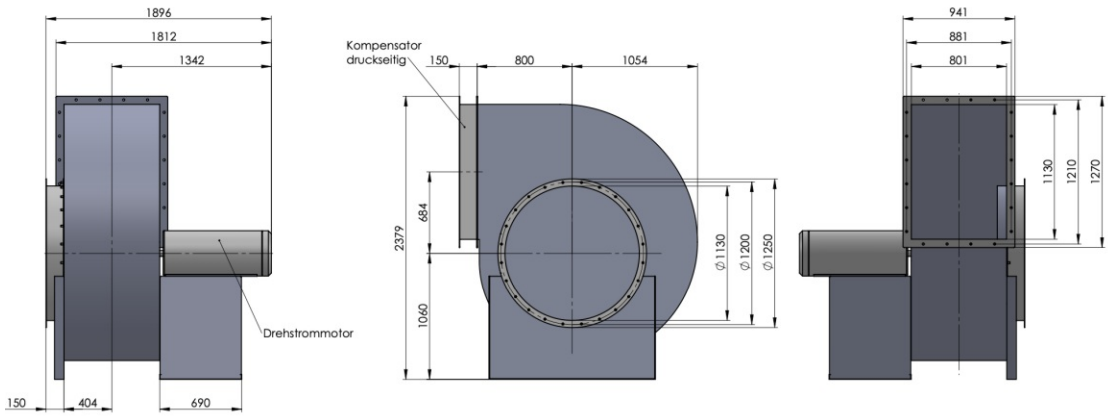

Figure 4.14: Radial Fan RS1120, www.gtg.at

Die approbierte gedruckte Originalversion dieser Diplomarbeit ist an der TU Wien Bibliothek verfügbar
The approved original version of this thesis is available in print at TU Wien Bibliothek.
TU Bibliothek WIEN Your knowledge hub

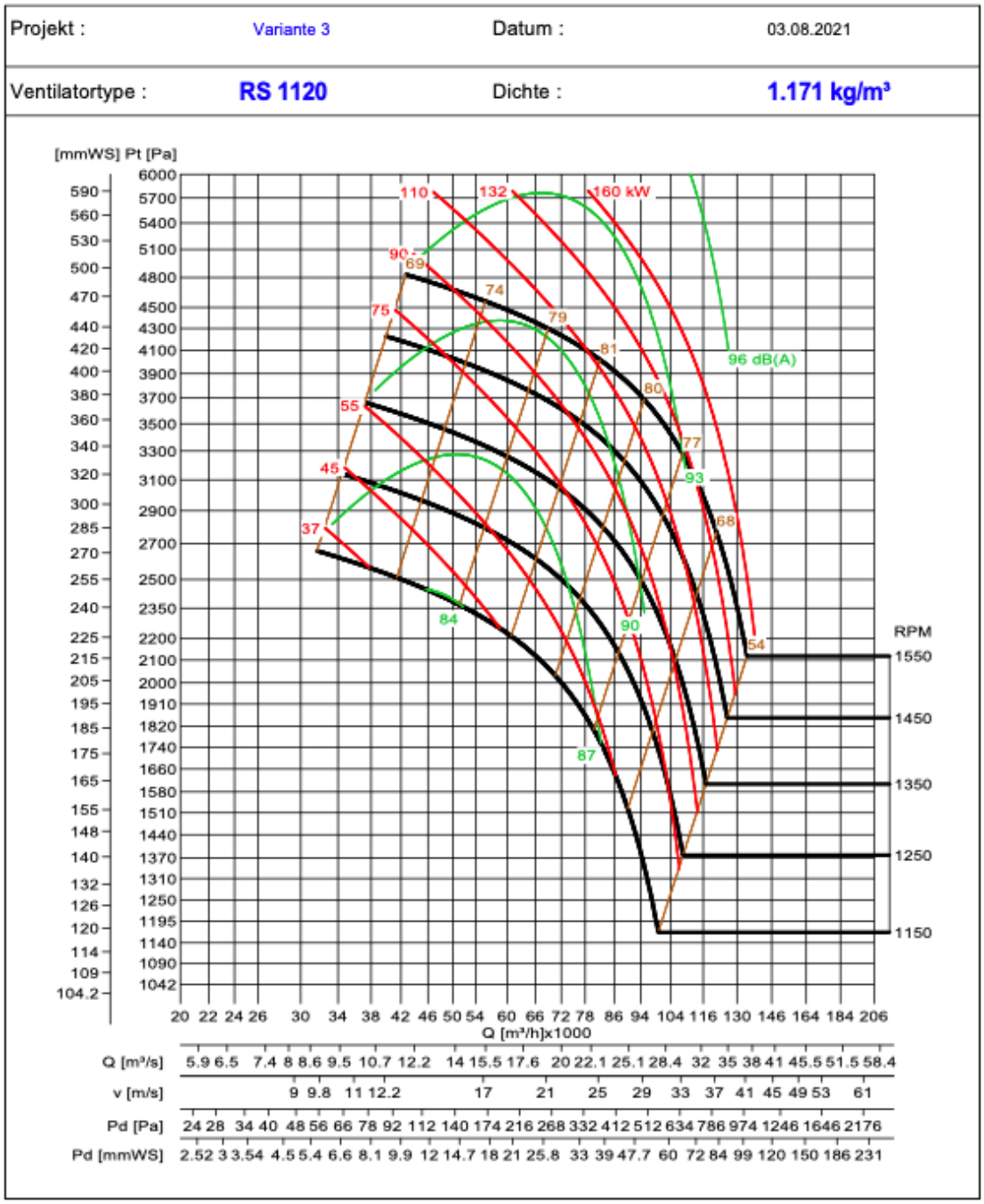

Figure 4.15: Radial Fan Data Sheet, www.gtg.at

Die approbierte gedruckte Originalversion dieser Diplomarbeit ist an der TU Wien Bibliothek verfügbar
The approved original version of this thesis is available in print at TU Wien Bibliothek.

4.3.5 Diffuser

The diffuser is an important wind tunnel component, which is a diverging channel converting kinetic energy into static pressure [27]. In other words, the purpose of the diffuser is to reduce the flow velocity while increasing the pressure with the least energy loss possible [3]. There are diffuser designs for different applications, while the geometry directly affects the flow characteristics and the energy losses inside the diffuser. The two main categories are diffusers with constant cross-section expansion and diffusers with a sudden cross-section expansion. Those types and their subcategories can be seen in figure 4.16 and figure 4.17. In closed-circuit wind tunnel systems, step diffusers are sometimes used [27]. Li et al. [23] stated that a sudden increase in the cross-sectional area leads to turbulent flow, for which reason a diffuser with a gradual expansion was used in this project´s open-circuit wind tunnel.

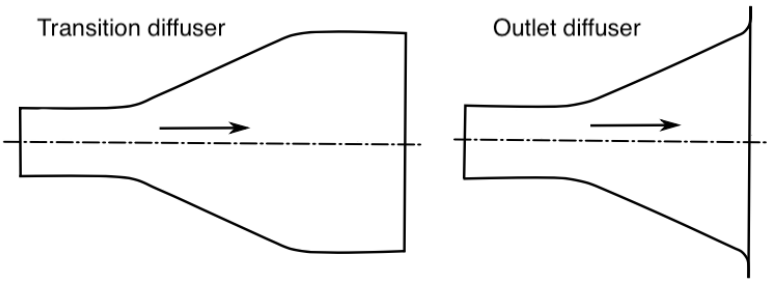

Figure 4.16: Diffuser with constant cross-section expansion, inspired by [27]

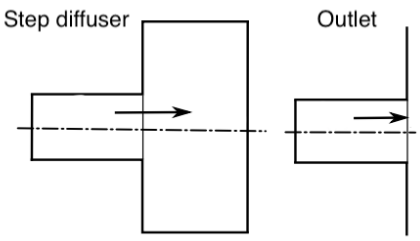

Figure 4.17: Diffuser with sudden cross-section expansion, inspired by [27]

Die approbierte gedruckte Originalversion dieser Diplomarbeit ist an der TU Wien Bibliothek verfügbar
The approved original version of this thesis is available in print at TU Wien Bibliothek.
TU Bibliothek WIEN Your knowledge hub

Since the test section is designed with a rectangular cross-section of 570×570 mm, and the axial ventilator flange has an inner diameter of 1120 mm, the transition diffuser (hereinafter referred to only as a diffuser) acts as a converter from a rectangular to a round cross-section. The transition will be achieved with an opening angle of 2φ which can be seen in figure 4.18.

As mentioned before, the goal is to decelerate the high-velocity flow with low pressure to a flow with low velocity and high pressure. This can be done with an opening angle of 2φ and should be achieved in the shortest possible distance [27].

This leads to the following conflicting claims [27]:

1. A high opening angle with a high rate of diffusion (A_{out}/A_{in}) leads to a higher risk of flow separation at the diffuser wall. Pressure loss, turbulence flow, pulsation, vibration, oscillating fan load and oscillation in test section velocities will occur. This phenomenon can be seen in figure 4.18. Thus, a relative angle, φ, has to be chosen.

2. A small opening angle inevitably leads to a longer channel distance, which raises the boundary layer thickness and friction losses. Apart from this, the cost of material and manufacturing increases.

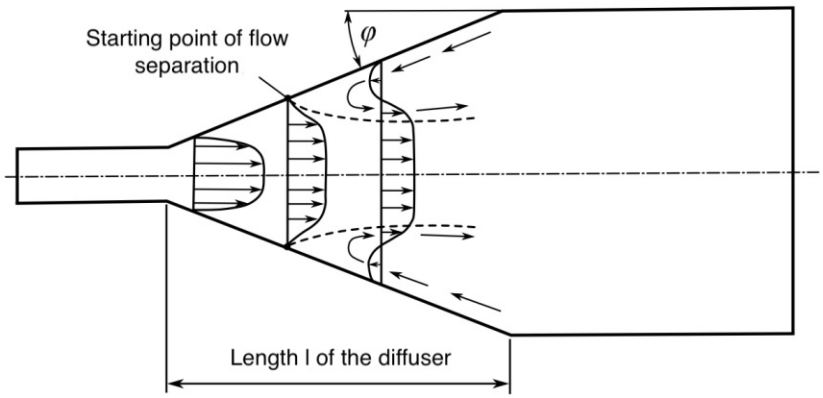

Figure 4.18: Diffuser with opening angle 2φ, inspired by [27]

Diffuser efficiency is sensitive to design errors, and the balancing act between length and angle is the key to an efficient diffuser. Since the definition of flow

Die approbierte gedruckte Originalversion dieser Diplomarbeit ist an der TU Wien Bibliothek verfügbar
The approved original version of this thesis is available in print at TU Wien Bibliothek.
TU Bibliothek WIEN Your knowledge hub

separation is subjective and, to a certain extent, arbitrarily, as Paßmann [27] states, many research studies have dealt with this issue. For example, Dixon and Hall [12] advise for an axial symmetric diffuser with an efficient pressure recovery at an opening angle of $2\varphi = 7°$ to $8°$. Mehta and Bradshaw [24] claimed that a diffuser for a low-speed wind tunnel works best with an expansion angle, 2φ, of $5°$ and $10°$ and a maximum ratio of cross-sectional areas of 2.5. Another example is the recommendation by Barlow et al. [3] stating that the opening angle of 2φ should be less than $7°$. The opinions in open literature differ, and therefore, a CFD-Simulation should assist.

In figure 4.23, the designed diffuser can be seen, which has an opening angle of $2\varphi = 7°$ and a ratio of cross sectional areas of $A_{out}/A_{in} = 3$. Due to economic reasons, the wall thickness was chosen to be 2 mm while a flange thickness of 4 mm is selected. The technical drawings can be seen in appendix B.1, while the results of the CFD simulation can be seen in section 4.4.6.

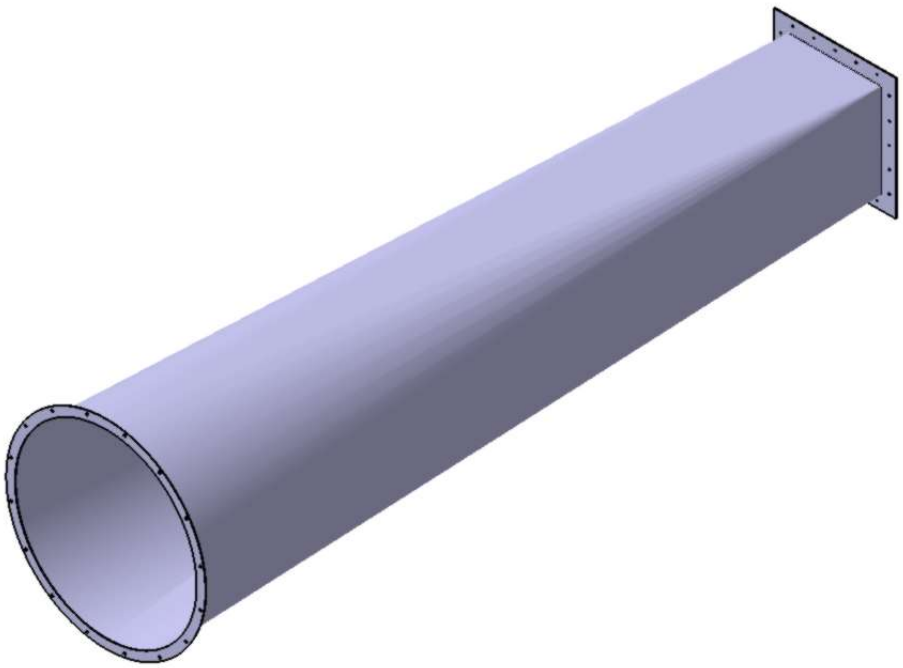

Figure 4.19: Diffuser

Die approbierte gedruckte Originalversion dieser Diplomarbeit ist an der TU Wien Bibliothek verfügbar
The approved original version of this thesis is available in print at TU Wien Bibliothek.
TU Bibliothek WIEN Your knowledge hub

4.4 CFD Simulation of the Wind Tunnel

4.4.1 Introduction

With the help of computational fluid dynamic simulations (CFD), the behaviour of a fluid can be predicted quickly and precisely. The simulation can be carried out early in the design process, and changes to the model can be adapted quickly. Time-consuming and expensive experiments can be avoided in most cases [5]. Therefore, a CFD simulation was used to investigate the occurrence of flow separations in the designed wind tunnel, reaching the required velocity inside the test chamber and overall efficiency. All accomplished and necessary steps of the CFD Simulation are explained in more detail in the following sections.

4.4.2 Modelling the Wind Tunnel

Designing a model of the fluid region and defining any solid that might be present is the first step of the simulation [5]. A helpful software package to generate advanced geometries and meshes, as well as mesh diagnostics, is "ICEM by Ansys". The user can draw the model from scratch directly, or he can import the finished CAD model. In the course of this project, an stl-file of the final wind tunnel was generated and imported into "ICEM" where the result can be seen in figure 4.20. Coloured points, lines, and areas representing the body's geometry are created automatically and can be manipulated.

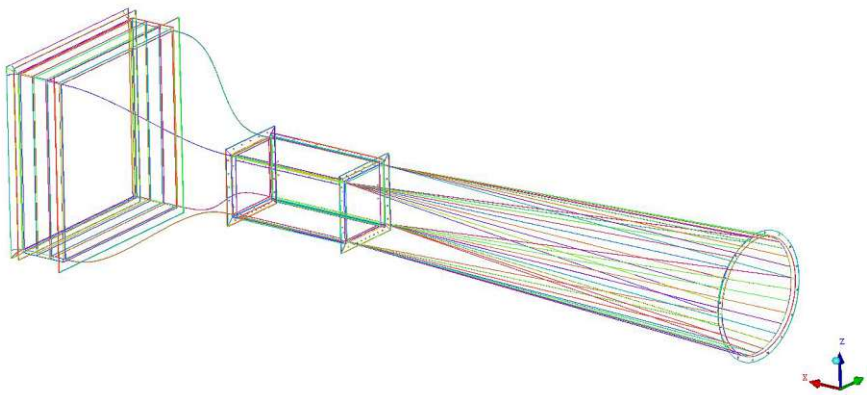

Figure 4.20: Model of the wind tunnel in ICEM

Die approbierte gedruckte Originalversion dieser Diplomarbeit ist an der TU Wien Bibliothek verfügbar
The approved original version of this thesis is available in print at TU Wien Bibliothek.
TU Bibliothek WIEN Your knowledge hub

4.4.3 Meshing / Pre-processing

In the next step, a mesh has to be created. The subsequent calculation uses the software package "Fluent by Ansys", which uses the finite volume method (FVM) when calculating the flow field variables with the mesh elements as the finite volumes [5]. Different mesh classifications like structured, unstructured and hybrid meshes can be applied to the model. An appropriate mesh is essential for an accurate solution, faster convergence and reduction of numerical diffusion [13, 32]. Before a pre-mesh can be generated, so-called "blocks" have to be carved out to picture the inner volume of the wind tunnel. The coloured points and lines from the previous step come into play. So-called "entities" have to be associated with the geometry of the wind tunnel. The final mesh can be seen in figure 4.21. One can observe that the inlet of the wind tunnel looks different to the wall. This is because outlet, inlet, as well as a solid have to be defined before the boundary and initial conditions in the next step 4.4.4. The mesh size and the location of its elements determine where the flow field variables are evaluated and the time-based expenditures. Where the flow changes rapidly, a finer mesh is required to obtain higher accuracy, while in areas of flow uniformity, a coarse mesh is sufficient [5]. The total cell number of the final mesh is just below 4000000.

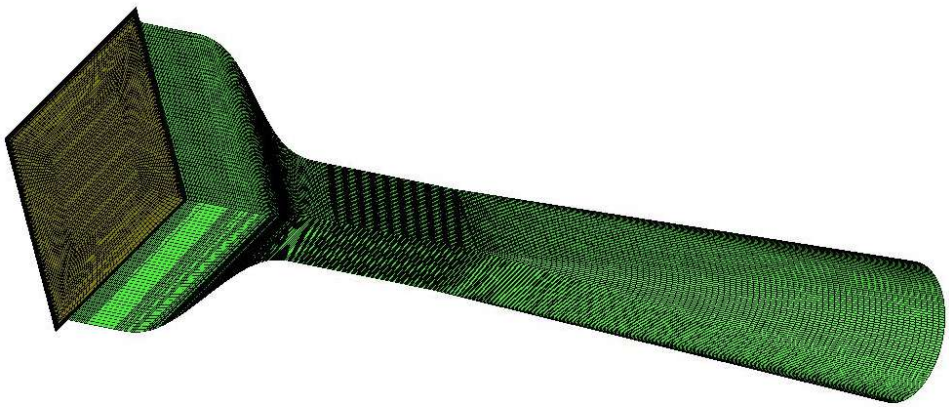

Figure 4.21: Mesh of the wind tunnel in ICEM

Die approbierte gedruckte Originalversion dieser Diplomarbeit ist an der TU Wien Bibliothek verfügbar
The approved original version of this thesis is available in print at TU Wien Bibliothek.
TU Bibliothek WIEN Your knowledge hub

4.4.4 Setup, Boundary Conditions and Turbulence Model

Now that the mesh is finished, it can be imported as an msh.-file to "Ansys Fluent", the numerical simulation software. All settings in the tree on the left side have to be adjusted to the particular circumstances. In this case, the flow is modelled using the "Transition SST-model" within the tab "Viscous-Model". This detailed shear-stress transport (SST) $k-\omega$ turbulence model was developed by Menter [25] to effectively blend the robust and accurate formulation of the $k-\omega$ model in the near-wall region with the free stream independence of the $k-\omega$ model in the far-field. This makes the SST $k-\omega$ model more accurate and reliable for a wider class of flows, especially for aerodynamics and turbomachinery at moderate Reynolds numbers [2]. Within the tab "Cell Zone Conditions", air density, specific heat, thermal conductivity, and viscosity have been set to constant values. The preset air density $\rho = 1.225\ kg/m^3$ was adopted. One of the most important settings is selecting the correct boundary conditions, where the inlet, outlet, wall and solid was related to a respective geometry of the mesh and material. The outlet represents the end of the diffuser and the beginning of the suction unit. A more advanced case of operation should be performed when simulating a wind tunnel while still being able to fall back on adequate reserves. In the appendix C.2 one can see that the suction unit is capable of generating an even higher volume flow rate, but with the chosen volume flow rate $\dot{V} = 24\ m^3/s$, a sufficient velocity inside the test chamber can be achieved. The mass flow rate $\dot{m}$ can be easily computed with $\dot{m} = \rho \cdot \dot{V} = 1.225\ kg/m^3 \cdot 24\ m^3/s$. Hence the outlet boundary conditions have been set to a mass flow rate of $\dot{m} = 29.4\ kg/s$. Air from the laboratory environment is drawn into the wind tunnel, whereby the inlet boundary conditions are set to a total gauge pressure of $0\ N/m^2$ and a turbulent intensity of 5%. A stationary wall was set to be the wall boundary condition. In table 4.2, all boundary conditions are summarized.

Inlet Boundary Conditions	Gauge Total Pressure $0\ N/m^2$
Outlet Boundary Conditions	Mass Flow Rate $29.4\ kg/s$
Wall Boundary Conditions	Stationary no-slip Wall

Table 4.2: Boundary Conditions

Die approbierte gedruckte Originalversion dieser Diplomarbeit ist an der TU Wien Bibliothek verfügbar
The approved original version of this thesis is available in print at TU Wien Bibliothek.
TU Bibliothek WIEN Your knowledge hub

4.4.5 Numerical Calculation

Fluid dynamic problems are nonlinear, and only with restrictive assumptions, as seen in the preceding chapter, the problem can be solved analytically. Therefore, the CFD solutions are calculated iteratively and have to be converged. Convergence means arriving at a solution, which is close to the exact solution within some error tolerance. The residual is a fundamental measurement to observe the convergence of an iterative solution. It quantifies the error in the solution of the system of equations and measures the local imbalance of a conserved variable in each control volume. As with the mesh created, the wind tunnel model consists of cells, while each cell has its residual value for each of the equations solved. Since an accurate numerical solution is requested, a low residual value is sought. Generally, a residual level of 10^{-4} characterises a loose convergence, levels of 10^{-5} are considered to be well converged, and levels of 10^{-6} describe an excellent convergence. Especially with complicated problems, it is not always possible to reach residual levels as low as 10^{-6} or even 10^{-5} [22].

Before the calculation can start, the number of iterations needs to be set. The required number of iterations is related to many factors. After some experience with different variants of the wind tunnel like shorter vs. longer diffuser, it was found that a reasonable number of iterations is within the range of 4500 to 5000. When starting the numerical calculation, the flow field must be initialised [2]. After selecting "run calculation", the progress, especially the mapping of the residuals like figure 4.22 should be observed from time to time. If inconsistencies are discovered, an immediate reaction and adjustments to the settings can be taken.

4.4.6 Interpretation / Post-processing

Post-processing can be seen as the result interpretation of the CFD simulation. It is important to proceed conscientiously since design errors, wrong setups, or incorrect adjustments to the boundary conditions can result in misleading outcomes. If that is the case, adjustments to the model design, the mesh, or the settings as described in chapter 4.4.4 can be performed. Even though this means that the cycle starts from the beginning. Visualising and interpreting the results in a precise manner is key to a successful CFD simulation. There are many possibilities to display

Die approbierte gedruckte Originalversion dieser Diplomarbeit ist an der TU Wien Bibliothek verfügbar
The approved original version of this thesis is available in print at TU Wien Bibliothek.
TU Bibliothek WIEN Your knowledge hub

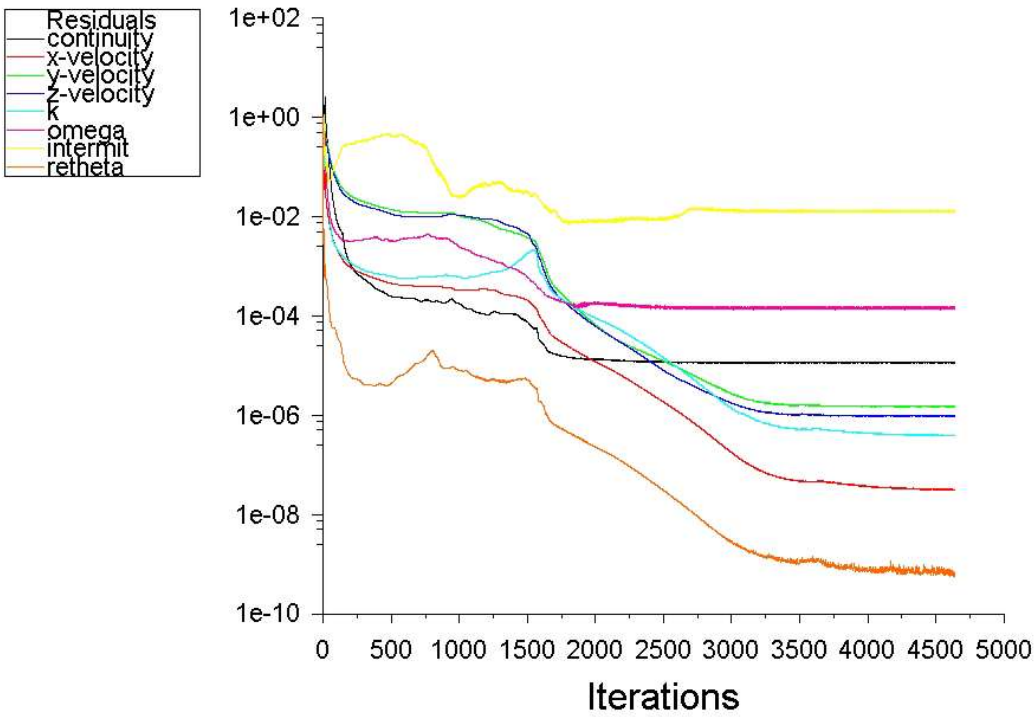

Figure 4.22: Residuals, WT No.3

different values like velocity magnitude, static pressure or turbulence intensity in different views or planes.

The repeating process of simulating and improving the wind tunnel will be discussed in the following. It is noted that all simulated models include the same settling chamber (without the meshes) as discussed in chapter 4.3.3 and the contraction cone as discussed in chapter 4.3.2.

CFD Simulation WT No.1

The first model includes:

- Test section as described in chapter 4.3.1
- Diffuser with a length of 3100 mm as described in section 4.3.5

The simulation of WT No.1 was performed with a coarse mesh to keep the simulation

Die approbierte gedruckte Originalversion dieser Diplomarbeit ist an der TU Wien Bibliothek verfügbar
The approved original version of this thesis is available in print at TU Wien Bibliothek.
TU Bibliothek WIEN Your knowledge hub

time initially as short as possible. It became clear that this setting was insufficient. The intake of the wind tunnel works fine without flow separation, and the velocity inside the test chamber looks satisfying at first sight. The flow pattern along the entire diffuser is not as good as desired. This can be seen in figure 4.23, where the visualised xy-plane sits in the centre of the wind tunnel. As discussed in chapter 4.3.5 flow separation can occur if the opening angle of the diffuser is chosen too large. Another reason for a poor flow quality might be the offset at the test chamber door. Taking a closer look at figure 4.23, it is evident that discontinuities occur at the upper edge of the test section. Therefore, changes to the diffuser and the test section have been made and again simulated separately.

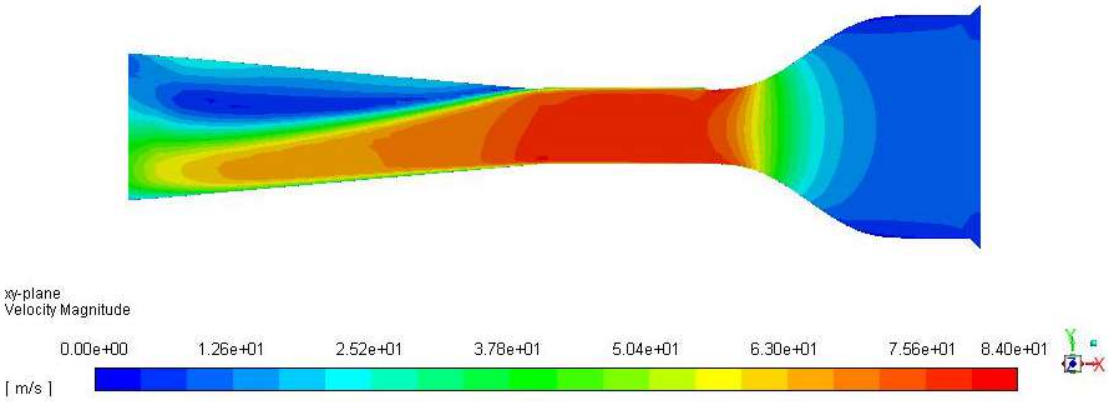

Figure 4.23: Velocity magnitude - wind tunnel No.1

CFD Simulation WT No.2

The second model includes:

- Test section with the offset as described in chapter 4.3.1
- Diffuser with a length of 4500 mm as described in chapter section 4.3.5

Since the large opening angle of the diffuser causes poor flow quality, the diffuser length was increased, and the opening angle was reduced. The exact geometry can be seen in chapter 4.3.5 as well as in the appendix B.1. All the required steps for a CFD simulation discussed from chapter 4.4.2 to chapter 4.4.5 have been executed again while only adjustments to the prior model, i.e. elongation of the diffuser,

Die approbierte gedruckte Originalversion dieser Diplomarbeit ist an der TU Wien Bibliothek verfügbar
The approved original version of this thesis is available in print at TU Wien Bibliothek.
TU Bibliothek WIEN Your knowledge hub

had to be made. For a better comparison of the different cases, the illustration of the velocity magnitude was done with the same settings as WT No.1. Flow separation in the diffuser still exists, but the flow contours along the upper edge of the diffuser have improved. Nevertheless, the velocities at the diffuser outlet are not uniform. Therefore, the impact of the door offset at the test section was next to be investigated.

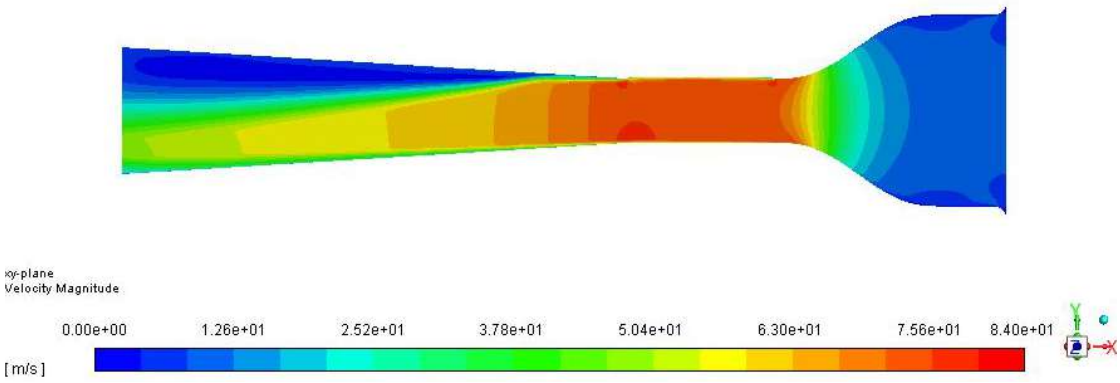

Figure 4.24: Velocity magnitude - wind tunnel No.2

CFD Simulation WT No.3

The third and final model includes:

- Test section without the offset as described in chapter 4.3.1
- Diffuser with a length of 4500 mm as described in section 4.3.5

The effects of the offset at the test section as described in chapter 4.3.1 is now investigated. Therefore, the improved model of chapter 4.3.1 is integrated and the mesh is applied as seen in figure 4.25

After keeping the boundary conditions as described in table 4.2 and the number of iterations to 5000, the solution was satisfying with the improved test section. The residuals, shown in figure figure 4.22, demonstrate that the simulation can be considered to be well converged. Figure 4.26 shows that the velocity magnitude distribution at the xy-plane is satisfying since no significant variations or distortions can be discovered inside the test chamber. An increasing but symmetrical flow

Die approbierte gedruckte Originalversion dieser Diplomarbeit ist an der TU Wien Bibliothek verfügbar
The approved original version of this thesis is available in print at TU Wien Bibliothek.
TU Bibliothek WIEN Your knowledge hub

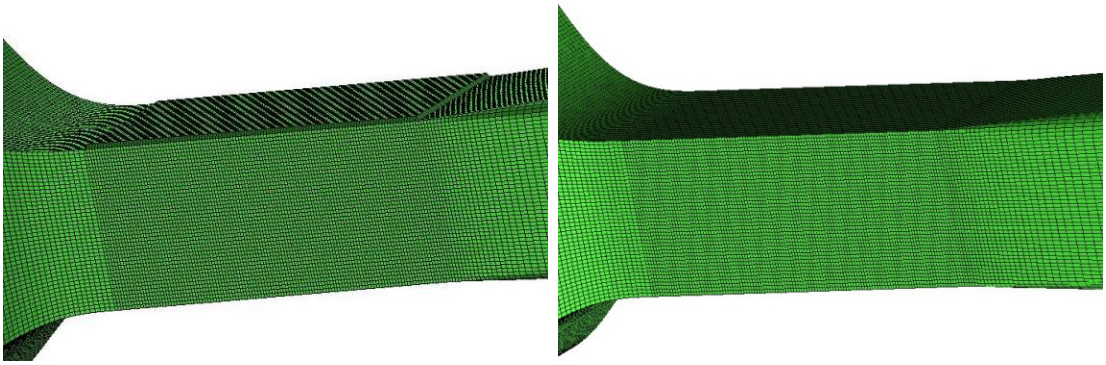

(a) Door with offset (b) Door without offset

Figure 4.25: Change to the mesh from (a) to (b)

velocity change is present throughout the diffuser in contrast to the inefficient figure 4.24, where asymmetrical flow separation occurs. An even longer diffuser could be integrated to prevent flow separation completely, but this would elongate the whole wind tunnel to unportable dimensions. Apart from spatial considerations, the velocity pattern inside the test chamber looks perfect, and the required velocity of 60 m/s is reached easily. Figure 4.28 confirms the good flow quality inside the test chamber because of the equally distributed pattern of velocity. The same confirms figure 4.29 since in the centre of the test section, the turbulence intensity approaches zero. High turbulence levels occur only near the walls, which is impossible to prevent.

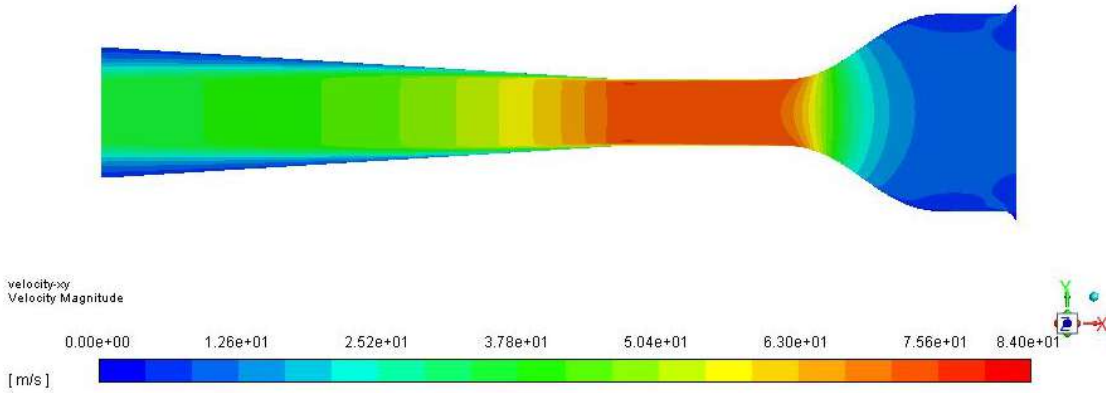

Figure 4.26: Velocity magnitude - wind tunnel No.3

Die approbierte gedruckte Originalversion dieser Diplomarbeit ist an der TU Wien Bibliothek verfügbar
The approved original version of this thesis is available in print at TU Wien Bibliothek.
TU Bibliothek WIEN Your knowledge hub

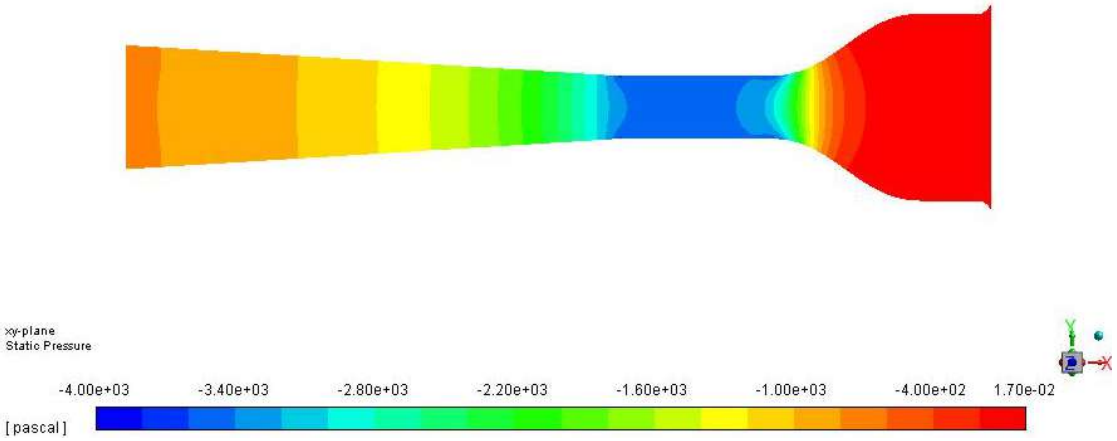

Figure 4.27: Static Pressure - wind tunnel No.3

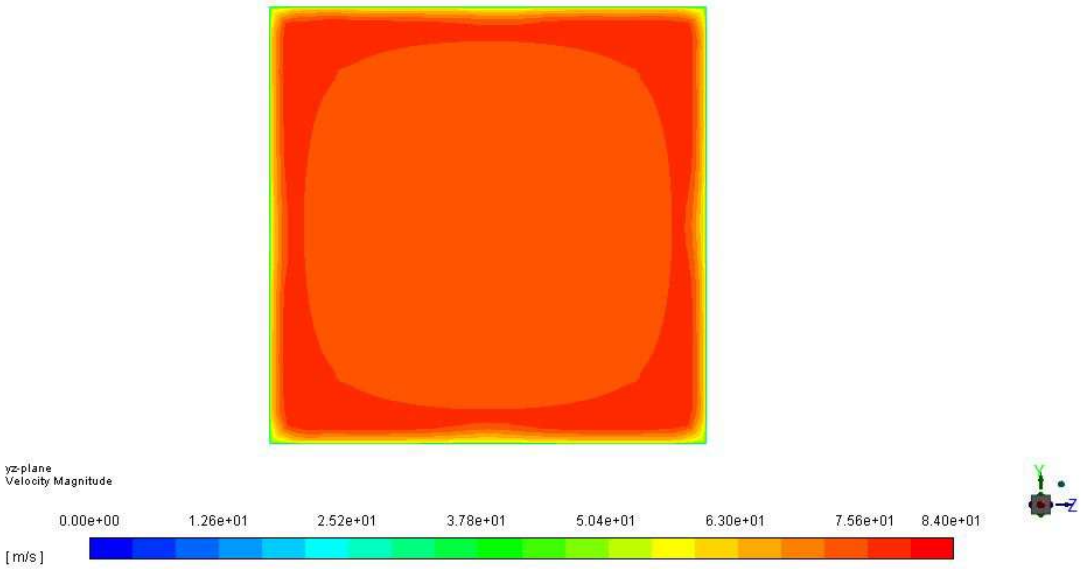

Figure 4.28: Velocity magnitude, yz-plane in test section - wind tunnel No.3

Die approbierte gedruckte Originalversion dieser Diplomarbeit ist an der TU Wien Bibliothek verfügbar
The approved original version of this thesis is available in print at TU Wien Bibliothek.

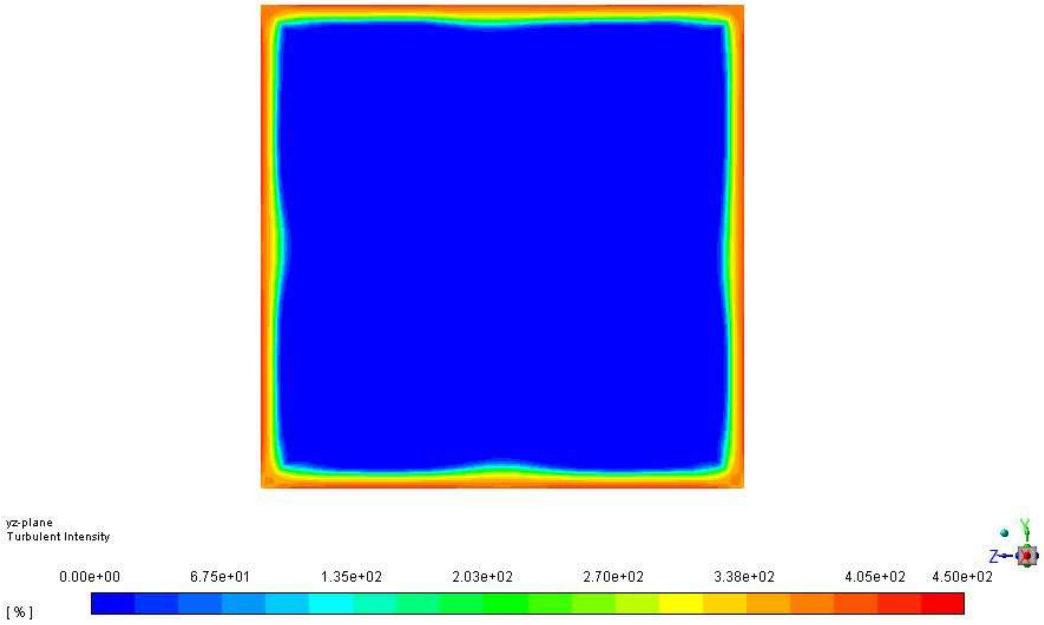

Figure 4.29: Turbulence intensity, yz-plane in test section - wind tunnel No.3

Die approbierte gedruckte Originalversion dieser Diplomarbeit ist an der TU Wien Bibliothek verfügbar
The approved original version of this thesis is available in print at TU Wien Bibliothek.

Die approbierte gedruckte Originalversion dieser Diplomarbeit ist an der TU Wien Bibliothek verfügbar
The approved original version of this thesis is available in print at TU Wien Bibliothek.
TU Bibliothek WIEN Your knowledge hub

Chapter 5

Statement of Costs

5.1 Introduction

An efficient wind tunnel facility for academic education and scientific research projects is a costly investment. Acquisition costs, maintenance costs, and operation costs must be included in the decision, whereby the acquisition costs make up the largest share. These funds must be founded through FFG, a national funding agency for research and development in Austria. Since complete wind tunnel facilities can be purchased, a comparison between one of them and the wind tunnel system developed within this thesis can be seen in the following.

5.2 Wind Tunnel by TecQuipment

With around sixty years of experience, TecQuipment designs, manufactures and supplies products for the global engineering educational market. They offer a wide range of technical products, including different sizes of wind tunnel systems. Based on the same requirements as for the developed wind tunnel, a quotation was requested for one of their biggest wind tunnel with a test section size of $600 \times 600 \times 1250\ mm$, which can be seen in figure 5.1.

Figure 5.1: Wind Tunnel by TecQuipment, www.tecquipment.com

After consultation with an employee of TecQuipment it became clear that it is not possible to purchase separate parts of their wind tunnel. Therefore only the complete system can be ordered at a price of 129, 087 GBP, which is around 152, 293 € with the current exchange rate. The included services can be seen in figure 5.2 while the complete quotation is displayed in appendix C.

TECQUIPMENT

Date: 07 July 2021
PROFORMA INVOICE/QUOTATION NO: Q00034696
AF1600S

	Delivery address:
Mr. Bernard Kunitzky **TU Vienna** Schuttelstrasse 27/21 Vienna 1020 Austria	Same as Invoice address

Your Ref: Our Ref: Q00034696

Total cost of goods	GBP	124,440.00
FCA (Including Packing)	GBP	3,520.00
Road Freight	GBP	1,127.00
Total price: DAP(R-PL) Vienna Austria. Incoterms ® 2020	**GBP**	**129,087.00**

Figure 5.2: Quotation by TecQuipment

Die approbierte gedruckte Originalversion dieser Diplomarbeit ist an der TU Wien Bibliothek verfügbar
The approved original version of this thesis is available in print at TU Wien Bibliothek.
TU Bibliothek WIEN Your knowledge hub

5.3 Costs of the Developed Wind Tunnel

As mentioned multiple times within this thesis, costs were taken into consideration in every single choice made. However, a well working and effective wind tunnel system require an investment which can be seen in the following sections.

5.3.1 Power Plant / Suction Unit

For the technical design of the wind tunnel and the dimensions of the diffuser, a power plant manufactured by the company GTG-Gebläse was chosen. After consultation with their specialists, three different variations have been taken into consideration, while the quotations associated with them are shown in appendix C.2. All of them include a radial fan instead of the most common used axial fan. Such a power plant, where the fan axis is parallel to the flow, is also included within the wind tunnel by TecQuipment in section 5.2. After consultation with their technical department, it was found that their wind tunnel is only capable of flow speeds around 35 m/s inside the test section. The velocities inside the test section of the designed wind tunnel within this work shall reach 60 m/s. Such high velocities can only be achieved with the help of radial fans. In appendix C.2, one can see three different suction units with the different speeds achievable inside the test chamber. In the end, variant number three was chosen, and the quotation belonging to it can be found in figure 5.3. A price difference between those three variations can undoubtedly be seen. However, the slightly higher investment for the most powerful ventilator is worth it because more representative flow conditions can be achieved in this wind tunnel. The final cost of the chosen power plant is 23.274, 00 €.

Die approbierte gedruckte Originalversion dieser Diplomarbeit ist an der TU Wien Bibliothek verfügbar
The approved original version of this thesis is available in print at TU Wien Bibliothek.
TU Bibliothek WIEN Your knowledge hub

GTG Gebläsetechnik Ges. m. b. H.
Perfektastrasse 79
A-1230 Wien
Firmenbuch: FN 279 638 h

Telefon: +43 1 603 58 19
Telefax: +43 1 600 77 19
e-mail: gtg@gtg.at
DVR Nr.: 101 39 47

BIC: RLN WAT WW
IBAN: AT93 3200 0000 0661 0802
Steuer Nr.: 092/1842
UID-Nr.: ATU 626 31 655

GTG
Gebläsetechnik Ges. m. b. H.

3			**Variante 3 - 60 m/s - 90 kW:**		
3.1	1	Stk.	Radialventilator RS 1120 RI - 90 kW	12.318,00	12.318,00
3.2	1	Stk.	Rohrschalldämpfer SIL-1120-2	3.654,00	3.654,00
3.3	1	Stk.	Frequenzumformer 90 kW	7.302,00	7.302,00
			Summe Variante 3 - 60 m/s - 90 kW:		**23.274,00**

Figure 5.3: Quotation Suction Unit by GTG-Gebläsetechnik, www.gtg.at

5.3.2 Components to be Manufactured

After consultation with employees of the Vienna University of Technology laboratory, a well-known manufacturer called "Innoweld-Metallverarbeitung GmbH" was recommended, since there have been quite a few cooperations in the past. The goal was to keep the production costs as low as possible by having a strong and robust construction throughout the whole wind tunnel and having solid corrosion resistance. Therefore the offer includes a coated version (material short cut: S235JR) and one version made of stainless steel (material short cut: 1.4301 2B). At the beginning of the design process, the expertise of "Innoweld" regarding the thickness of the material was consulted.

The complete quotation can be seen in appendix C.3, while every component with its prices is listed in the following. The final costs of the chosen manufactured components, including setup- and shipping costs, are listed in section 5.3.2.

Die approbierte gedruckte Originalversion dieser Diplomarbeit ist an der TU Wien Bibliothek verfügbar
The approved original version of this thesis is available in print at TU Wien Bibliothek.
TU Bibliothek WIEN Your knowledge hub

Settling Chamber

As seen in appendix B.1, the settling chamber consists of the main body, an inflow profile, and the rack for the settling chamber. Every price including the different Materials can be seen in figure 5.4.

Menge	MEH	Bezeichnung	Preis	Gesamt EUR
1,00	STK	Laserzuschnitt Zg.Nr.: Settling Chamber inflow S235JR gekantet mit Folgebügen, geschweißt inkl. Beschichtung	1.136,36	1.136,36
1,00	STK	Laserzuschnitt Zg.Nr.: Settling Chamber inflow 1.4301 2B gekantet mit Folgebügen, geschweißt	1.126,16	1.126,16
1,00	STK	Laserzuschnitt Zg.Nr.: Settling Chamber Korpus S235JR gekantet, geschweißt inkl. Beschichtung	2.047,40	2.047,40
1,00	STK	Laserzuschnitt Zg.Nr.: Settling Chamber Korpus 1.4301 2B gekantet, geschweißt	2.059,00	2.059,00
2,00	STK	Formrohrrahmen geschweißt 50x50x3mm Zg.Nr.: Rack für Settling Chamber S235JR / 3,00 mm inkl. Löcher, geschweißt, Oberfläche roh	295,00	590,00

Figure 5.4: Quotation Settling Chamber

Die approbierte gedruckte Originalversion dieser Diplomarbeit ist an der TU Wien Bibliothek verfügbar
The approved original version of this thesis is available in print at TU Wien Bibliothek.
TU Bibliothek WIEN Your knowledge hub

Contraction Cone

As seen in appendix B.1, the contraction cone has no discrete rack since it is directly screwed to the settling chamber on one side and to the test chamber on the other. Two different materials are listed again in figure 5.5.

Menge	MEH	Bezeichnung	Preis	Gesamt EUR
1,00	STK	Laserzuschnitt Zg.Nr.: ContractionCone S235JR gekantet/gerollt, geschweißt inkl. Beschichtung	1.937,15	1.937,15
1,00	STK	Laserzuschnitt Zg.Nr.: ContractionCone 1.4301 2B gekantet/gerollt, geschweißt	2.075,61	2.075,61

Figure 5.5: Quotation Contraction Cone

Test Section

The test section consists of many components made out of bare steel profiles as seen in appendix B.1. The price for the frame of the test section as well as for the rack can be seen in figure 5.6

Menge	MEH	Bezeichnung	Preis	Gesamt EUR
1,00	STK	Formrohrrahmen geschweißt 50x50x3mm Zg.Nr.: Rack für Test Section S235JR / 3,00 mm inkl. Löcher, geschweißt, Oberfläche roh	390,00	390,00
1,00	STK	Laserzuschnitt Zg.Nr.: Test Section S235JR / 5,00 mm gekantet, geschweißt, inkl. Senkungen, inkl. Gewinde, inkl. Schrauben, Oberfläche roh	649,26	649,26

Figure 5.6: Quotation Test Section

Die approbierte gedruckte Originalversion dieser Diplomarbeit ist an der TU Wien Bibliothek verfügbar
The approved original version of this thesis is available in print at TU Wien Bibliothek.
TU Bibliothek WIEN Your knowledge hub

Diffuser

As seen in appendix B.1, the diffuser has no discrete rack since it is directly screwed to the test chamber on one side and to the suction unit on the other. Two different materials and prices for the diffuser are listed in figure 5.7.

Menge	MEH	Bezeichnung	Preis	Gesamt EUR
1,00	STK	Laserzuschnitt Zg.Nr.: Diffuser S235JR gekantet mit Folgebügen, geschweißt inkl. Beschichtung	4.176,85	4.176,85
1,00	STK	Laserzuschnitt Zg.Nr.: Diffuser 1.4301 2B gekantet mit Folgebügen, geschweißt	4.746,22	4.746,22

Figure 5.7: Quotation Diffuser

Final Costs of the Manufactured Components

If choosing the coated steel version (material short cut: S235JR) over the stainless steel components (material short cut: 1.4301 2B), it would lead to a saving of 710 €. However, the durability of stainless steel is the main reason why the decision has been made in favour of the slightly higher priced version as seen in table 5.1.

Component	Price
Settling chamber inflow	1126.16 €
Settling chamber housing	2059.00 €
Settling chamber rack	590.00 €
Contraction cone	2075.61 €
Test section framework	649.26 €
Test section rack	390.00 €
Diffuser	4746.22 €
	11636.25 €

Table 5.1: Costs of the Manufactured Components

Die approbierte gedruckte Originalversion dieser Diplomarbeit ist an der TU Wien Bibliothek verfügbar
The approved original version of this thesis is available in print at TU Wien Bibliothek.
TU Bibliothek WIEN Your knowledge hub

5.3.3 Prefabricated Parts

Meshes

As mentioned in section 4.3.3, the meshes for the settling chamber need to have a particular porosity. Not many manufacturers can deliver such precise dimensions. One of them is Jaera GmbH., while their quotation for two suitable meshes can be seen in figure 5.8 as well as in the appendix C.4. In each case, 2 running meters are needed since they are sold with a width of 1.3 m. In total the cost for the meshes are 502 €.

Pos.	Bezeichnung	Menge	Lieferzeit	Preis pro.	Preis ges.
1	Drahtgewebe aus Edelstahl 1.4301 Rollenware Maschenweite : 0,8 mm Drahtstärke : 0,22 mm Breite : 1300 mm Gewicht / lfdm.: 0,6 kg // Durchlass: 61,5 %	1 lfdm.	aus freibl. Vorrat	133,00 €	133,00 €
2	Drahtgewebe aus 1.4301 Rollenware Maschenweite : 1,4 mm Drahtstärke : 0,25 mm Breite : 1000 mm Gewicht / lfdm.: 0,48 kg // Durchlass: 72 %	1 lfdm.	aus freibl. Vorrat	118,00 €	118,00 €

Figure 5.8: Quotation Meshes

T-Profile for Settling Chamber

A T-profile is needed for better support for the two plates of honeycomb grid inside the settling chamber. This component can be purchased at any length, while the price per kilogram for the dimensions of $35 \times 35 \times 4.5$ mm is 197.2 €. In this case, the manufacturer Posamentir GmbH. was chosen. For a length of 1740 mm and a weight of around 4.3 kg (DIN 1026 S235JRG2), this results in 8.5 € material costs plus 11 € charges for cutting expenditures. The respective quotation can be seen in the appendix C.4.

Honeycomb

Also, the honeycomb grid needs to have certain dimensions. Schöftner Technik GmbH. is one of the few manufacturers who can deliver the required quality. The quotation for a suitable honeycomb grid can be seen in figure 5.9 as well as in the

Die approbierte gedruckte Originalversion dieser Diplomarbeit ist an der TU Wien Bibliothek verfügbar
The approved original version of this thesis is available in print at TU Wien Bibliothek.
TU Bibliothek WIEN Your knowledge hub

appendix C.4. It should be mentioned that 150 € have to be budgeted extra for such delicate freight. Thus, the total cost of the honeycomb are 691.20 €.

Art. Nr.	Beschreibung	Menge	Einzelpreis	Steuern	Betrag
	Aluminium Honeycomb Core - expandiert Werkstoff: Alu 3000, 50µ, mikro-perforiert Zellgröße: ø6,35mm, 54kg/m³ Abmessungen (expandiert): 2500×1250mm Dicke/Höhe: 35mm	2 Stk.	203,0000	USt 20%	406,00 €
	Zuschnitt auf 1740×870	1,00	0,0000		0,00 €
	Verpackung	1,00	45,0000	USt 20%	45,00 €
				Netto:	**451,00 €**
				Steuern:	**90,20 €**
				Gesamt:	**541,20 €**

Zahlungsbedingungen:
Vorauskasse

Toleranz Dicke: +-0,2mm

Figure 5.9: Quotation Honeycomb

Frames for Meshes

The meshes inside the settling chamber are tacked to a frame made out of MDF. The price per square meter of this material with a thickness of 20 mm is usually around 15 €/m^2. In total 3.2 m^2 of MDF are needed. With a waste due to cutting of around 10 Percent, 3.5 m^2 should be calculated, bringing this component to a cost of 52.5 €.

Acrylic Glas

Vibrations inside the test chamber are expected, for which reason the thickness of the acrylic glass panels was chosen to be 15mm. Such thick panels are expensive,

Component	Price
Door 1280 × 660 mm	211.93 €
Upper/Lower Window 1300 × 585 mm	382.38 €
Back Window 1300 × 570 mm	186.40 €
	780.71 €

Table 5.2: Costs of Acrylic-Glas

Die approbierte gedruckte Originalversion dieser Diplomarbeit ist an der TU Wien Bibliothek verfügbar
The approved original version of this thesis is available in print at TU Wien Bibliothek.
TU Bibliothek WIEN Your knowledge hub

and cut-offs should be avoided. One manufacturer where pre-cut panels can be ordered is Nordic Panel GmbH. The prices for each component can be seen in table 5.2 while the quotation can be found in appendix C.4.

Small Parts

The costs of all small parts, such as fastening components, are listed in table 5.3. It should be noted that this list can be seen as a reference point while, in some cases, a higher price may result. Minimum purchase quantities represent a cost uncertainty, e.g. for knurled screws, at least 100 pieces must be ordered. However, the respective quotation can be seen in the appendix C.4.

Component	Quantity	Price
Hexagon head screw DIN 933 - M10×20	70	27.58 €
Hexagon head screw DIN 933 - M10×70	10	8.03 €
Hexagon nut DIN 934 - M10	80	30.56 €
Metal Washer UNI 1739 - 10×1.5	160	16.72 €
Knurled screw DIN 464 - M5×18	8	64.48 €
Packaging, shipping, taxes		38.40 €
Handles	2	7 €
Retractable levelling caster	8	163.18 €
		355.95 €

Table 5.3: Costs of Small Part

Die approbierte gedruckte Originalversion dieser Diplomarbeit ist an der TU Wien Bibliothek verfügbar
The approved original version of this thesis is available in print at TU Wien Bibliothek.
TU Bibliothek WIEN Your knowledge hub

Final Costs of the Prefabricated Parts

The final costs of all prefabricated parts is listed in table 5.4.

Component	Price
T-Profile for Settling Chamber	19.50 €
Meshes	502.00 €
Honeycomb	691.20 €
Acrylic Glas	780.71 €
Frames for Meshes	52.5 €
Small Parts	355.95 €
	2401.86 €

Table 5.4: Costs of the Prefabricated Parts

Die approbierte gedruckte Originalversion dieser Diplomarbeit ist an der TU Wien Bibliothek verfügbar
The approved original version of this thesis is available in print at TU Wien Bibliothek.
TU Bibliothek WIEN Your knowledge hub

5.3.4 Costs for Assembly

Since many different manufacturers are involved in providing all wind tunnel components, the assembly represents another challenge. As already mentioned, this wind tunnel facility shall be set up in the laboratory for the Institute of Energy Systems and Thermodynamics at the Vienna University of Technology. Therefore, the expected number of hours needed to set up the wind tunnel and the expected hourly wage were estimated. It is assumed that two persons are needed for the assembly, requiring approximately 20 hours. The total costs for assembly amounted to 3000€.

5.3.5 Costs of the complete Wind Tunnel

The final costs of the complete wind tunnel can be seen in table 5.5, where all the main cost factors are listed. The suction unit represents the largest share, but the expensive radial fan is needed to reach the required velocity inside the test chamber. The manufactured components have the second biggest share, but the opportunities to save further costs, such as different materials or smaller material thickness, already have been heavily maxed out. The share of the prefabricated parts is the smallest, while some minor savings are possible because some of the parts may already be in possession of the laboratory. The costs for assembly are challenging to predict and not easy to reduce because the assembly has to be performed by skilled employees who can deal with difficulties during the assembly process.

Component	Price
Suction Unit	23274.00 €
Manufactured Components	11636.25 €
Prefabricated Parts	2401.86 €
Assembly Costs	3000.00 €
	40312.11 €

Table 5.5: Costs of the complete Wind Tunnel

Die approbierte gedruckte Originalversion dieser Diplomarbeit ist an der TU Wien Bibliothek verfügbar
The approved original version of this thesis is available in print at TU Wien Bibliothek.
TU Bibliothek WIEN Your knowledge hub

Die approbierte gedruckte Originalversion dieser Diplomarbeit ist an der TU Wien Bibliothek verfügbar
The approved original version of this thesis is available in print at TU Wien Bibliothek.
TU Bibliothek WIEN Your knowledge hub

Chapter 6

Conclusions and Outlook

Wind tunnel facilities are essential and indispensable appliances because the results of aerodynamic experiments are fundamental for research and development within wind energy harvesting. To purchase a complete wind tunnel unit is convenient with all the available features from a well-known manufacturer. With such a purchase, the wind tunnel will work fine together with all the instruments and software. If not, customer support would deal with the upcoming issues. The possibility of guarantee claims is also attractive for companies and universities. However, the high price constitutes a disadvantage. Further, how well the essential parts, i.e. the contraction cone and diffuser, are designed remains unknown because the manufacturer will not provide any information about flow separation and inefficiencies of the system. Another disadvantage is that the whole unit has to be purchased, and if certain parts, like the suction unit or monitoring tools, already exist, it is not possible to buy only individual parts.

A wind tunnel, especially for the Vienna University of Technology, was developed in this work, realising a cost-effective possibility for aerodynamic tests for wind turbine models. The fundamentals of energy generation through wind power and modelling of wind turbines have been discussed for a better understanding of the matter. The main aim of this work was the detailed development of a wind tunnel. Each part was designed as efficient and cost-effective as possible. Multiple simulations have shown the weaknesses of tunnel components and were then improved until the simulation results have been satisfying. After listing the costs of each component and the assembly, the decision whether to buy a complete wind tunnel from a manufacturer as listed in section 5.2 or to construct a wind tunnel as designed

within this thesis project becomes more apparent. It should be pointed out once more that a complete wind tunnel, like the one in section 5.2, costs around 152,000 € including instruments. The wind tunnel developed within this thesis work costs around 40,000 € while observation instruments with all the required electronics are not included. However, with the tremendous price gap of around 110,000 € between those two variants, it can be assumed that even the priciest instruments for flow observation and mountings can be added while still saving costs by choosing not to buy a complete wind tunnel facility. When designing a wind tunnel, it is advisable to start with the part where the investigated body of interest will be observed. As in this study, the test chamber has to be the first section developed since its geometry significantly influences both upstream and downstream parts. Also, the demanded flow velocity inside the test section is crucial for the technical specifications and size of the suction unit. Therefore, precise requirements for using the wind tunnel simplify the right choice of a sufficient suction unit. Within this project, three different power plants have been taken into consideration. Initially, the existing radial compressor owned by the Vienna University of Technology was intended to be used but could not generate the demanded volume flow rate. Because companies mostly use axial fans for open circuit wind tunnel facilities, it was sought to implement an axial suction unit for financial reasons. Finally, a radial fan was chosen because a relatively high flow velocity was required. That drastically increases the costs, but it is noted that the demanded flow velocity inside the test section is twice as high as achieved by the reference wind tunnel of a well-known company. After choosing the final suction unit, the diffuser shall be designed wisely since its design is substantially for the overall efficiency of the wind tunnel. As seen in this work, only minor changes to the diffuser matter significantly to flow separation and, therefore, to the efficiency of this critical part. Then the contraction cone with the precedent settling chamber was designed. The flow simulation confirmed the efficient design of the contraction cone based on Bell and Mehta´s[24] polynomial as well as the efficiency of the whole wind tunnel.

Subsequently to this work, attachment parts like pitot-tubes and other observation instruments could be selected. If a quick implementation of wind tunnel models inside the test chamber is sought, a foundation and body for the tower could be designed to fit. If the wind tunnel has been commissioned at the laboratory hall and the sound pollution exceeds a worrying level, a silencer at the suction unit could be implemented, and investigations of power loss could be performed.

Die approbierte gedruckte Originalversion dieser Diplomarbeit ist an der TU Wien Bibliothek verfügbar
The approved original version of this thesis is available in print at TU Wien Bibliothek.
TU Bibliothek WIEN Your knowledge hub

Bibliography

[1] Amrani, D. (2012). A comparative study of sound speed in air at room temperature between a pressure sensor and a sound sensor. *Physics Education 48*, Publisher: IOP Publishing, 65–71.

[2] Ansys, F. ANSYS FLUENT 12.0 Theory Guide - 4.5.2 Shear-Stress Transport (SST) - Model https://www.afs.enea.it/project/neptunius/docs/fluent/html/th/node67.htm (accessed May 30, 2021).

[3] Barlow, J. B., *Low-speed wind tunnel testing*, 3. ed..; Wiley: New York, NY [u.a.], 1999; xii+713.

[4] Bartl, J., Mühle, F., Schottler, J., Sætran, L., Peinke, J., Adaramola, M., and Hölling, M. (2018). Wind tunnel experiments on wind turbine wakes in yaw: effects of inflow turbulence and shear. *Wind Energy Science 3*, 329–343.

[5] Bertholds, A. (2012). CFD Simulations of the New University of Sydney Boundary Layer Wind Tunnel.

[6] Betz, A., *Wind-Energie und ihre Ausnutzung durch Windmühlen*; Vandenhoeck & Ruprecht: Göttingen, 1926; v+64.

[7] Blanco, M. I. (2009). The economics of wind energy. *Renewable and sustainable energy reviews 13*, 1372–1382.

[8] Bouriga, M., Taher, R., Morency, F., and Weiss, J. (2015). Numerical investigation of secondary flows in a constant-width wind-tunnel contraction. *The Aeronautical Journal 119*, Publisher: Cambridge University Press, 613–630.

[9] Castellani, F., Astolfi, D., Peppoloni, M., Natili, F., Buttà, D., and Hirschl, A. (2019). Experimental Vibration Analysis of a Small Scale Vertical Wind Energy System for Residential Use. *Machines 7*, 35.

Die approbierte gedruckte Originalversion dieser Diplomarbeit ist an der TU Wien Bibliothek verfügbar
The approved original version of this thesis is available in print at TU Wien Bibliothek.
TU Bibliothek WIEN Your knowledge hub

[10] Chaudhry, H. N., Calautit, J. K., Hughes, B. R., and Sim, L. F. (2015). CFD and Experimental Study on the Effect of Progressive Heating on Fluid Flow inside a Thermal Wind Tunnel. *Computation 3*, Number: 4 Publisher: Multidisciplinary Digital Publishing Institute, 509–527.

[11] Chong, T., Joseph, P., and Davies, P. (2009). Design and performance of an open jet wind tunnel for aero-acoustic measurement. *Applied Acoustics 70*, 605–614.

[12] Dixon, S., and Hall, C., *Fluid Mechanics and Thermodynamics of Turbomachinery | ScienceDirect*, 6th ed.; Elsevier Inc.: UK, 2010.

[13] Envenio Top 6 Reasons to Choose Structured Grids in CFD - Design Engineering https://www.design-engineering.com/cfd-automeshing-1004028397-1004028397/ (accessed May 29, 2021).

[14] Gasch, R., *Wind power plants: fundamentals, design, construction and operation*, 2. ed..; Springer: Berlin [u.a.], 2012; xviii+548.

[15] Hau, E., *Wind turbines: fundamentals, technologies, application, economics. With 41 tables*, 2. ed..; Springer: Berlin [u.a.], 2006; xviii+783.

[16] Hau, E., *Windkraftanlagen: Grundlagen. Technik. Einsatz. Wirtschaftlichkeit*; Springer Berlin / Heidelberg: Berlin, Heidelberg, 2017.

[17] Hoghooghi, H., Ahmadabadi, M. N., and Manshadi, M. D. (2016). Optimization of a subsonic wind tunnel nozzle with low contraction ratio via ball-spine inverse design method. *Journal of Mechanical Science and Technology 30*, 2059–2067.

[18] Husain, Z., Abdullah, M., and YAP, T. C. (2005). Two-Dimensional Analysis of Tandem/Staggered Airfoils Using Computational Fluid Dynamics. *International Journal of Mechanical Engineering Education 33*, 195–207.

[19] Hyvärinen, A., and Segalini, A. (2017). Effects From Complex Terrain on Wind-Turbine Performance. *Journal of Energy Resources Technology 139*, DOI: 10.1115/1.4036048.

[20] Jonkman, J., Butterfield, S., Musial, W., and Scott, G. Definition of a 5-MW Reference Wind Turbine for Offshore System Development, NREL/TP-500-38060, 947422, 2009, NREL/TP–500–38060, 947422.

[21] Kaldellis, J. K., and Zafirakis, D. (2011). The wind energy (r) evolution: A short review of a long history. *Renewable energy 36*, 1887–1901.

Die approbierte gedruckte Originalversion dieser Diplomarbeit ist an der TU Wien Bibliothek verfügbar
The approved original version of this thesis is available in print at TU Wien Bibliothek.
TU Bibliothek WIEN Your knowledge hub

[22] Kuron, M. Engineering.com, 3 Criteria for Assessing CFD Convergence https://www.engineering.com/story/3-criteria-for-assessing-cfd-convergence (accessed June 2, 2021).

[23] Li, Z., Moradi, I., Nguyen, Q., Karimipour, A., Afrand, M., Tlili, I., and Incecik, A. (2020). Three-dimensional simulation of wind tunnel diffuser to study the effects of different divergence angles on speed uniform distribution, pressure in outlet, and eddy flows formation in the corners. *Physics of Fluids 32*, Publisher: American Institute of Physics, 052006.

[24] Mehta, R. D., and Bradshaw, P. (1979). Design rules for small low speed wind tunnels. *Aeronautical journal 83*, Place: Cambridge, UK Publisher: Cambridge University Press, 443–453.

[25] Menter, F. R. (1994). Two-equation eddy-viscosity turbulence models for engineering applications. *AIAA Journal 32*, Publisher: American Institute of Aeronautics and Astronautics, 1598–1605.

[26] Oh, K.-Y., Nam, W., Ryu, M. S., Kim, J.-Y., and Epureanu, B. I. (2018). A review of foundations of offshore wind energy convertors: Current status and future perspectives. *Renewable and Sustainable Energy Reviews 88*, 16–36.

[27] Paßmann, M., *Auslegung der Testsektion eines geschlossenen Windkanals für ORC-Fluide: Kontraktion, Diffusor und ein modulares Gesamtkonzept*, 1st ed. 2016..; Forschungsreihe der FH Münster; Springer Fachmedien Wiesbaden : Imprint: Springer Spektrum: Wiesbaden, 2016; xxiv+127.

[28] Rehman, S., Alam, M., Alhems, L. M., Rafique, M. M., et al. (2018). Horizontal axis wind turbine blade design methodologies for efficiency enhancement—A review. *Energies 11*, 506.

[29] Sassi, M. A. Nonlinear dynamic analysis of wind turbine towers subject to design wind and seismic loads, Accepted: 2017-01-19T21:59:16Z Artwork Medium: born digital Interview Medium: born digital, Text, Colorado: Colorado School of Mines, 2015.

[30] Scheiman, J., and Brooks, J. D. (2012). Comparison of Experimental and Theoretical Turbulence Reduction from Screens, Honeycomb, and Honeycomb-Screen Combinations. *Journal of Aircraft*, DOI: 10.2514/3.57538.

[31] Sedighi, H., Akbarzadeh, P., and Salavatipour, A. (2020). Aerodynamic performance enhancement of horizontal axis wind turbines by dimples on blades: Numerical investigation. *Energy 195*, 117056.

Die approbierte gedruckte Originalversion dieser Diplomarbeit ist an der TU Wien Bibliothek verfügbar
The approved original version of this thesis is available in print at TU Wien Bibliothek.
TU Bibliothek WIEN Your knowledge hub

[32] Semlitsch, B. Large eddy simulation of turbulent compressible jets, Ph.D. Thesis, KTH Royal Institute of Technology, 2014.

[33] Singh, A., Chauhan, J., Gupta, S., and Dwivedi, V. In, Ghaziabad, 2012.

[34] Surek, D., and Stempin, S., Ähnlichkeitsgesetze der Strömungsmechanik In *Technische Strömungsmechanik*; Springer Fachmedien Wiesbaden: Wiesbaden, 2017, pp 85–94.

[35] Thapar, V., Agnihotri, G., and Sethi, V. K. (2011). Critical analysis of methods for mathematical modelling of wind turbines. *Renewable Energy 36*, 3166–3177.

[36] Wang, J., Wang, C., Campagnolo, F., and Bottasso, C. L. (2019). Wake behavior and control: comparison of LES simulations and wind tunnel measurements. *Wind Energy Science 4*, 71–88.

[37] Welsh, A. Low Turbulence Wind Tunnel Design and Wind Turbine Wake Characterization, Wisconsin-Milwaukee, 2013.

[38] Zabarjad Shiraz, M., Dilimulati, A., and Paraschivoiu, M. (2020). Wind power potential assessment of roof mounted wind turbines in cities. *Sustainable Cities and Society 53*, 101905.

Die approbierte gedruckte Originalversion dieser Diplomarbeit ist an der TU Wien Bibliothek verfügbar
The approved original version of this thesis is available in print at TU Wien Bibliothek.
TU Bibliothek WIEN Your knowledge hub

Appendix A

Tables and diagrams

A.1 Function Points, Bell and Mehta

The profile of the contraction wall can be seen in Fig.A.1 while all function points regarding to this profile can be seen in Tab.A.1.

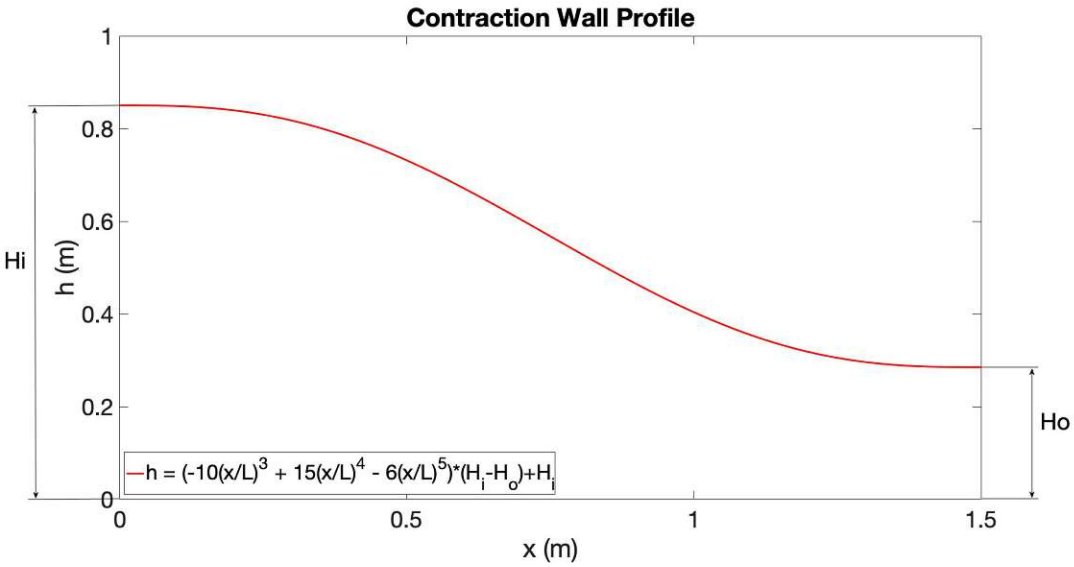

Figure A.1: Contraction Wall Profile

Die approbierte gedruckte Originalversion dieser Diplomarbeit ist an der TU Wien Bibliothek verfügbar
The approved original version of this thesis is available in print at TU Wien Bibliothek.
TU Bibliothek WIEN Your knowledge hub

Table A.1: Contraction Cone Dimensions - Bell Mehta´s Polynomial

Value of x in meter	Value of h in meter
0	0.85=H_i
0.0152	0.85
0.0303	0.85
0.0455	0.8498
0.0606	0.8496
0.0758	0.8493
0.0909	0.8489
0.1061	0.8482
0.1212	0.8474
0.1364	0.8463
0.1515	0.845
0.1667	0.8435
0.1818	0.8417
0.197	0.8396
0.2121	0.8372
0.2273	0.8345
0.2424	0.8316
0.2576	0.8283
0.2727	0.8246
0.2879	0.8207
0.303	0.8164
0.3182	0.8118
0.3333	0.8068
0.3485	0.8015
0.3636	0.7959
0.3788	0.79
0.3939	0.7837

Continued on next page

Die approbierte gedruckte Originalversion dieser Diplomarbeit ist an der TU Wien Bibliothek verfügbar
The approved original version of this thesis is available in print at TU Wien Bibliothek.
TU Bibliothek WIEN Your knowledge hub

Table A.1 – continued from previous page

Value of x in meter	Value of h in meter
0.4091	0.7772
0.4242	0.7703
0.4394	0.7631
0.4545	0.7556
0.4697	0.7478
0.4848	0.7397
0.5	0.7314
0.5152	0.7228
0.5303	0.714
0.5455	0.705
0.5606	0.6957
0.5758	0.6862
0.5909	0.6765
0.6061	0.6667
0.6212	0.6567
0.6364	0.6465
0.6515	0.6363
0.6667	0.6259
0.6818	0.6154
0.697	0.6048
0.7121	0.5942
0.7273	0.5835
0.7424	0.5729
0.7576	0.5621
0.7727	0.5515
0.7879	0.5408
0.803	0.5302
0.8182	0.5196

Continued on next page

Die approbierte gedruckte Originalversion dieser Diplomarbeit ist an der TU Wien Bibliothek verfügbar
The approved original version of this thesis is available in print at TU Wien Bibliothek.
TU Bibliothek WIEN Your knowledge hub

Table A.1 – continued from previous page

Value of x in meter	Value of h in meter
0.8333	0.5091
0.8485	0.4987
0.8636	0.4885
0.8788	0.4783
0.8939	0.4683
0.9091	0.4585
0.9242	0.4488
0.9394	0.4393
0.9545	0.43
0.9697	0.421
0.9848	0.4122
1	0.4036
1.0152	0.3953
1.0303	0.3872
1.0455	0.3794
1.0606	0.3719
1.0758	0.3647
1.0909	0.3578
1.1061	0.3513
1.1212	0.345
1.1364	0.3391
1.1515	0.3335
1.1667	0.3282
1.1818	0.3232
1.197	0.3186
1.2121	0.3143
1.2273	0.3104
1.2424	0.3067

Continued on next page

Die approbierte gedruckte Originalversion dieser Diplomarbeit ist an der TU Wien Bibliothek verfügbar
The approved original version of this thesis is available in print at TU Wien Bibliothek.
TU Bibliothek WIEN Your knowledge hub

Table A.1 – continued from previous page

Value of x in meter	Value of h in meter
1.2576	0.3034
1.2727	0.3005
1.2879	0.2978
1.303	0.2954
1.3182	0.2933
1.3333	0.2915
1.3485	0.29
1.3636	0.2887
1.3788	0.2876
1.3939	0.2868
1.4091	0.2861
1.4242	0.2857
1.4394	0.2854
1.4545	0.2852
1.4697	0.285
1.4848	0.285
1.5	0.285=H_o

Die approbierte gedruckte Originalversion dieser Diplomarbeit ist an der TU Wien Bibliothek verfügbar
The approved original version of this thesis is available in print at TU Wien Bibliothek.
TU Bibliothek WIEN Your knowledge hub

Appendix B

Drawings

B.1 Designed Wind Tunnel

Die approbierte gedruckte Originalversion dieser Diplomarbeit ist an der TU Wien Bibliothek verfügbar
The approved original version of this thesis is available in print at TU Wien Bibliothek.
TU Bibliothek WIEN Your knowledge hub

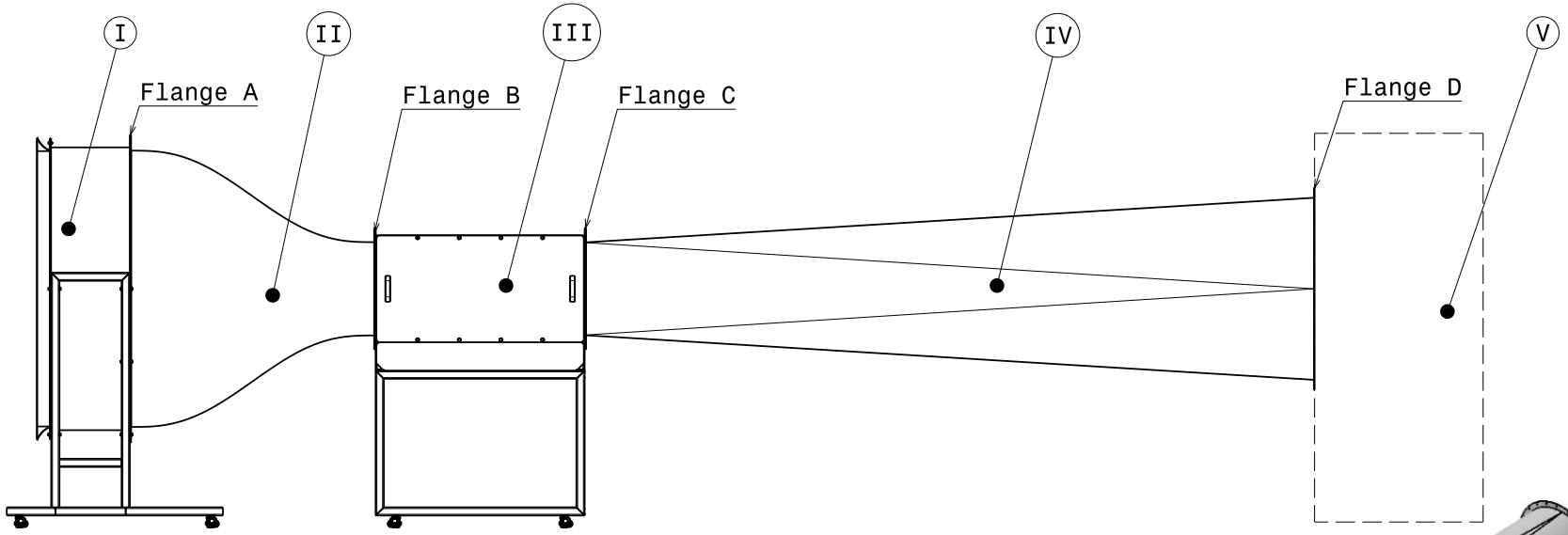

Components Assembly Wind Tunnel:

Number	Component/Type	Quantity
I	Settling Chamber / Assembly I	1
II	Contraction Cone / Part II	1
III	Test Section / Assembly III	1
IV	Diffuser / Part IV	1
V	Suction Unit / Purchased part	1

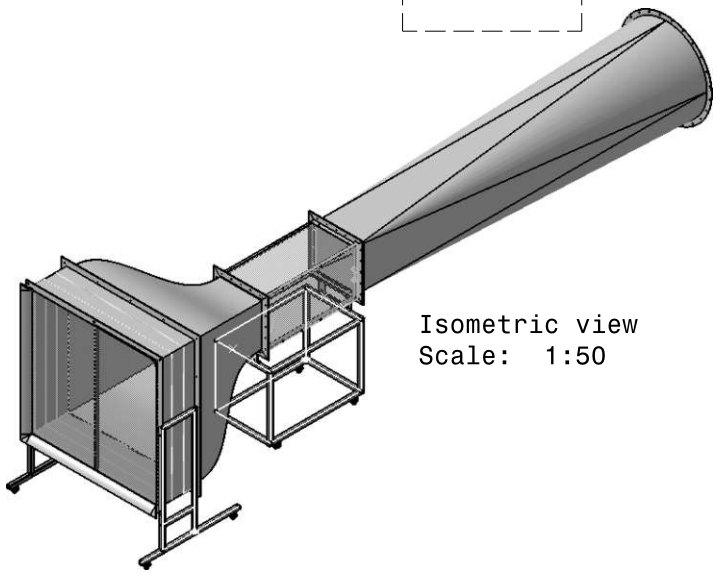

Isometric view
Scale: 1:50

Parts for Flange Connection:

Flange	Part	Quantity
A	Hexagon head screw DIN 933 - M10 x 20	10
	Hexagon head screw DIN 558 - M10 x 70	6
	Bright metal washer UNI 1739 10x1.5	32
	Hexagon nut DIN 934 - M10	16
B	Hexagon head screw DIN 933 - M10 x 20	20
	Bright metal washer UNI 1739 10x1.5	40
	Hexagon nut DIN 934 - M10	20
C	Hexagon head screw DIN 933 - M10 x 20	20
	Bright metal washer UNI 1739 10x1.5	40
	Hexagon nut DIN 934 - M10	20
D	Hexagon head screw DIN 933 - M10 x 20	16
	Bright metal washer UNI 1739 10x1.5	32
	Hexagon nut DIN 934 - M10	16

DESIGNED BY: B. Kunitzky DATE: 07.2021	Wind Tunnel	
CHECKED BY: XXX DATE: XXX		
SIZE A3		
SCALE 1:30	Type: Assembly	SHEET 1/1

This drawing is our property; it can't be reproduced or communicated without our written agreement.

Die approbierte gedruckte Originalversion dieser Diplomarbeit ist an der TU Wien Bibliothek verfügbar
The approved original version of this thesis is available in print at TU Wien Bibliothek.

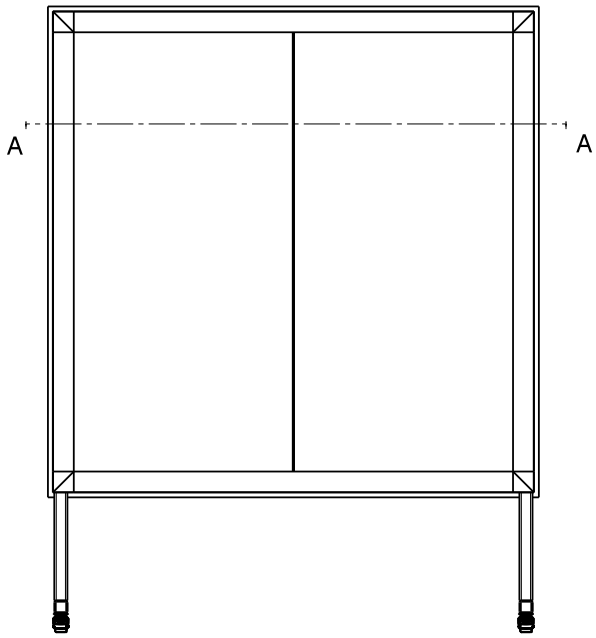

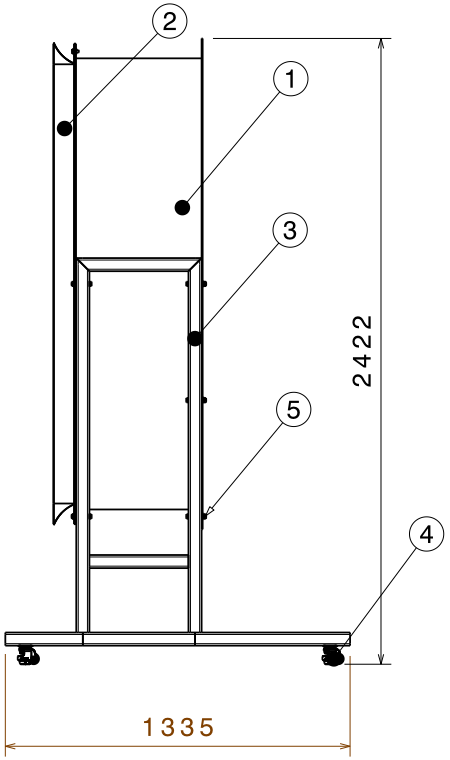

Isometric view
Scale: 1:40

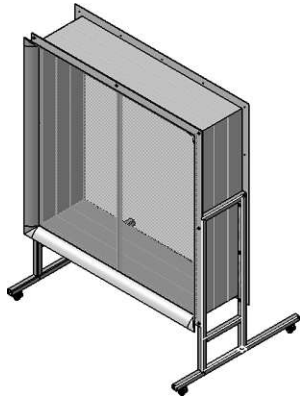

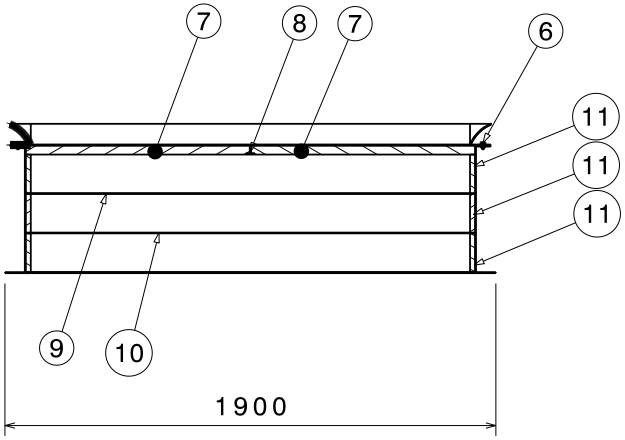

Section cut: A-A

Parts list: Assembly I

Number	Component	Quantity
1	Housing	1
2	Inflow	1
3	Rack for settling chamber	2
4	Adjustable caster, LYBC 40mm (PP)*	4
5	Screw-nut connection (PP)*: -M10x70 hexagon head screw, DIN 558-4.6 -Washer 10mm, 2 pieces each, DIN 9021 -M10 Nut, DIN 934 -Spring washer 10mm, DIN127	10
6	Screw-nut connection (PP)*: -M10x20 hexagon head screw, DIN 933 -Washer 10mm, 2 pieces each, DIN 9021 -M10 Nut, DIN 934 -Spring washer 10mm, DIN127	14
7	Honeycomb (PP)*	2
8	Bar, T-Profile, Steel 35x35x4.5 (PP)*	1
9	Mesh A (PP)*	1
10	Mesh B (PP)*	1
11	Frame for Meshes	3

*(PP) - purchased part

DESIGNED BY: B. Kunitzky DATE: 07.2021	Settling Chamber		
CHECKED BY: XXX DATE: XXX			
SIZE A3			
SCALE 1:20	WEIGHT (kg)	Type: Assembly I	SHEET 1/1

This drawing is our property; it can't be reproduced or communicated without our written agreement.

I	_
H	_
G	_
F	_
E	_
D	_
C	_
B	_
A	_

Die approbierte gedruckte Originalversion dieser Diplomarbeit ist an der TU Wien Bibliothek verfügbar
The approved original version of this thesis is available in print at TU Wien Bibliothek.

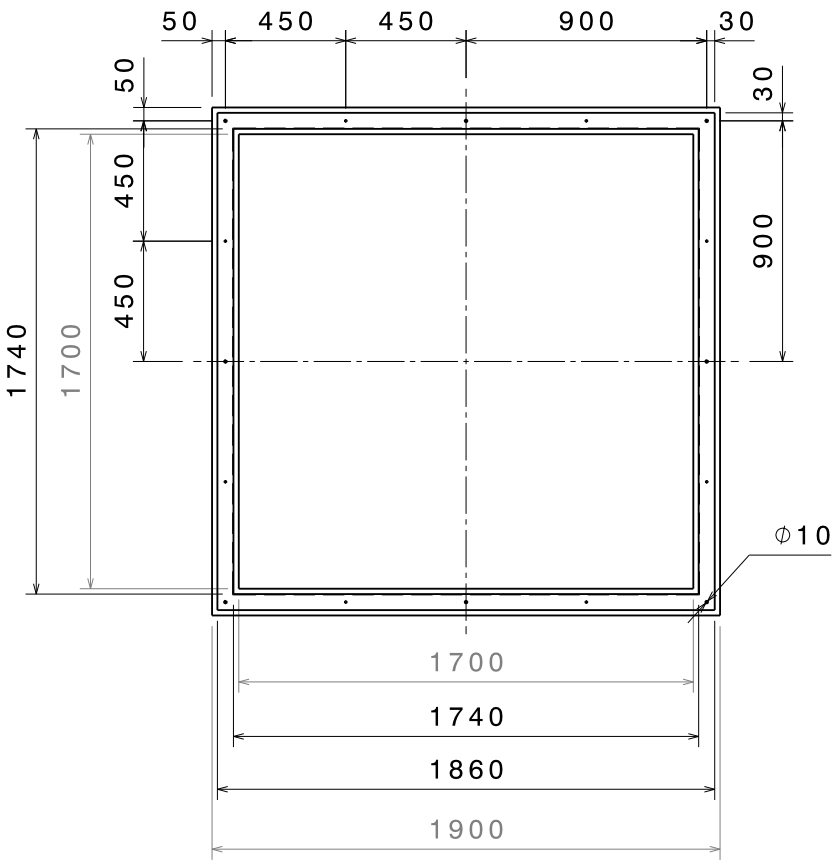

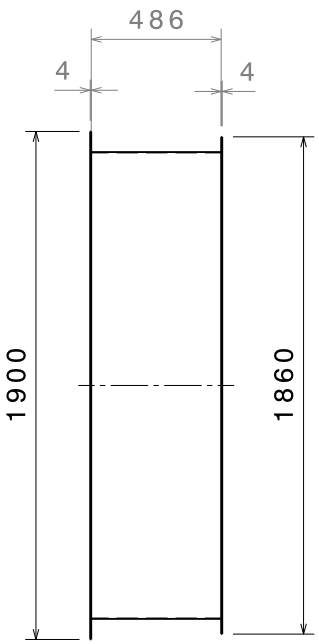

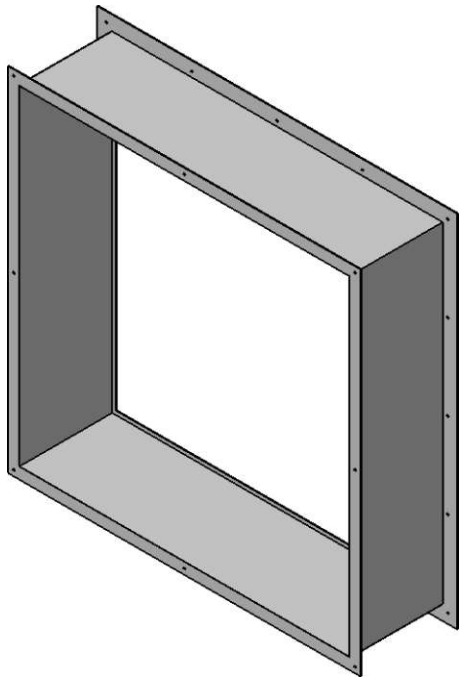

Isometric view
Scale: 1:20

Wall thickness 2mm, flange thickness 4mm,
all drilled holes - diameter 10mm

DESIGNED BY: B. Kunitzky DATE: 06.2021	Housing		
CHECKED BY: XXX DATE: XXX			
SIZE A3	Material: 1.4301 2B (Stainless Steel)		
SCALE 1:20	WEIGHT (kg)	Type: Part for Assembly I	SHEET 1/1

I	_
H	_
G	_
F	_
E	_
D	_
C	_
B	_
A	_

This drawing is our property; it can't be reproduced or communicated without our written agreement.

Die approbierte gedruckte Originalversion dieser Diplomarbeit ist an der TU Wien Bibliothek verfügbar
The approved original version of this thesis is available in print at TU Wien Bibliothek.
TU Bibliothek WIEN Your knowledge hub

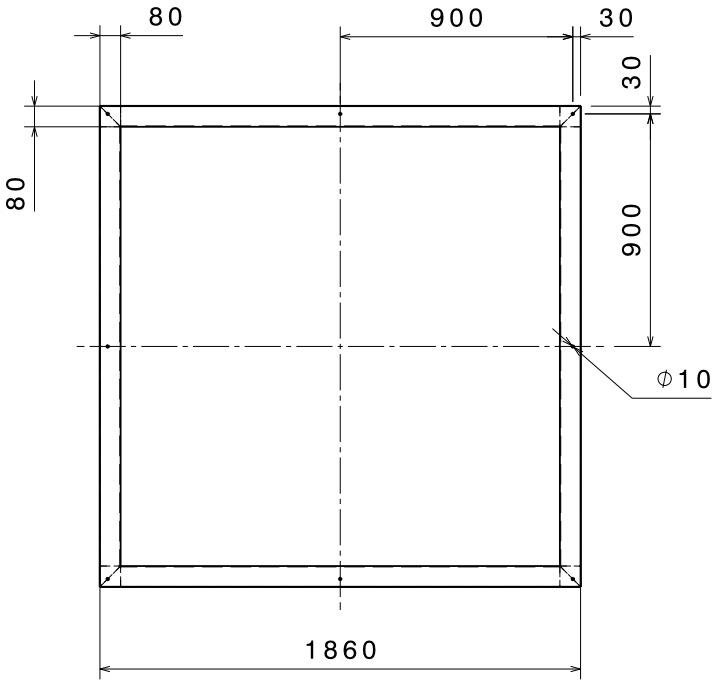

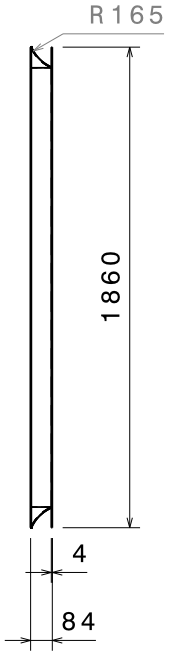

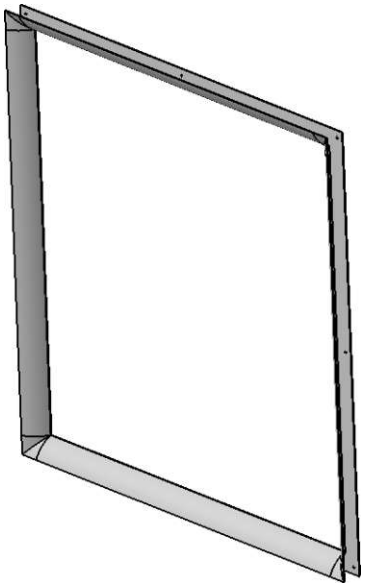

Isometric view

Wall thickness 2mm, Flange thickness 4mm

DESIGNED BY: B.Kunitzky DATE: 06.2021	Inflow		
CHECKED BY: XXX DATE: XXX			
SIZE A3	Material: 1.4301 2B (Stainless Steel)		
SCALE 1:20	Type: Part for Settling Chamber	SHEET 1/1	

This drawing is our property; it can't be reproduced or communicated without our written agreement.

I	_
H	_
G	_
F	_
E	_
D	_
C	_
B	_
A	_

Die approbierte gedruckte Originalversion dieser Diplomarbeit ist an der TU Wien Bibliothek verfügbar
The approved original version of this thesis is available in print at TU Wien Bibliothek.

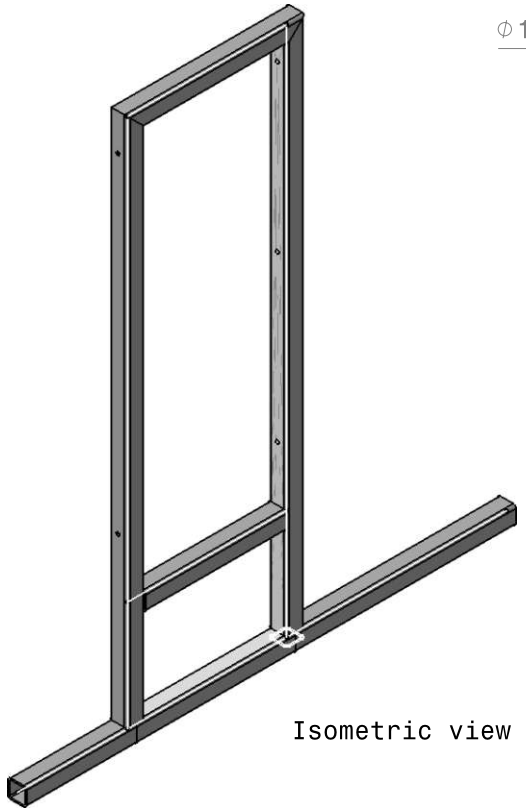

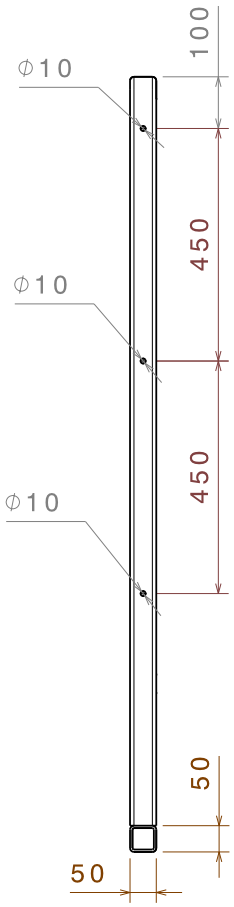

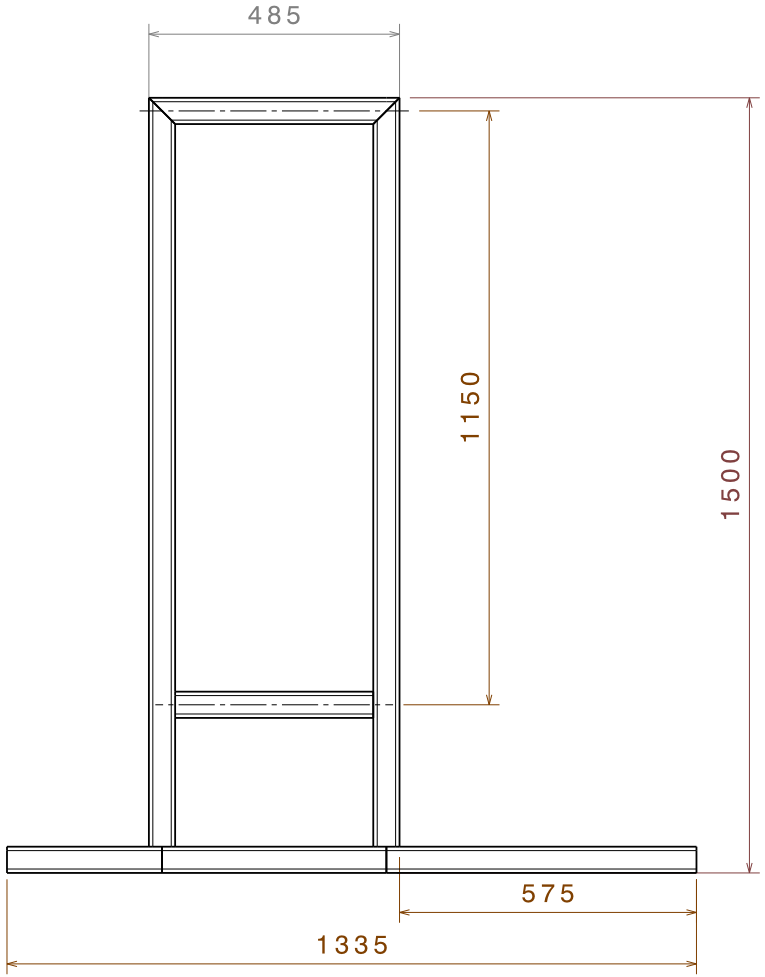

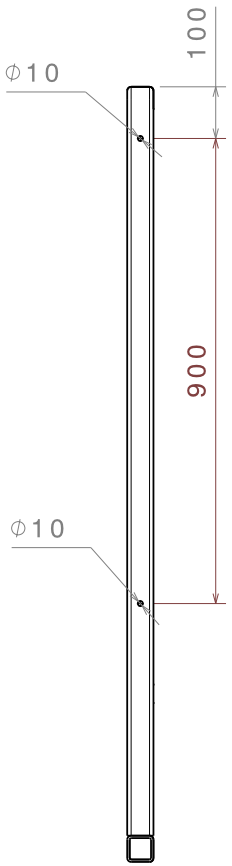

DESIGNED BY: B. Kunitzky DATE: 06.2021	Rack for settling chamber		
CHECKED BY: XXX DATE: XXX			
SIZE A3	Material: Steel 50x50x,2.5		
SCALE 1:10	WEIGHT (kg)	Type: Part for settling chamber	SHEET 1/1

This drawing is our property; it can't be reproduced or communicated without our written agreement.

Die approbierte gedruckte Originalversion dieser Diplomarbeit ist an der TU Wien Bibliothek verfügbar
The approved original version of this thesis is available in print at TU Wien Bibliothek.

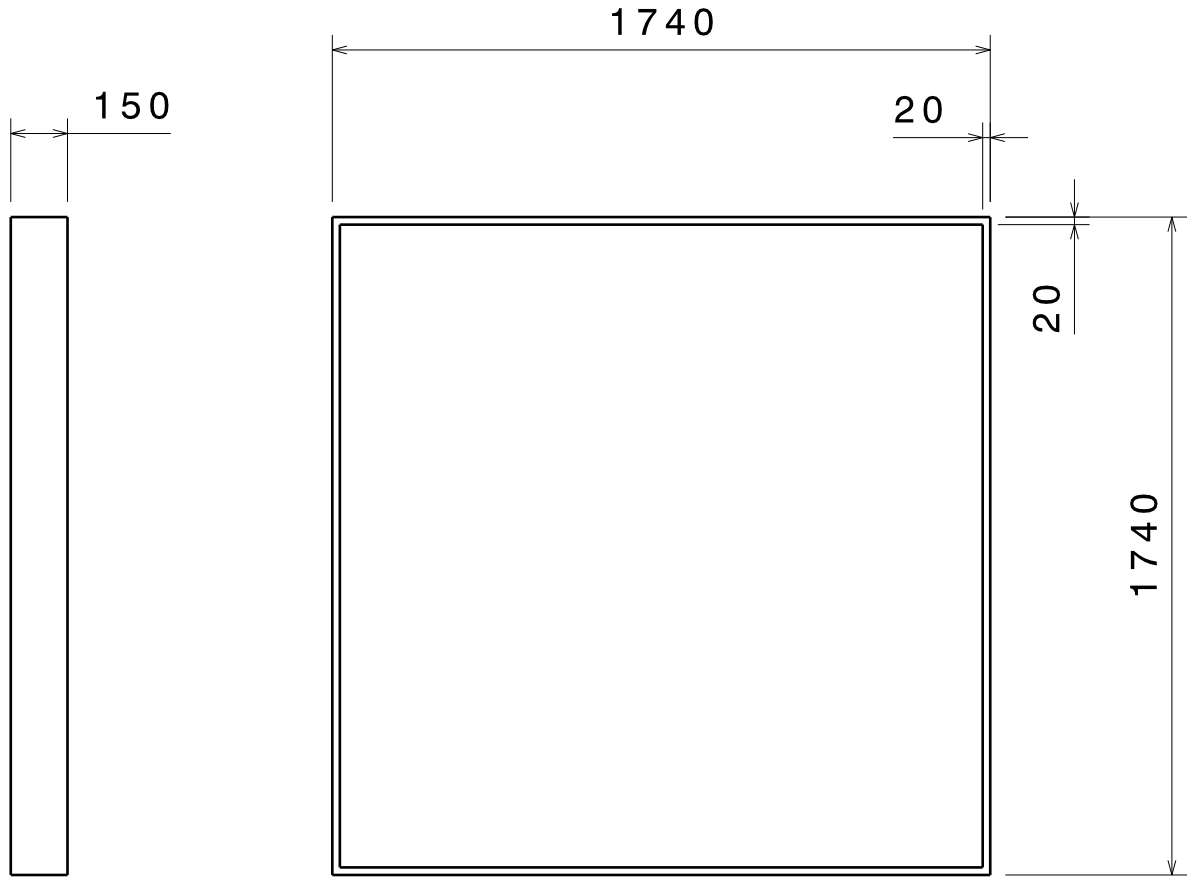

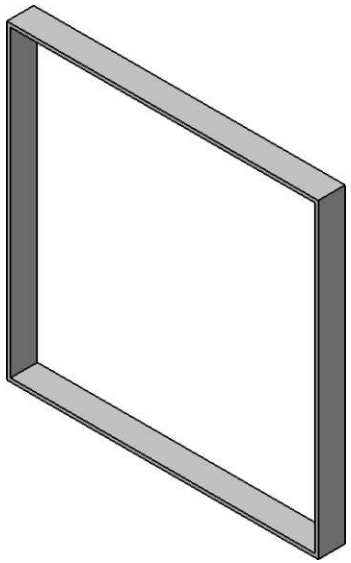

Isometric view
Scale: 1:30

DESIGNED BY: B.Kunitzky DATE: 06.2021	Frame for Meshes		
CHECKED BY: XXX DATE: XXX			
SIZE A4	Material: MDF		
SCALE 1:20	Type: Part for settling chamber	SHEET 1/1	

This drawing is our property; it can't be reproduced or communicated without our written agreement.

I	_
H	_
G	_
F	_
E	_
D	_
C	_
B	_
A	_

Die approbierte gedruckte Originalversion dieser Diplomarbeit ist an der TU Wien Bibliothek verfügbar
The approved original version of this thesis is available in print at TU Wien Bibliothek.
TU WIEN Bibliothek Your knowledge hub

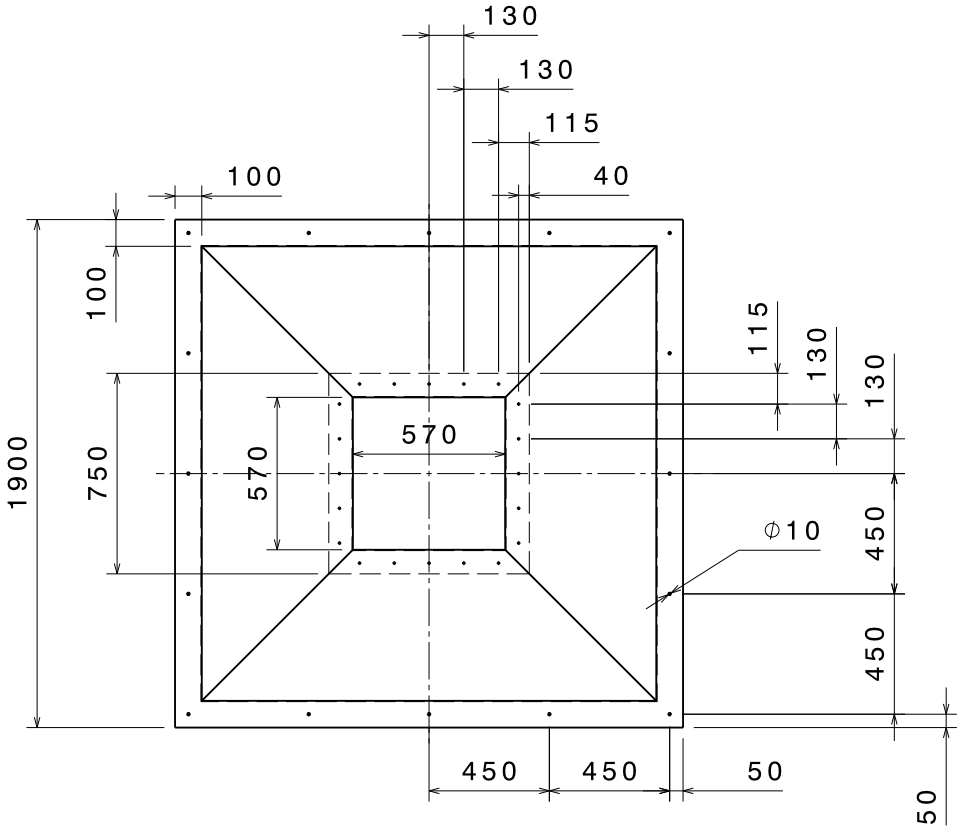

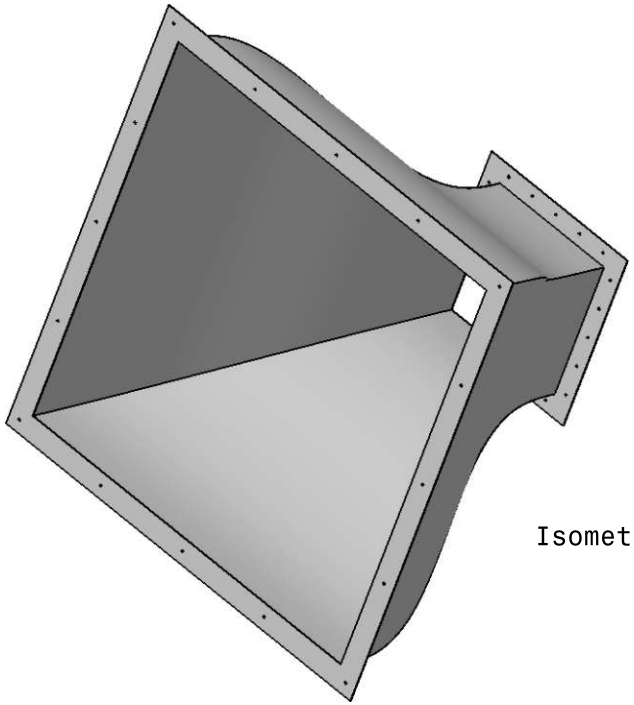

Isometric view

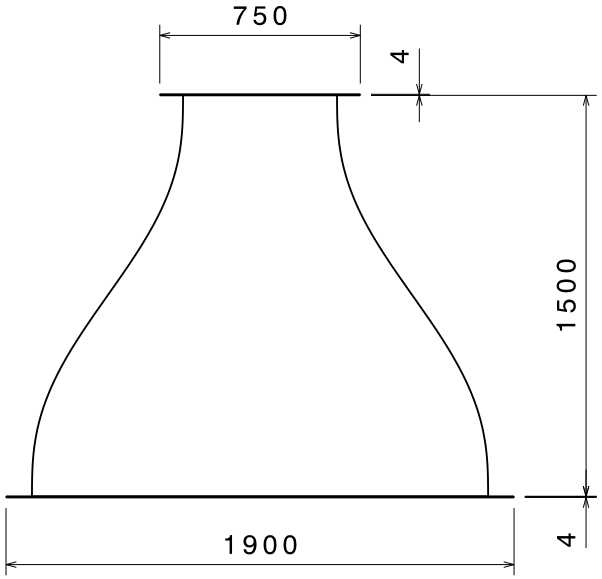

Wall thickness 2mm, flange thickness 4mm,
all drilled holes - diameter = 10mm

DESIGNED BY: B.Kunitzky DATE: 06.2021	Contraction Cone		
CHECKED BY: XXX DATE: XXX			
SIZE A3	Material: 1.4301 2B (Stainless Steel)		
SCALE 1:20	Type: Part II	SHEET 1/1	

I	_
H	_
G	_
F	_
E	_
D	_
C	_
B	_
A	_

This drawing is our property; it can't be reproduced or communicated without our written agreement.

Die approbierte gedruckte Originalversion dieser Diplomarbeit ist an der TU Wien Bibliothek verfügbar
The approved original version of this thesis is available in print at TU Wien Bibliothek.
TU Wien Bibliothek Your knowledge hub

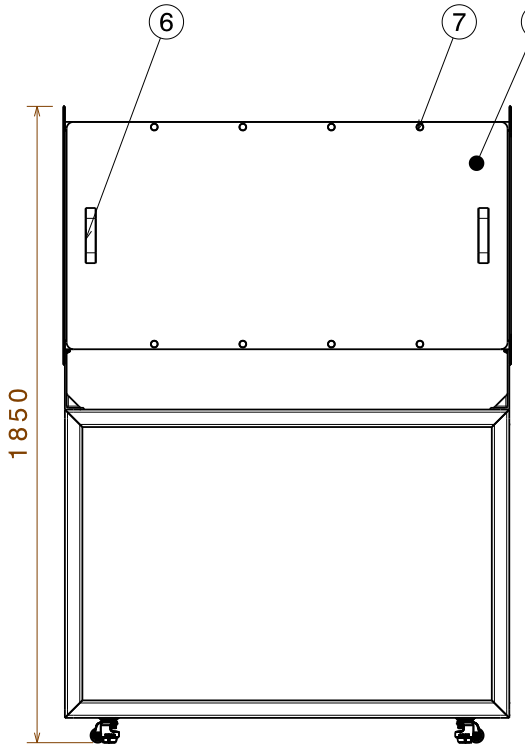

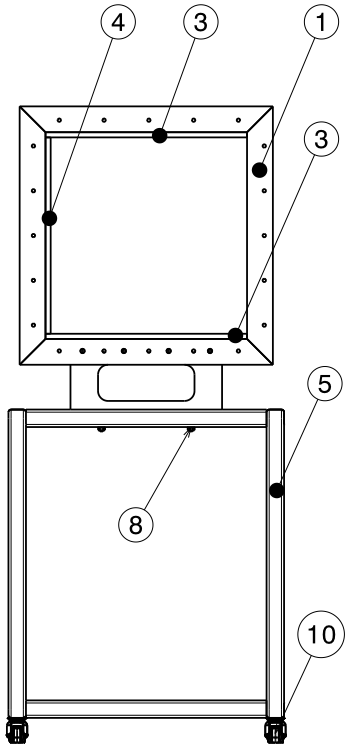

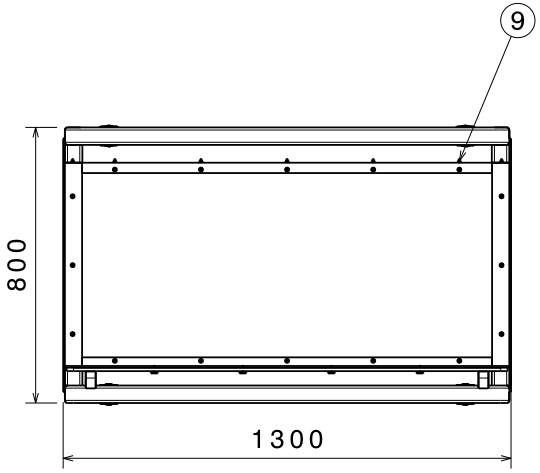

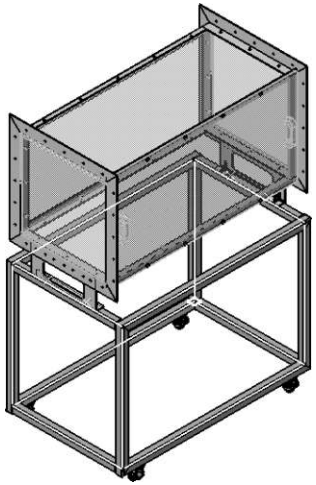

Isometric view
Scale: 1:25

Parts list: Assembly III

Number	Component	Quantity
1	Framework for test section	1
2	Door	1
3	Upper / lower window	2
4	Back window	1
5	Rack for test section	1
6	Handle + screws (PP)*	2
7	Knurled screw DIN 653, M5x18 (PP)*	8
8	Screw-nut-washer connection M10 (PP)*: -M10x70 hexagon head screw DIN 558 - 4.6 -M10 nut DIN 934 -Spring washer 10mm, DIN 127 -Washer 10mm, DIN 9021	4
9	Screw-nut-washer connection M5 (PP)*: -M5x30 countersunk screw, DIN 10642 -M5 nut DIN 934 -Spring washer 5mm, DIN 7980	48
10	Adjustable heavy duty caster, LYBC 40mm (PP)*	4

(PP) - purchased parts

DESIGNED BY: B. Kunitzky DATE: 06.2021	Test Section	
CHECKED BY: XXX DATE: XXX		
SIZE A3		
SCALE 1:15	WEIGHT (kg)	Type: Assembly III — SHEET 1/1

This drawing is our property; it can't be reproduced or communicated without our written agreement.

I	_
H	_
G	_
F	_
E	_
D	_
C	_
B	_
A	_

Die approbierte gedruckte Originalversion dieser Diplomarbeit ist an der TU Wien Bibliothek verfügbar
The approved original version of this thesis is available in print at TU Wien Bibliothek.

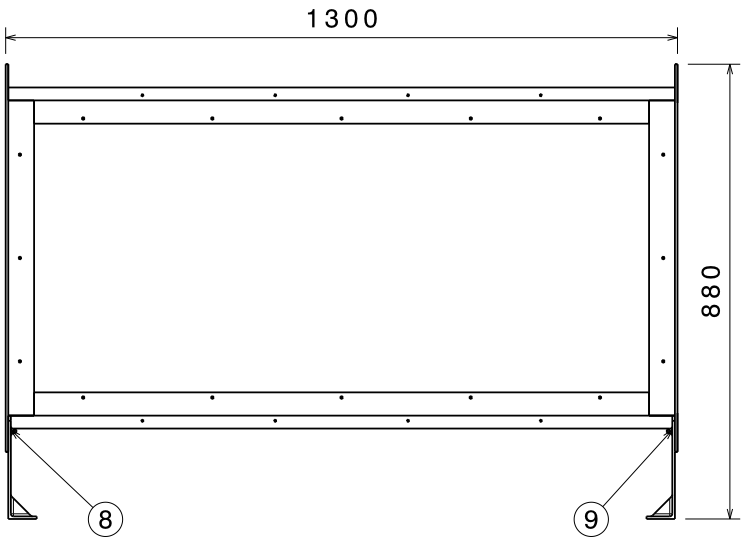

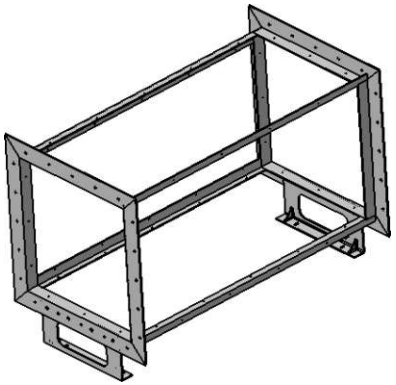

Isometric view
Scale: 1:20

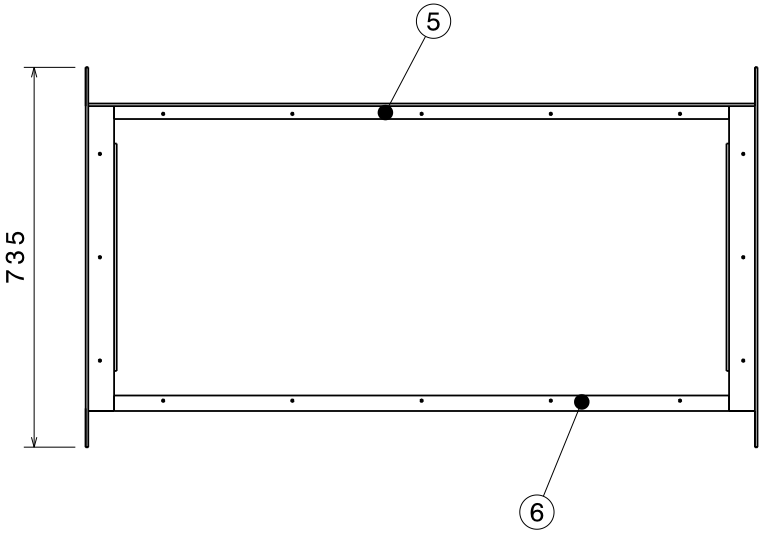

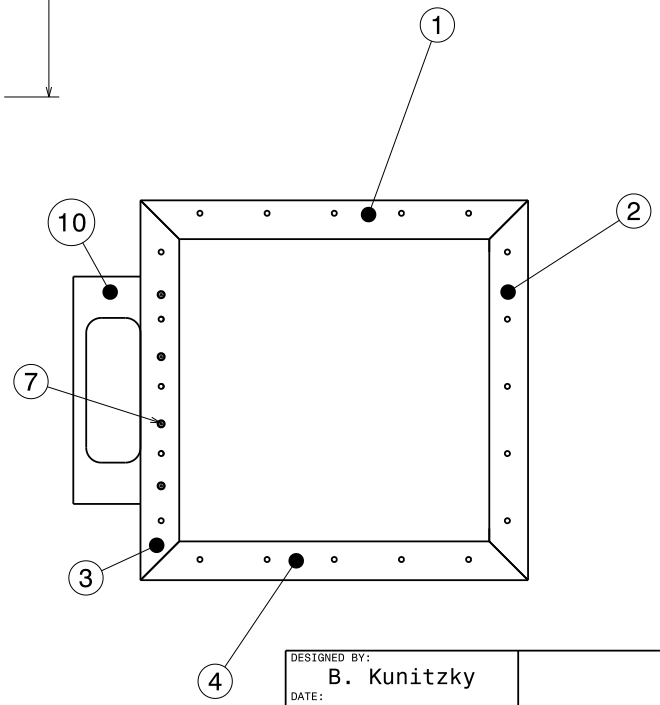

Parts list: Framework test section

Number	Component	Quantity
1	Flange angle - back	2
2	Flange angle - upper	2
3	Flange angle - lower	2
4	Flange angle - front	2
5	Longitudinal angle - back	2
6	Longitudinal angle - front	2
7	Countersunk screw M6x20 - 8,8 - UNI 5933 (PP)*	8
8	Metal washer UNI 1739 6x1 (PP)*	8
9	Nut DIN 934 - M6 (PP)*	8
10	Mount for framework	2

*(PP)-purchased parts

DESIGNED BY: B. Kunitzky
DATE: 06.2021
CHECKED BY: XXX
DATE: XXX

Framework test section

SIZE: A3
SCALE: 1:20
WEIGHT (kg):
Type: Assembly for test section
SHEET: 1/1

This drawing is our property; it can't be reproduced or communicated without our written agreement.

Die approbierte gedruckte Originalversion dieser Diplomarbeit ist an der TU Wien Bibliothek verfügbar
The approved original version of this thesis is available in print at TU Wien Bibliothek.

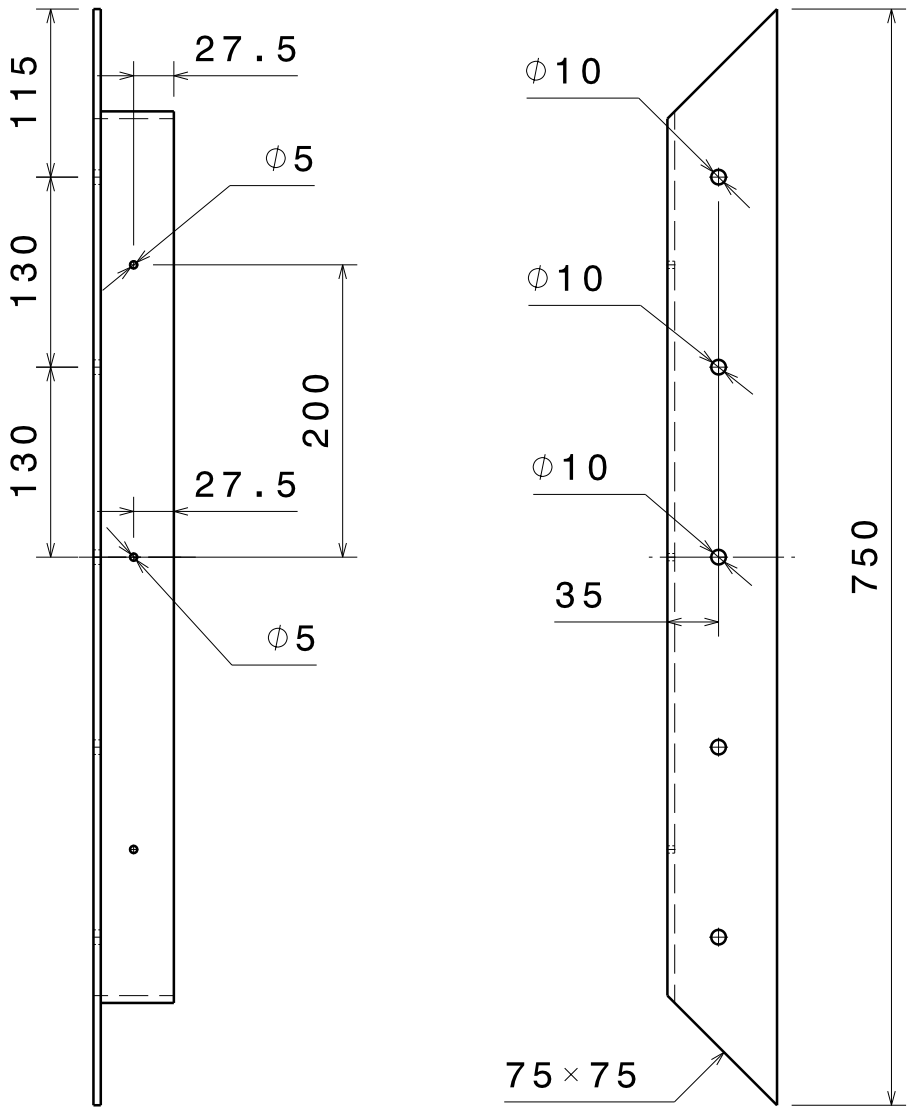

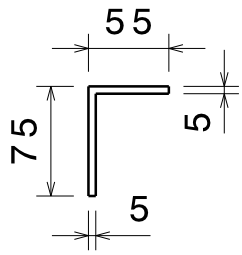

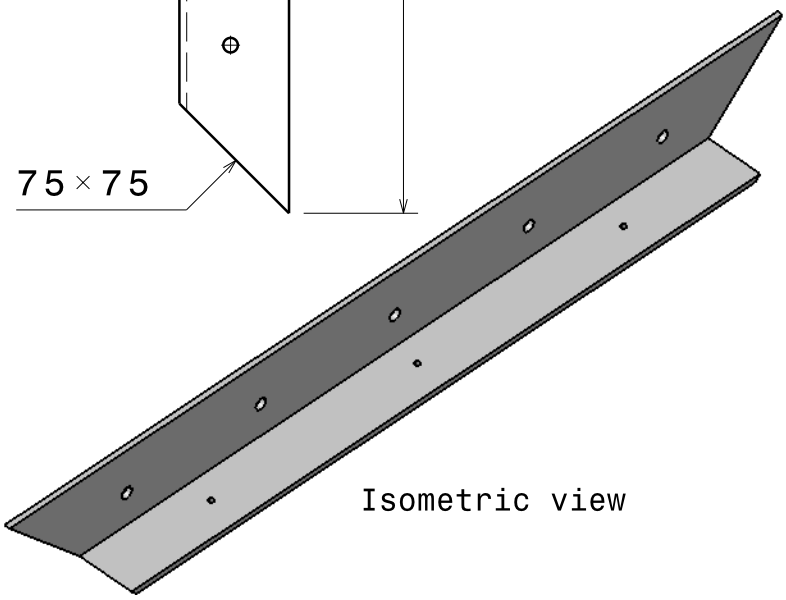

Isometric view

DESIGNED BY: B. Kunitzky DATE: 07.2021	Flange angle - back	I	_
CHECKED BY: XXX DATE: XXX		H	_
		G	_
		F	_
		E	_
SIZE A4	Material: Steel L-Profile: 75x55x5	D	_
		C	_
SCALE 1:5	Type: Part for framework test section / SHEET 1/1	B	_
		A	_

This drawing is our property; it can't be reproduced or communicated without our written agreement.

Die approbierte gedruckte Originalversion dieser Diplomarbeit ist an der TU Wien Bibliothek verfügbar
The approved original version of this thesis is available in print at TU Wien Bibliothek.
TU Bibliothek WIEN Your knowledge hub

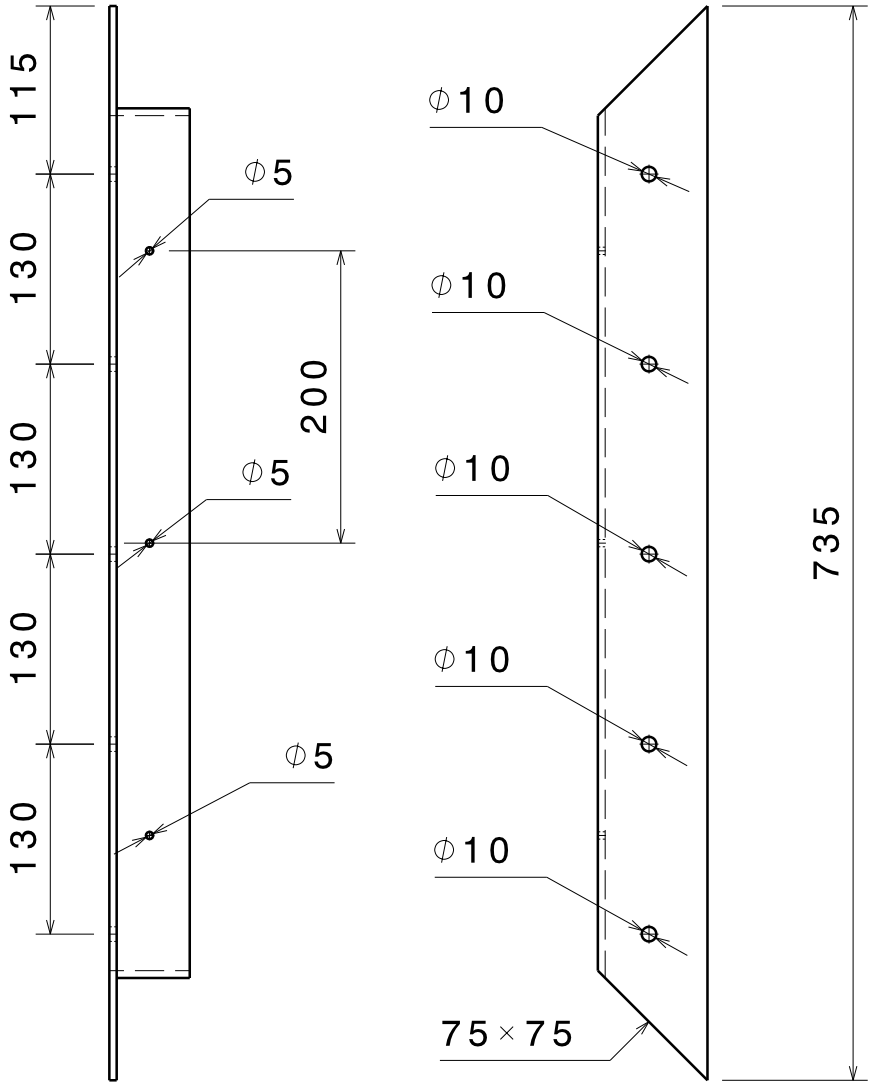

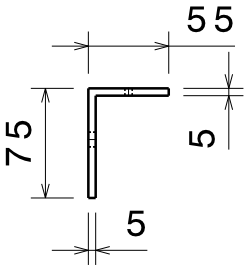

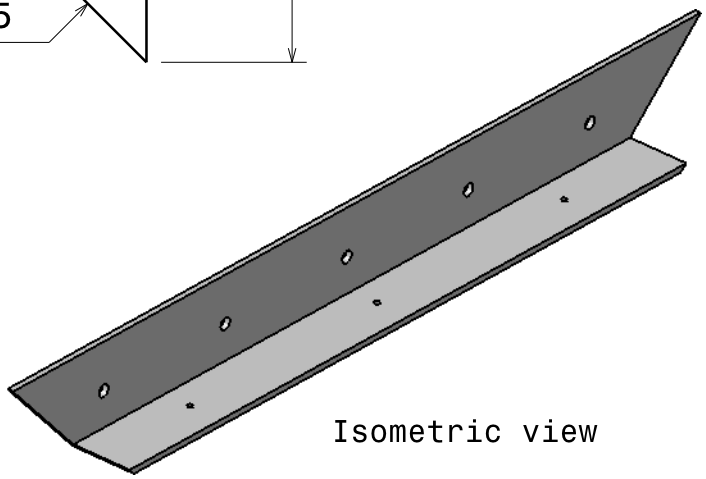

Isometric view

DESIGNED BY: B. Kunitzky DATE: 07.2021	Flange angle - upper	I	_
CHECKED BY: XXX DATE: XXX		H	_
		G	_
		F	_
		E	_
SIZE A4	Material: Steel L-Profile 75x55x5	D	_
		C	_
SCALE 1:5	Type: Part for framework test section / SHEET 1/1	B	_
		A	_

This drawing is our property; it can't be reproduced or communicated without our written agreement.

Die approbierte gedruckte Originalversion dieser Diplomarbeit ist an der TU Wien Bibliothek verfügbar
The approved original version of this thesis is available in print at TU Wien Bibliothek.
TU Bibliothek WIEN Your knowledge hub

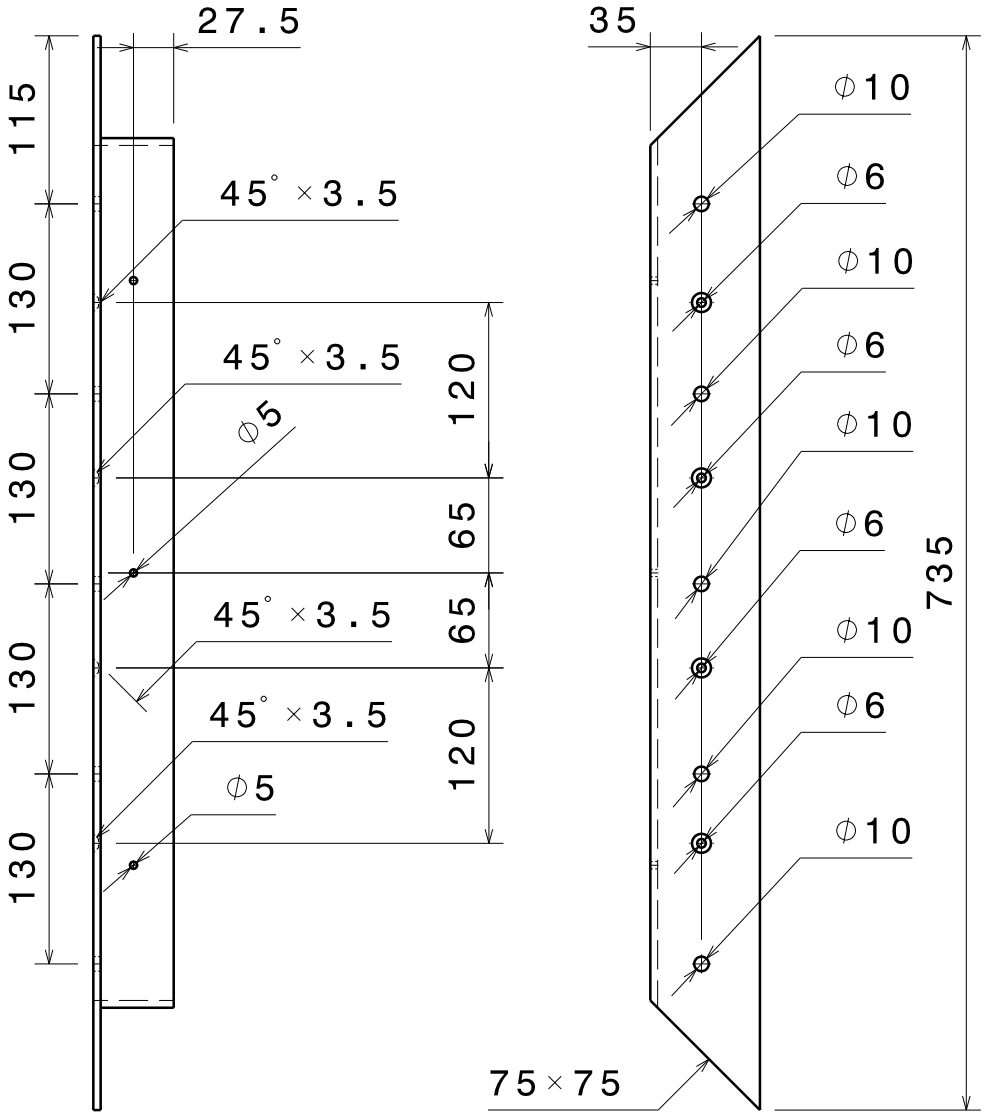

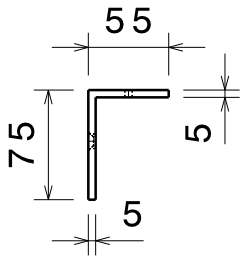

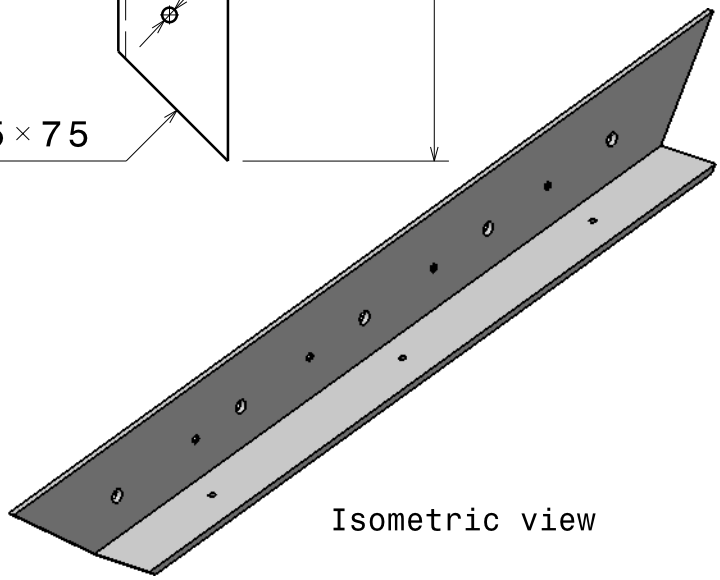

Isometric view

DESIGNED BY: B. Kunitzky DATE: 07.2021	Flange angle - lower	I	_
CHECKED BY: XXX DATE: XXX		H	_
		G	_
		F	_
SIZE A4	Material: Steel L-Profile 75x55x5	E	_
		D	_
SCALE 1:5	Type: Part for framework test section / SHEET 1/1	C	_
		B	_
This drawing is our property; it can't be reproduced or communicated without our written agreement.		A	_

Die approbierte gedruckte Originalversion dieser Diplomarbeit ist an der TU Wien Bibliothek verfügbar
The approved original version of this thesis is available in print at TU Wien Bibliothek.
TU Bibliothek WIEN Your knowledge hub

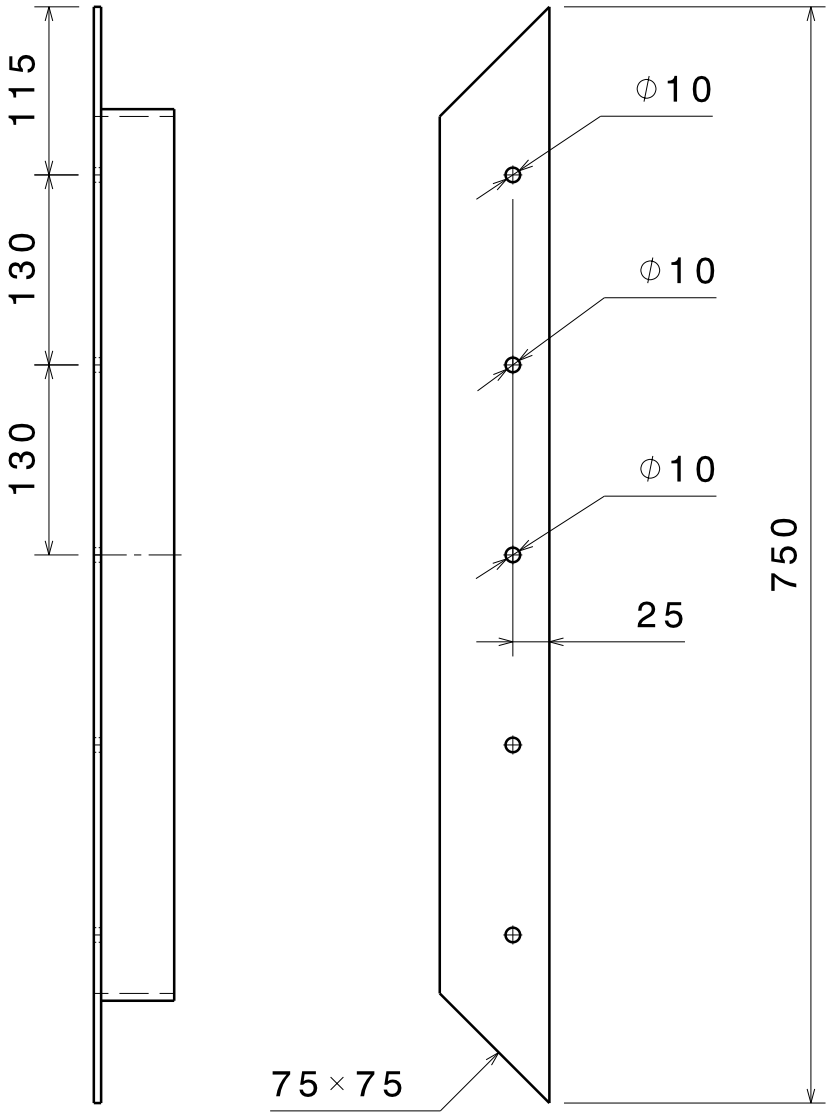

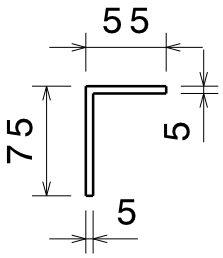

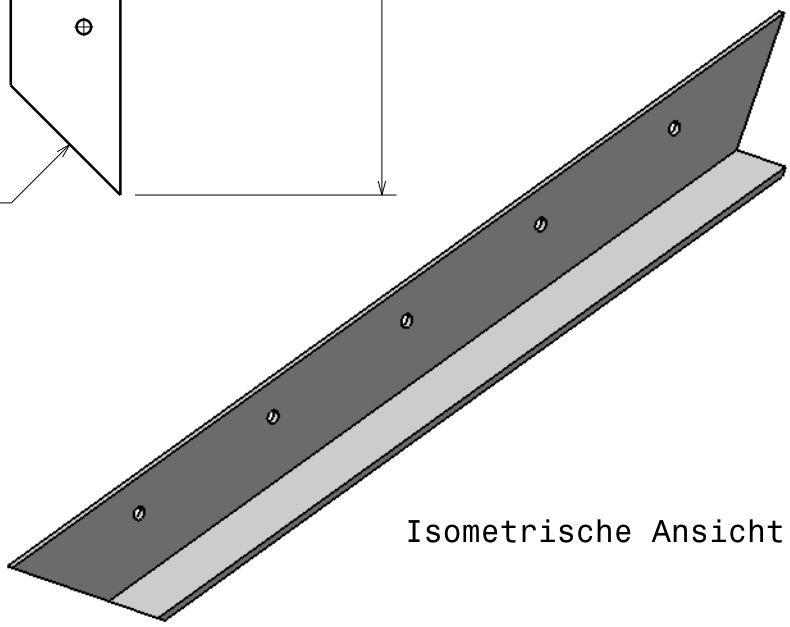

Isometrische Ansicht

DESIGNED BY: B. Kunitzky DATE: 07.2021	Flange angle - front	I	_
CHECKED BY: XXX DATE: XXX		H	_
		G	_
		F	_
		E	_
SIZE A4	Material: Steel L-Profile: 75x55x5	D	_
		C	_
SCALE 1:5	Type: Part for framework test section / SHEET 1/1	B	_
		A	_

This drawing is our property; it can't be reproduced or communicated without our written agreement.

Die approbierte gedruckte Originalversion dieser Diplomarbeit ist an der TU Wien Bibliothek verfügbar
The approved original version of this thesis is available in print at TU Wien Bibliothek.
TU Bibliothek WIEN Your knowledge hub

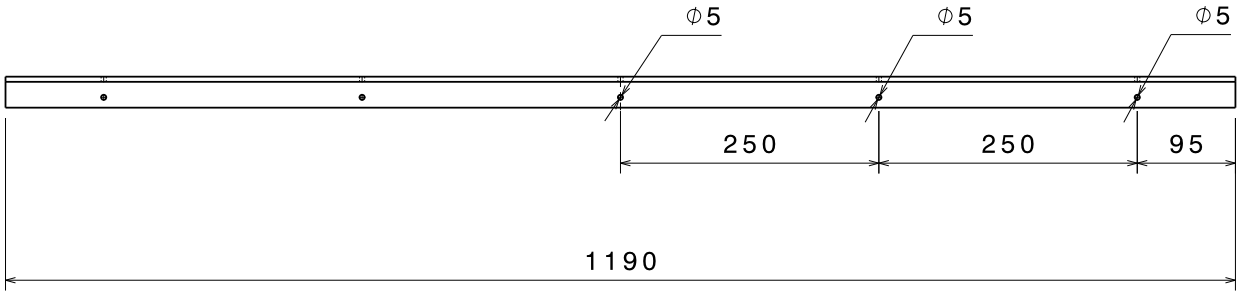

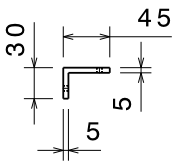

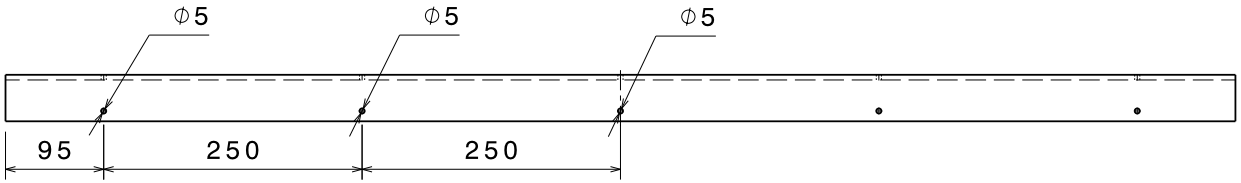

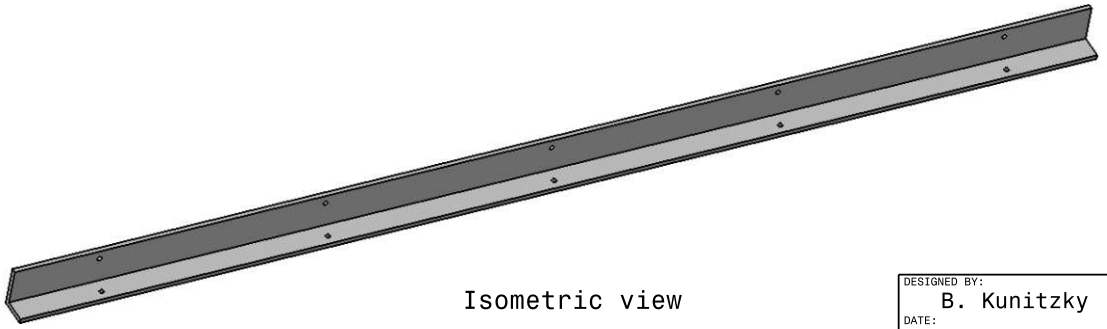

Isometric view

DESIGNED BY: B. Kunitzky DATE: 07.2021	Longitudinal angle - back		
CHECKED BY: XXX DATE: XXX			
SIZE A3	Material: Steel L-Profile 45x30x5		
SCALE 1:5	Type: Part for framework test section	SHEET 1/1	

This drawing is our property; it can't be reproduced or communicated without our written agreement.

Die approbierte gedruckte Originalversion dieser Diplomarbeit ist an der TU Wien Bibliothek verfügbar
The approved original version of this thesis is available in print at TU Wien Bibliothek.

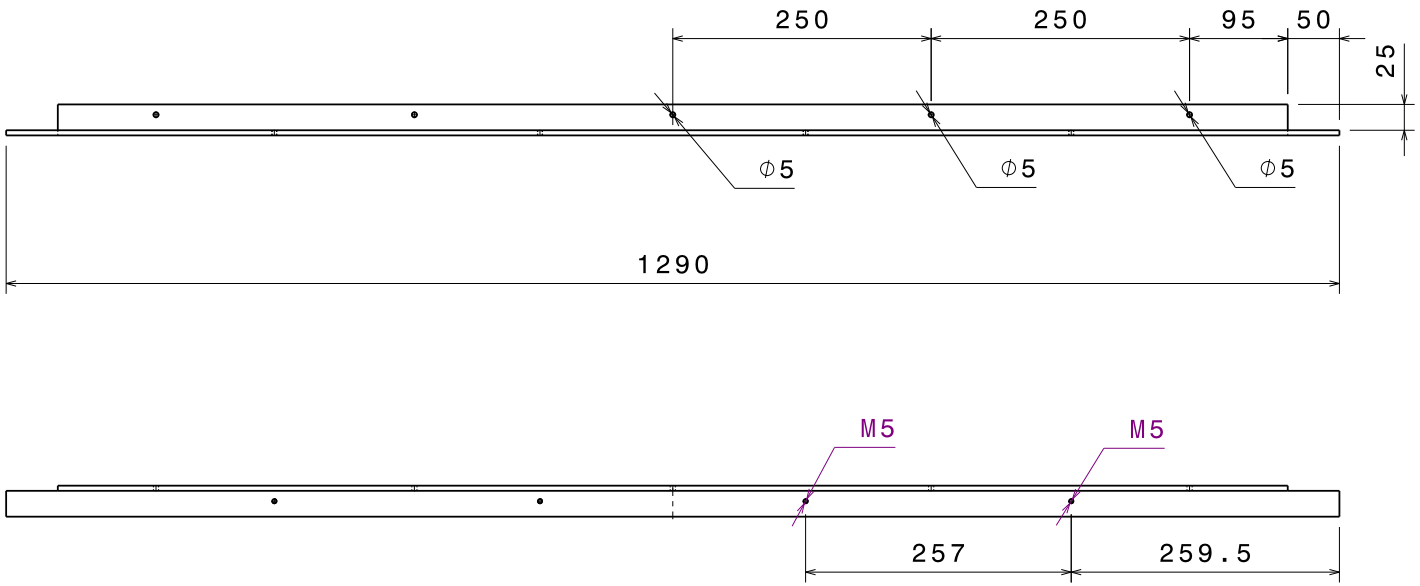

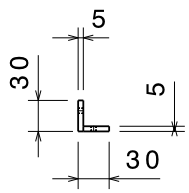

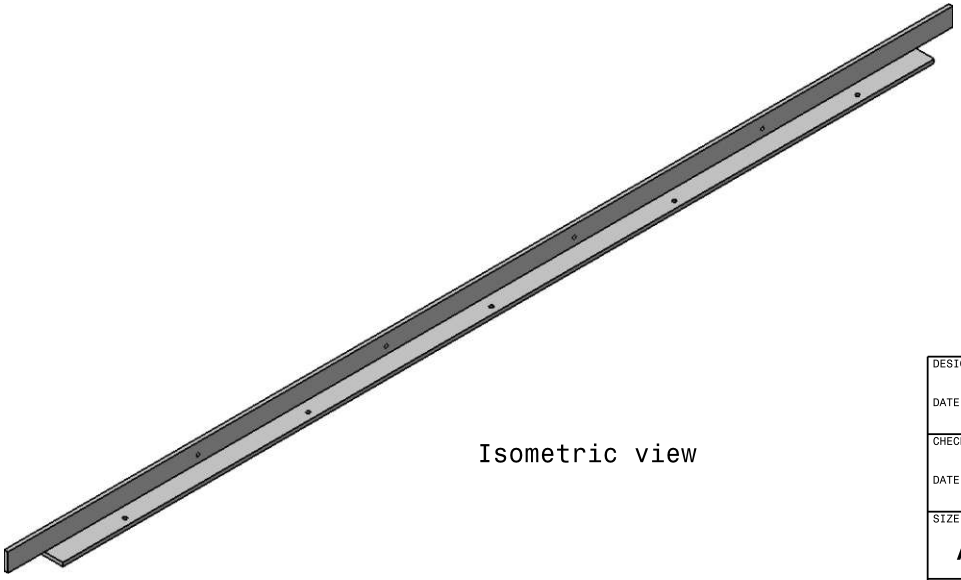

Isometric view

DESIGNED BY: B. Kunitzky	Longitudinal angle - front
DATE: 07.2021	
CHECKED BY: XXX	
DATE: XXX	
SIZE A3	Material: Steel L-Profile 30x30x5
SCALE 1:5	Type: Part for framework test section — SHEET 1/1

This drawing is our property; it can't be reproduced or communicated without our written agreement.

Die approbierte gedruckte Originalversion dieser Diplomarbeit ist an der TU Wien Bibliothek verfügbar
The approved original version of this thesis is available in print at TU Wien Bibliothek.

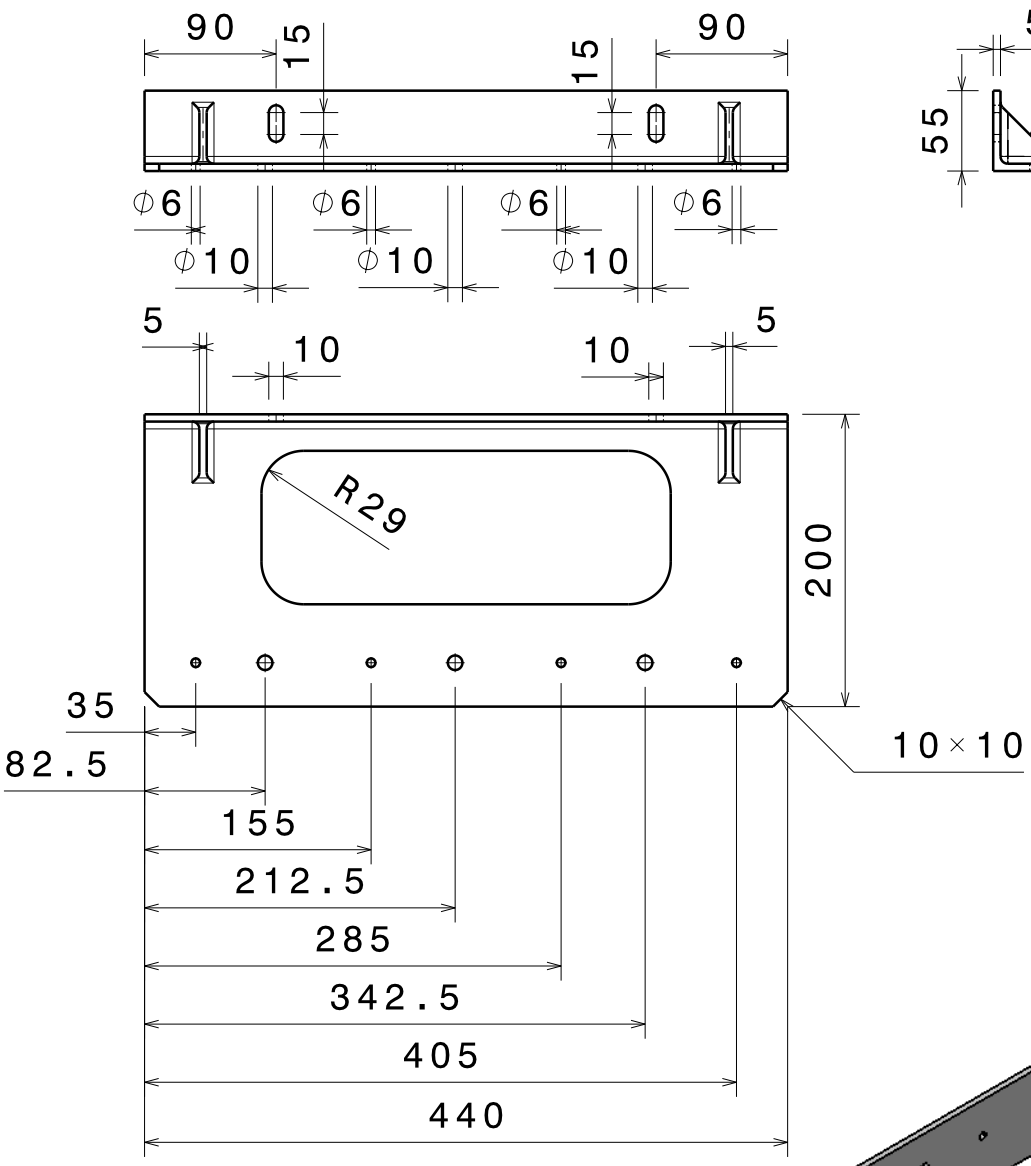

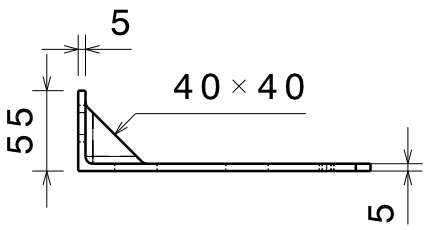

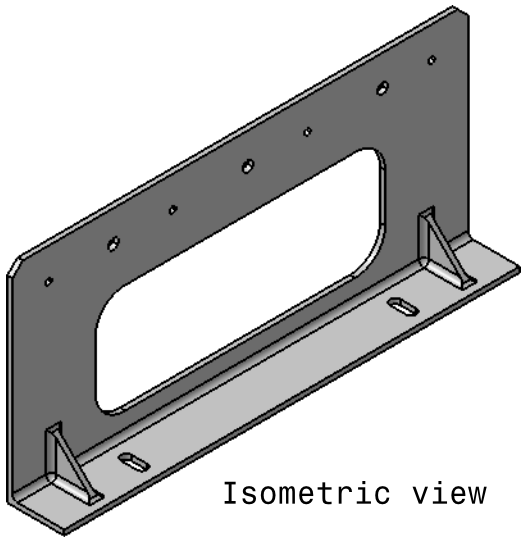

Isometric view

Attention: Holes are asymmetric,
due to asymmetry of the test section

DESIGNED BY: B.Kunitzky DATE: 07.2021	Mount for framework		
CHECKED BY: XXX DATE: XXX			
SIZE A4	Material: Steel		
SCALE 1:5	Type: Part for framework test section	SHEET 1/1	

I	_
H	_
G	_
F	_
E	_
D	_
C	_
B	_
A	_

This drawing is our property; it can't be reproduced or communicated without our written agreement.

Die approbierte gedruckte Originalversion dieser Diplomarbeit ist an der TU Wien Bibliothek verfügbar
The approved original version of this thesis is available in print at TU Wien Bibliothek.
TU Bibliothek WIEN Your knowledge hub

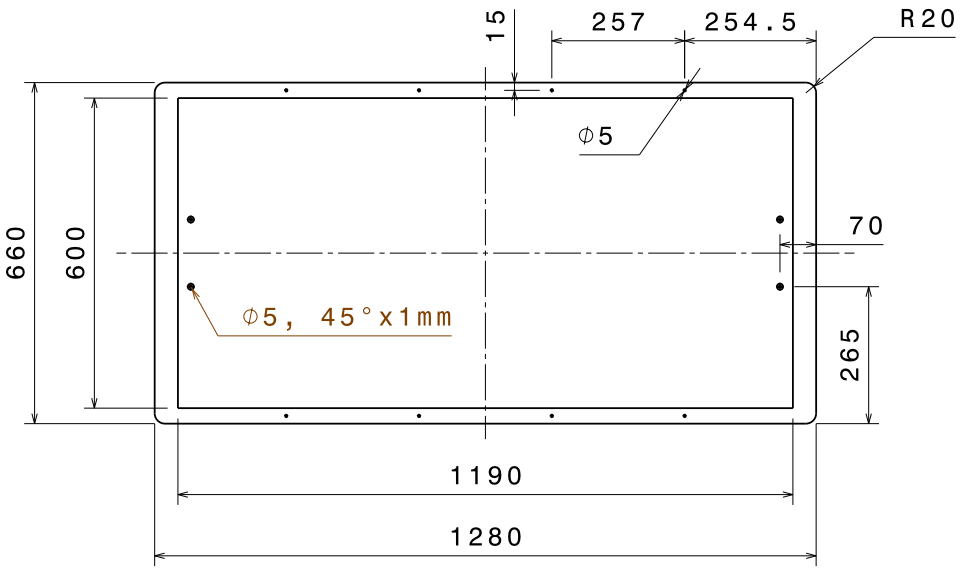

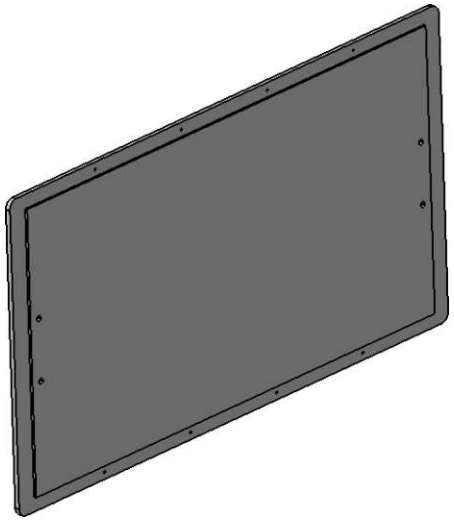

Isometric view
Scale: 1:10

All drilled holes have an inner diameter of 5mm.

DESIGNED BY: B. Kunitzky DATE: 07.2021	Door		
CHECKED BY: XXX DATE: XXX			
SIZE A3	Material: Acrylic glas		
SCALE 1:10	WEIGHT (kg)	Type: Part for test section	SHEET 1/1

This drawing is our property; it can't be reproduced or communicated without our written agreement.

I	_
H	_
G	_
F	_
E	_
D	_
C	_
B	_
A	_

Die approbierte gedruckte Originalversion dieser Diplomarbeit ist an der TU Wien Bibliothek verfügbar
The approved original version of this thesis is available in print at TU Wien Bibliothek.

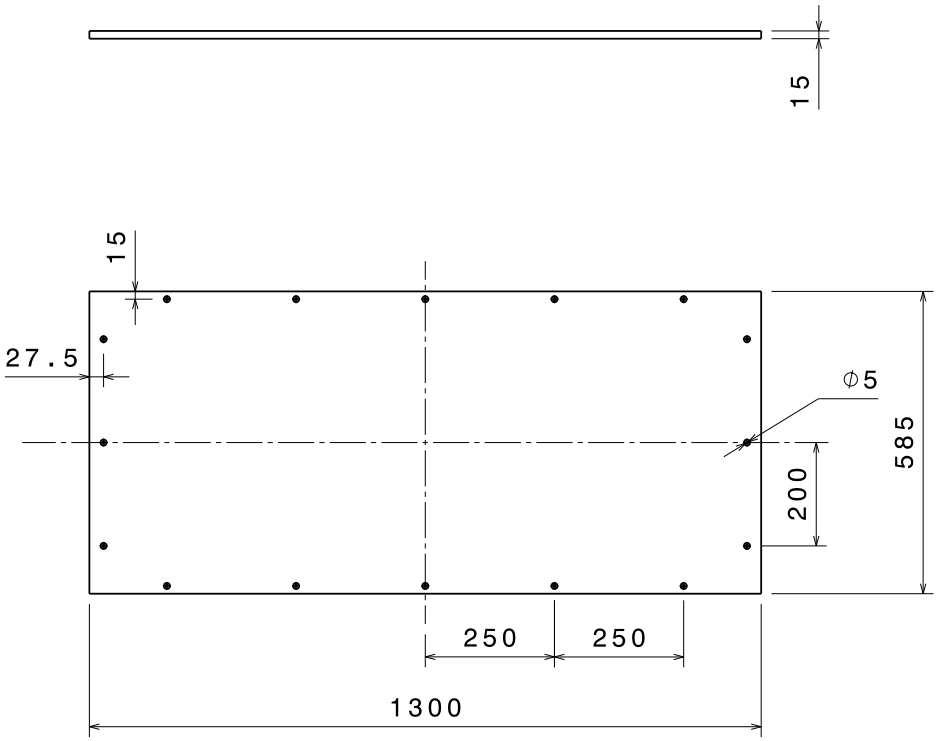

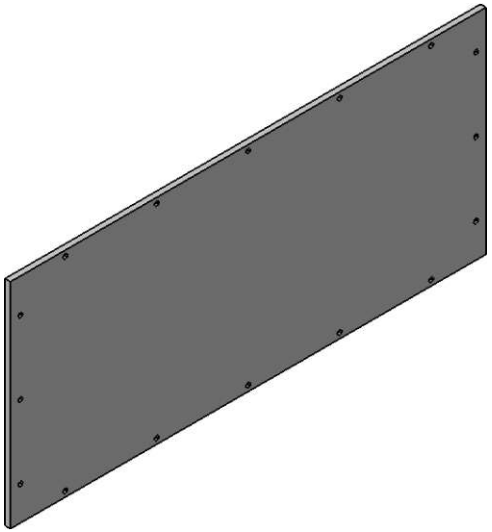

Isometric view
Scale 1:10

All drilled holes have an inner diameter of 5mm,
and a chamfer of 45°x1mm

DESIGNED BY: B. Kunitzky		Upper / lower window
DATE: 07.2021		
CHECKED BY: XXX		
DATE: XXX		
SIZE A3		Material: Acrylic glas
SCALE 1:10	Type: Part for test section	SHEET 1/1

This drawing is our property; it can't be reproduced or communicated without our written agreement.

I	_
H	_
G	_
F	_
E	_
D	_
C	_
B	_
A	_

Die approbierte gedruckte Originalversion dieser Diplomarbeit ist an der TU Wien Bibliothek verfügbar
The approved original version of this thesis is available in print at TU Wien Bibliothek.

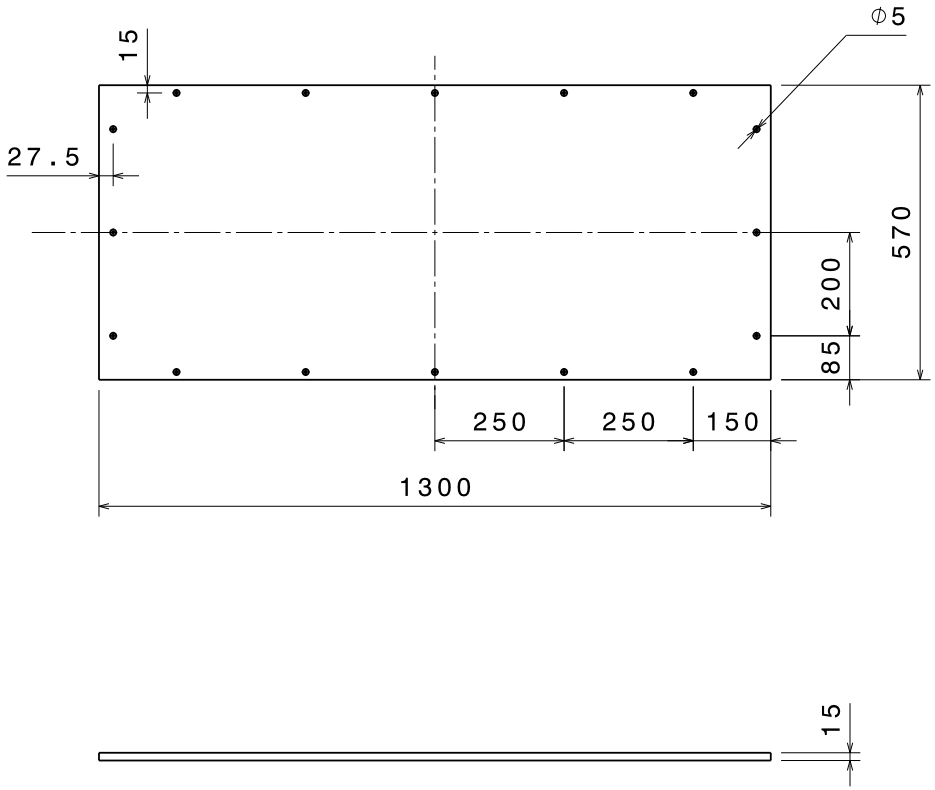

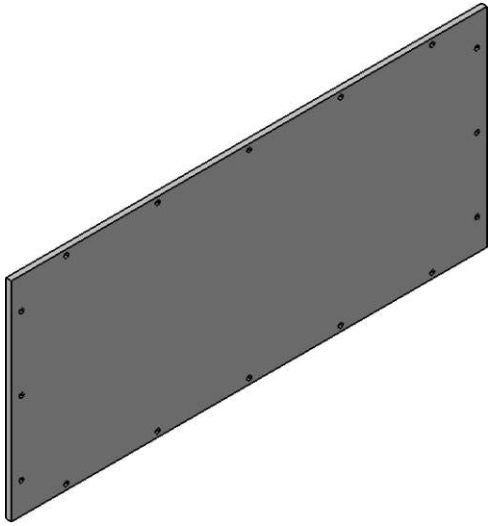

Isometric view
Sale: 1:10

All drilled holes have an inner diameter of 5mm
with a chamfer of 45°x1mm

DESIGNED BY: B. Kunitzky DATE: 07.2021	Back window		
CHECKED BY: XXX DATE: XXX			
SIZE A3	Material: Acrylic glas		
SCALE 1:10	Type: Part for test section	SHEET 1/1	

This drawing is our property; it can't be reproduced or communicated without our written agreement.

I	_
H	_
G	_
F	_
E	_
D	_
C	_
B	_
A	_

Die approbierte gedruckte Originalversion dieser Diplomarbeit ist an der TU Wien Bibliothek verfügbar
The approved original version of this thesis is available in print at TU Wien Bibliothek.
TU Bibliothek WIEN Your knowledge hub

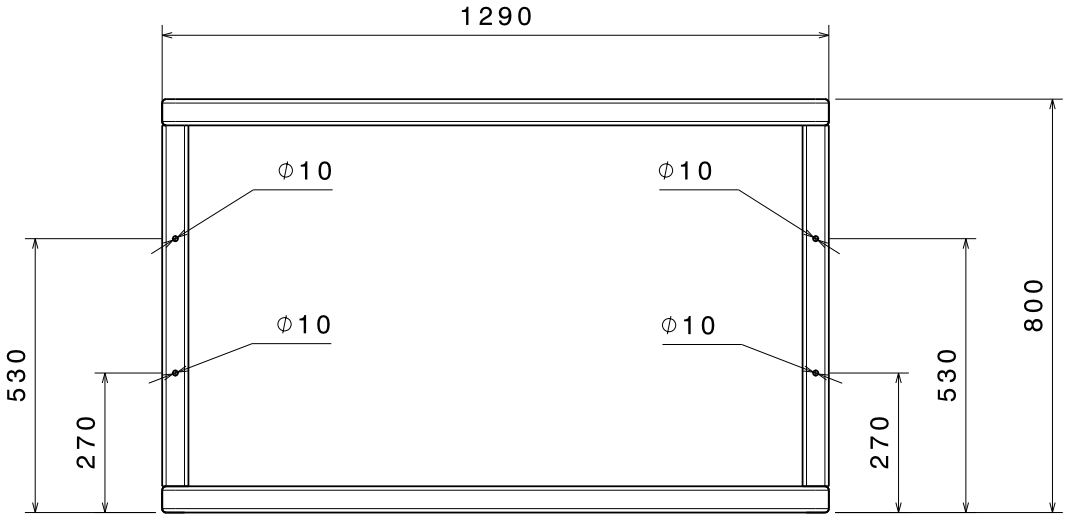

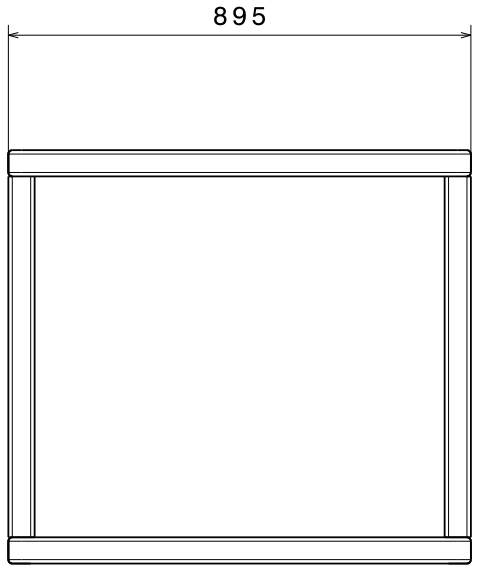

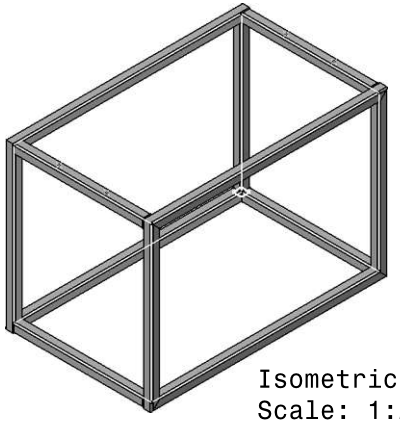

Isometric view
Scale: 1:20

DESIGNED BY: B. Kunitzky DATE: 07.2021	Rack for test section		
CHECKED BY: XXX DATE: XXX			
SIZE A3	Material: Steel profile: 50x50x2.5		
SCALE 1:10	Type: Part for test section	SHEET 1/1	

This drawing is our property; it can't be reproduced or communicated without our written agreement.

I	_
H	_
G	_
F	_
E	_
D	_
C	_
B	_
A	_

Die approbierte gedruckte Originalversion dieser Diplomarbeit ist an der TU Wien Bibliothek verfügbar
The approved original version of this thesis is available in print at TU Wien Bibliothek.
TU Wien Bibliothek Your knowledge hub

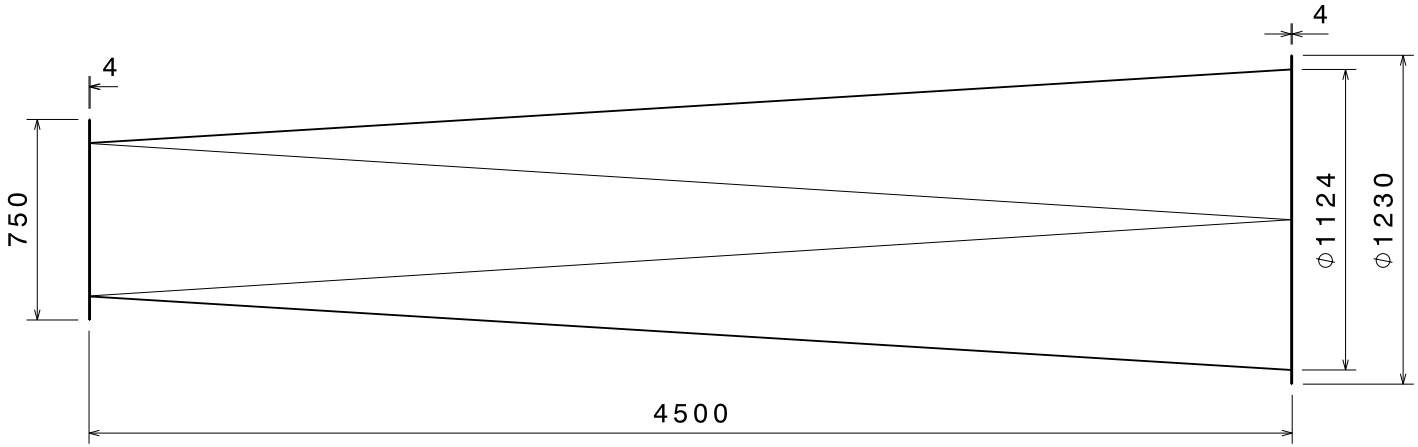

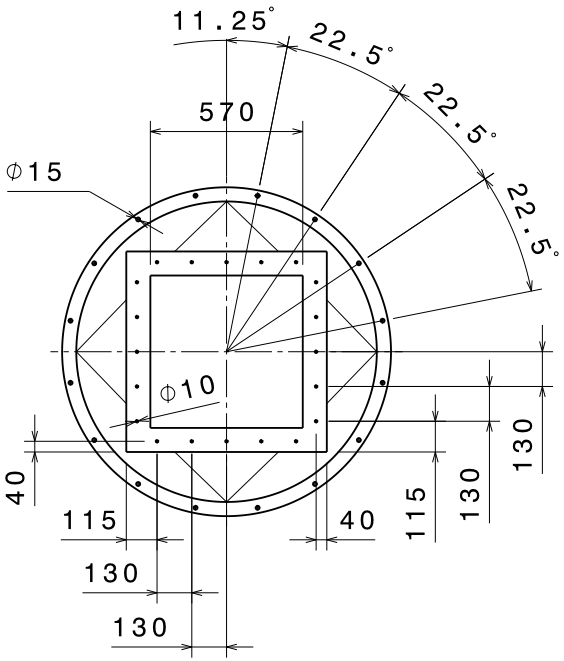

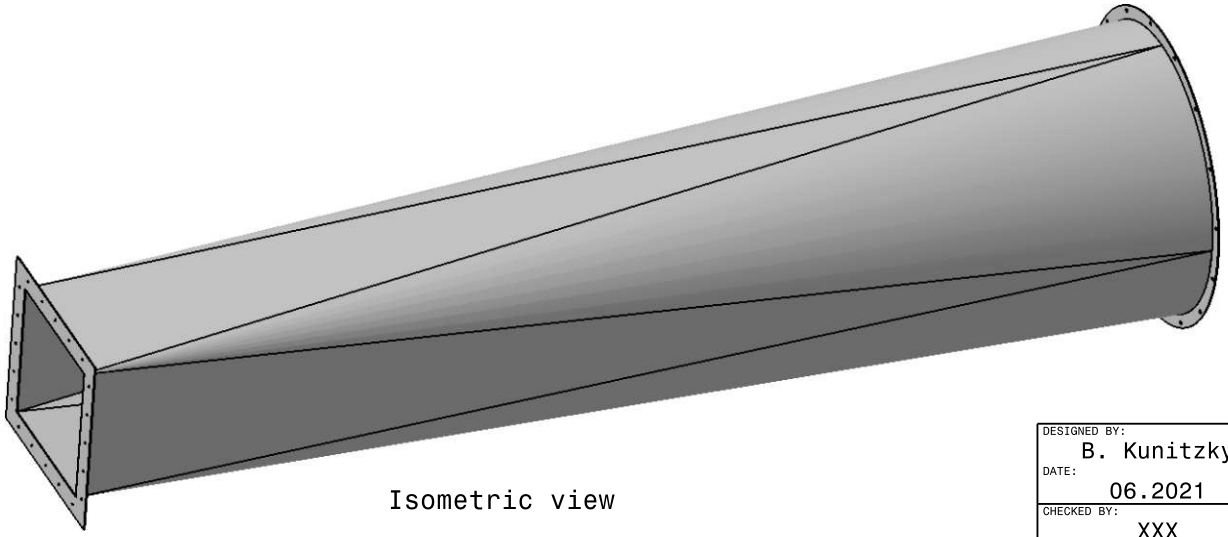

Isometric view

Wall thickness 2mm, flange thickness 4mm

DESIGNED BY: B. Kunitzky DATE: 06.2021	Diffuser		
CHECKED BY: XXX DATE: XXX			
SIZE A3	Material: 1.4301 2B (Stainless Steel)		
SCALE 1:20	WEIGHT (kg)	DRAWING NUMBER Part IV	SHEET 1/1

I	–
H	–
G	–
F	–
E	–
D	–
C	–
B	–
A	–

This drawing is our property; it can't be reproduced or communicated without our written agreement.

Die approbierte gedruckte Originalversion dieser Diplomarbeit ist an der TU Wien Bibliothek verfügbar
The approved original version of this thesis is available in print at TU Wien Bibliothek.
TU Bibliothek WIEN Your knowledge hub

Appendix C

Quotations

C.1 Quotation of the Wind Tunnel by TecQuipment

Die approbierte gedruckte Originalversion dieser Diplomarbeit ist an der TU Wien Bibliothek verfügbar
The approved original version of this thesis is available in print at TU Wien Bibliothek.
TU Bibliothek WIEN Your knowledge hub

TECQUIPMENT

Date: 07 July 2021
PROFORMA INVOICE/QUOTATION NO: Q00034696
AF1600S

	Delivery address:
Mr. Bernard Kunitzky **TU Vienna** Schuttelstrasse 27/21 Vienna 1020 Austria	Same as Invoice address

Your Ref: Our Ref: Q00034696

Total cost of goods	GBP	124,440.00
FCA (Including Packing)	GBP	3,520.00
Road Freight	GBP	1,127.00
Total price: DAP(R-PL) Vienna Austria. Incoterms ® 2020	**GBP**	**129,087.00**

Terms and Conditions:	Standard Terms and Conditions apply and are available upon request from TecQuipment Ltd
Payment Terms:	50% Payment with Order, 50% Payment Prior to Shipment
Despatch time:	Available for Shipment within 29 weeks subject to confirmation at time of order. (Please refer to individual delivery times or contact us with your requirements).
Shipment method:	Road Freight
Currency:	GB STERLING
Validity:	Up to 31 January 2022.
Origin:	United Kingdom
Power supply:	240V 1Ph 50Hz / 415V 3Ph 50Hz (please refer to our Technical Datasheets for detailed electrical requirements).

Estimated Weight: 2,657.90 Kgs Estimated Volume: 25.82 Cu. Mt.

5 Years Parts and Labour Warranty from Date of Invoice as defined in the Standard Terms and Conditions
Please Note: The minimum order value is £100.00. The above prices do not include taxes, duty or VAT.

For and on behalf of:
TecQuipment Limited

Annette Jones

Die approbierte gedruckte Originalversion dieser Diplomarbeit ist an der TU Wien Bibliothek verfügbar
The approved original version of this thesis is available in print at TU Wien Bibliothek.
TU Bibliothek WIEN Your knowledge hub

PROFORMA INVOICE/QUOTATION NO: Q00034696
TU Vienna
Your Ref:

Item	Reference	Description	Qty	Total Ex-works
1.0	AF1600S	**AF1600S SUBSONIC WIND TUNNEL SET** AF1600 Subsonic Wind Tunnel and related ancillaries including a Three Component Balance, Traverse and Instrumentation.	1	91,800.00
		Recommended ancillaries:		
1.1	AFA1	**MULTI-TUBE MANOMETER** A tilting 36-tube manometer for use with the AF100 Series Subsonic Wind Tunnel, other TecQuipment products, or as a general purpose instrument.	1	3,552.00
1.2	AFA11	**SMOKE GENERATOR** This smoke generator and probe is an optional ancillary to TecQuipment's AF1450 and AF1600 Subsonic Wind Tunnels. It allows the observation of airflow in subsonic wind tunnels. Comes with: 1X Smoke generator 1X Swan neck probe 2X Probe tips 1X Bottle of smoke oil 1X Length of tubing Manual and safety data	1	3,576.00
		Available Experiment Models:		
1.3	AF1600B	**NACA 0012 AEROFOIL WITH TAPPINGS** A 150 mm chord 600 mm span NACA0012 aerofoil with pressure tappings for use with the AF1600 Subsonic Wind Tunnel.	1	3,012.00
1.4	AF1600C	**NACA 2412 AEROFOIL WITH FLAP** A 150 mm chord NACA2412 unsymmetrical section aerofoil with 600 mm span and adjustable flap for use with the AF1600 Subsonic Wind Tunnel.	1	2,688.00
1.5	AF1600D	**SET OF 2 NACA 0012 AEROFOILS** A set of two aerofoils both of NACA0012 profile and 150 mm chord for use with the AF1600 Subsonic Wind Tunnel.	1	1,296.00
1.6	AF1600F	**BOUNDARY LAYER MODEL** A flat boundary layer model to illustrate the phenomena of boundary layer development and separation. For use with the AF1600 Subsonic Wind Tunnel.	1	5,280.00
1.7	AF1600G	**AIRCRAFT MODEL LOW WING** A model aircraft with low wing configuration for use in TecQuipment's AF1600 Wind tunnel	1	1,320.00
1.8	AF1600H	**AIRCRAFT MODEL HIGH WING** A model aircraft with high wing configuration for use in TecQuipment's AF1600 Wind tunnel	1	1,320.00
1.9	AF1600J	**THREE DIMENSIONAL DRAG MODELS**		

Die approbierte gedruckte Originalversion dieser Diplomarbeit ist an der TU Wien Bibliothek verfügbar
The approved original version of this thesis is available in print at TU Wien Bibliothek.
TU Bibliothek WIEN Your knowledge hub

PROFORMA INVOICE/QUOTATION NO: Q00034696
TU Vienna
Your Ref:

Item	Reference	Description	Qty	Total Ex-works
		Five drag investigation models for use with the TecQuipment AF1600 wind tunnel - a streamlined shape, a sphere, hemisphere, "dimpled" sphere, and a flat plate. All the models have the same frontal area for easy comparison	1	1,596.00
2.0	INSTCOM	**Inst, Commissioning & Training**	1	9,000.00
		Installation: Unpacking, and checking off parts to the packing contents lists (quantity and quality). Connection to mains services as required (suitable local services should already be in place and should be safe for the TecQuipment representative to connect to. Commissioning: Initial set up (including the removal of transit devices, filling with oil and fluids where applicable (certain oils and fluids must be provided locally, refer to the product data sheet)). Check performance to the satisfaction of the TecQuipment representative on site. Briefing to operators of how connections are made and any safety related issues to the connections. **Training** Safety (including recommended PPE), levels, norms and pre start checks Start up and shut down procedures from the manual Regular maintenance and briefing on the TecQuipment terms of warranty and spare parts and support procedure Experimental set up and techniques to take readings Performance of up to two experiments from the manual, not including manipulation and mathematical treatment of the data. ****Please note that ICT will only occur once travel restrictions due to Covid-19 are lifted. Such restrictions should not impact on the shipment of or payment for the physical goods**		
			Totals	124,440.00

Die approbierte gedruckte Originalversion dieser Diplomarbeit ist an der TU Wien Bibliothek verfügbar
The approved original version of this thesis is available in print at TU Wien Bibliothek.
TU Bibliothek WIEN Your knowledge hub

BANK PAYMENT DETAILS

Money transfer and cheque payments

BARCLAYS BANK PLC,
15 Colmore Row,
Birmingham,
B3 2BH, UK

Sort Code: 20-07-71
Account Name: TecQuipment Ltd,
A/C No: 63952975
Swift Code: BARCGB22
IBAN: GB75 BARC 2007 7163 9529 75

US Dollar money transfer and cheque payments

BARCLAYS BANK PLC,
15 Colmore Row,
Birmingham,
B3 2BH, UK

Sort Code: 20-07-71
Account Name: TecQuipment Ltd,
A/C No: 62483966
Swift Code: BARCGB22
IBAN: GB18 BARC 2007 7162 4839 66

Die approbierte gedruckte Originalversion dieser Diplomarbeit ist an der TU Wien Bibliothek verfügbar
The approved original version of this thesis is available in print at TU Wien Bibliothek.
TU Bibliothek WIEN Your knowledge hub

C.2 Quotation of the Suction Unit

Die approbierte gedruckte Originalversion dieser Diplomarbeit ist an der TU Wien Bibliothek verfügbar
The approved original version of this thesis is available in print at TU Wien Bibliothek.
TU Bibliothek WIEN Your knowledge hub

GTG
Gebläsetechnik Ges. m. b. H.

Technische Universität Wien
z. H. Hr. Bernhard Kunitzky
Karlsplatz 13
A-1040 Wien

Kunden Nr.: 2355
Von: Georg Grossauer
Datum: 04.08.2021

Angebot Nr. 1210311

Wir danken für Ihre Anfrage und bieten auf Grundlage unserer Allgemeinen Geschäftsbedingungen wie folgt an:

Pos	Menge		Text	Einzelpreis EUR	Gesamtpreis EUR
1			**Variante 1 - 50 m/s - 55 kW:**		
1.1	1	Stk.	Radialventilator RS 1000 RI - 55 kW	9.169,00	9.169,00
1.2	1	Stk.	Rohrschalldämpfer SIL-1000-2	3.278,00	3.278,00
1.3	1	Stk.	Frequenzumformer 55 kW	5.156,00	5.156,00
			Summe Variante 1 - 50 m/s - 55 kW:		**17.603,00**

GTG Gebläsetechnik Ges. m. b. H.
Perfektastrasse 79
A-1230 Wien
Firmenbuch: FN 279 638 h

Telefon: +43 1 603 58 19
Telefax: +43 1 600 77 19
e-mail: gtg@gtg.at
DVR Nr.: 101 39 47

BIC: RLN WAT WW
IBAN: AT93 3200 0000 0661 0802
Steuer Nr.: 092/1842
UID-Nr.: ATU 626 31 655

Die approbierte gedruckte Originalversion dieser Diplomarbeit ist an der TU Wien Bibliothek verfügbar
The approved original version of this thesis is available in print at TU Wien Bibliothek.
TU Bibliothek WIEN Your knowledge hub

Pos	Menge		Text	Einzelpreis EUR	Gesamtpreis EUR
2			**Variante 2 - 54 m/s - 75 kW:**		
2.1	1	Stk.	Radialventilator RS 1000 - 75 kW	9.736,00	9.736,00
2.2	1	Stk.	Rohrschalldämpfer SIL-1000-2	3.278,00	3.278,00
2.3	1	Stk.	Frequenzumformer 75 kW	6.344,00	6.344,00
			Summe Variante 2 - 54 m/s - 75 kW:		**19.358,00**
3			**Variante 3 - 60 m/s - 90 kW:**		
3.1	1	Stk.	Radialventilator RS 1120 RI - 90 kW	12.318,00	12.318,00
3.2	1	Stk.	Rohrschalldämpfer SIL-1120-2	3.654,00	3.654,00
3.3	1	Stk.	Frequenzumformer 90 kW	7.302,00	7.302,00
			Summe Variante 3 - 60 m/s - 90 kW:		**23.274,00**

Die approbierte gedruckte Originalversion dieser Diplomarbeit ist an der TU Wien Bibliothek verfügbar
The approved original version of this thesis is available in print at TU Wien Bibliothek.
TU Bibliothek WIEN Your knowledge hub

Pos	Menge		Text	Einzelpreis EUR	Gesamtpreis EUR
			Radialventilator einseitig saugend Type RS 1120 Leistungsdaten: + 70.000 m3/h + 2.37 Pa Pstat + 1.318 min-1 (ca. 44 Hz) Anlauf, Drehzahlregelung: + über Frequenzumformer (nicht im Lieferumfang enthalten) Auslegungsdaten: + Saubere Luft; 20 ° C + Auslegungsdichte 1,17 kg/m3 Ausführung: + Radialventilator einseitig saugend + direkt getrieben, Laufrad auf der Motorwelle - esec 4 + Werkstoff Stahlblech Oberflächenschutz: + Stahlteile entfettet und handentrostet + Anstrich Herstellerstandard Ausblasposition: + nach Kundenwunsch + RD/LG 180 - 235 nur auf Anfrage Zubehör - inklusive: + Drehstrommotor 90 kW; 4-polig 400 V; 50 Hz; Iso F; IP 55; B 3 ca. 157 A bei 400 V Effizienzklasse IE-3 + Kaltleiter + Inspektionsöffnung + Gummischwingungsdämpfer + Wellenabdichtung - Standard		

GTG Gebläsetechnik Ges. m. b. H.
Perfektastrasse 79
A-1230 Wien
Firmenbuch: FN 279 638 h

Telefon: +43 1 603 58 19
Telefax: +43 1 600 77 19
e-mail: gtg@gtg.at
DVR Nr.: 101 39 47

BIC: RLN WAT WW
IBAN: AT93 3200 0000 0661 0802
Steuer Nr.: 092/1842
UID-Nr.: ATU 626 31 655

Die approbierte gedruckte Originalversion dieser Diplomarbeit ist an der TU Wien Bibliothek verfügbar
The approved original version of this thesis is available in print at TU Wien Bibliothek.
TU Bibliothek WIEN Your knowledge hub

Pos	Menge		Text	Einzelpreis EUR	Gesamtpreis EUR
			Rohrschalldämpfer: + Ausführung ohne Kern + Länge ca. 2500 mm + verzinkte Ausführung + inkl. Übergangsstück zur Ausblasseite des Ventilators Frequenzumformer: + SIEMENS G120P + Gehäuse IP 55 + Bedienelement IOP-2-BT		

Die approbierte gedruckte Originalversion dieser Diplomarbeit ist an der TU Wien Bibliothek verfügbar
The approved original version of this thesis is available in print at TU Wien Bibliothek.
TU Bibliothek WIEN Your knowledge hub

Pos	Menge		Text	Einzelpreis EUR	Gesamtpreis EUR
			Hinweise - Berechnungsgrundlagen: + Die angegebene Luftgeschwindigkeit soll im Querschnitt 570 x 570 mm erreicht werden. + Danach folgt ein Übergang auf Rohrleitung NW 1000 bzw. NW 1120 mm. + An diesen Übergang wird der Ventilator angeschlossen. + Diese Bauteile sind nicht in unserem Angebotsumfang enthalten. + Nach dem Ventilator kann mittels Übergangsstück eckig/rund der Schalldämpfer angeschlossen werden (optional angeboten). + Unser Lieferumfang umfasst nur die Lieferung der im Angebot angeführten Teile, exkl. Einbringung, Montage, Verkabelung etc.		

Die approbierte gedruckte Originalversion dieser Diplomarbeit ist an der TU Wien Bibliothek verfügbar
The approved original version of this thesis is available in print at TU Wien Bibliothek.
TU Bibliothek WIEN Your knowledge hub

Pos	Menge	Text	Einzelpreis EUR	Gesamtpreis EUR
Summe Variante 1 - 50 m/s - 55 kW:				17.603,00
Summe Variante 2 - 54 m/s - 75 kW:				19.358,00
Summe Variante 3 - 60 m/s - 90 kW:				23.274,00

Angebotsgültigkeit:
1 Monat; Änderungen und Irrtum vorbehalten

Lieferung:
DAP frachtfrei geliefert an Ihre Adresse in Wien

Gewährleistungsfrist:
24 Monate nach Lieferung - ausgenommen Verschleiß und Verschleißte

Lieferzeit:
+ aktuell ca.16 Arbeitswochen (August und KW 52 - KW 2 Betriebsurlaub)
+ Auf Grund der aktuellen Situation weisen wir ausdrücklich darauf hin, dass die Angaben zu Lieferzeiten nur unter Vorbehalt gelten. Maßnahmen im Zusammenhang mit dem Coronavirus sowie die derzeit auf den internationalen Märkten vorherrschende Verknappung der Rohmaterialien lassen zur Zeit keine exakten Angaben zu den Lieferzeiten zu.

Preisstellung:
Preis pro Stück; netto exkl. USt

Zahlung:
Innerhalb von 14 Tagen ab Rechnungsdatum abzüglich 2 % Skonto oder nach 30 Tagen ohne Abzug; vorbehaltlich Bestätigung durch unsere Kreditüberprüfung.

Wir danken für Ihr Interesse und stehen für allfällige Rückfragen jederzeit gerne zur Verfügung.

Mit freundlichen Grüßen!

GTG Gebläsetechnik Ges. m. b. H.
Perfektastraße 79
A-1230 Wien

Georg Grossauer

Die approbierte gedruckte Originalversion dieser Diplomarbeit ist an der TU Wien Bibliothek verfügbar
The approved original version of this thesis is available in print at TU Wien Bibliothek.
TU Bibliothek WIEN Your knowledge hub

Lieferbedingungen:
Grundlage unserer Verkaufsgeschäfte bilden ausschließlich unsere „Allgemeinen Geschäftsbedingungen“ in der jeweils gültigen Fassung, welche unter www.gtg.at eingesehen werden können. In unserem Angebot/unserer Auftragsbestätigung sind alle technischen Angaben enthalten, die uns bekannt gegeben worden sind. Bei Betriebsbedingungen, die davon oder von unserer Auftragsbestätigung abweichen, wird keinerlei Haftung übernommen.

Gewährleistung:
Die Gewährleistungsdauer ist in unserem Angebot/unserer Auftragsbestätigung angeführt und beginnt ab erfolgter Lieferung. Von der Gewährleistung ausgeschlossen sind Verbrauchs- und Verschleißteile wie z. B. Lager, Schwingungsdämpfer, Kompensatoren, Dichtungen, Keilriemen und -scheiben sowie alle Schäden, die durch Transport, Montage, fehlerhafte Inbetriebnahme, unsachgemäße Lagerung, mangelhafte Wartung und dergleichen eintreten.

Abwicklung von Gewährleistungsansprüchen:
Falls der Verdacht eines Gewährleistungsanspruches besteht, sind wir umgehend davon schriftlich zu verständigen. Der beanstandete Teil ist an uns zur Überprüfung zu senden. Falls der Gewährleistungsanspruch zu Recht besteht, wird die Ware von uns repariert oder ein neuer Teil zur Verfügung gestellt. Falls die Mängelrüge zu Unrecht erfolgte, erhalten Sie von uns einen Kostenvoranschlag zu Reparatur oder Neukauf. Für den reparierten/getauschten Teil beginnt die Gewährleistungsdauer neu zu laufen, längstens jedoch für 12 Monate. Allfällige Transport- und Montagekosten gehen zu Lasten des Käufers. Wir weisen darauf hin, dass sechs Monate nach Lieferung gemäß § 924 GewRÄG die Beweislast zur Feststellung eines Mangels, der schon bei der Auslieferung bestanden haben soll, beim Käufer liegt.

Folgeschaden-Ausschlussklausel:
Besteller und Lieferer sind sich grundsätzlich einig, dass bei eventuellen Schadenersatzansprüchen dem Besteller keine Ansprüche auf Ersatz von mittelbaren Schäden zustehen. Schäden, die nicht am Liefergegenstand selbst entstanden sind, z. B. Produktionsausfall, Stand- , Anreise- und Montagezeiten, Zinsverlust und entgangener Gewinn, sind ausgeschlossen, soweit nicht ein vorsätzliches Tun oder Unterlassen des Lieferers zweifelsfrei vorliegt.

Zahlung:
siehe Angebotsblatt; vorbehaltlich Bestätigung durch unsere Kreditversicherung

Preisstellung:
siehe Angebotsblatt; transportverpackt; pro Stück; exkl. USt; exkl. Montage; exkl. Inbetriebnahme

Lieferzeit:
siehe Angebotsblatt; August und KW 51 - KW 2 Betriebsurlaub

Gerichtsstand und Erfüllungsort:
Gerichtsstand und Erfüllungsort ist Wien

Gültigkeit:
Änderungen und Irrtum vorbehalten

Eigentumsvorbehalt:
Der Eigentumsvorbehalt ist ausdrücklich vereinbart und kann auch durch keine anders lautenden Bedingungen ausgeschlossen werden. Bis zur vollständigen Bezahlung bleibt die Ware unser Eigentum.

Ausführung:
Der Schalldruckpegel wurde gemäß DIN 45 635 Teil 1 und Teil 38 ermittelt. Die angegebenen Werte gelten bei Freifeldmessung in 5 m Entfernung, Ventilator saug- und druckseitig angeschlossen, Toleranz ± 4 dB(A). Die Fördertoleranz beträgt ± 5 %. Die Ventilatoren sind nach DIN 24166 in Genauigkeitsklasse 2 und gemäß den gültigen CE - Vorschriften gefertigt. Das Laufrad ist statisch und dynamisch mindestens nach DIN ISO 1940 T 1 G 6.3 gewuchtet. Für Schwingungen im eingebauten Zustand gelten die Werte der ISO 14694 (E) BV-3 „Table 5 – *in situ*“ gemessen an Teilen, die nicht durch Antrieb oder Luftstrom Vibrationen ausgesetzt sind (z. B. Lagerung bei Riemenantrieb, Motor bei Direktantrieb).

Funkenschutz:
Funkensichere Ventilatoren sind in Anlehnung an DIN EN 14986 2004 08 funkensicher oder nach ATEX ausgeführt.

Die approbierte gedruckte Originalversion dieser Diplomarbeit ist an der TU Wien Bibliothek verfügbar
The approved original version of this thesis is available in print at TU Wien Bibliothek.
TU Bibliothek WIEN Your knowledge hub

Ausblaspositionen:

Die Drehrichtung wird bestimmt, in dem man die der Ansaugöffnung gegenüberliegende Seite betrachtet, also die Antriebsseite. Soll sich das Laufrad im Uhrzeigersinn drehen, wird das mit den Buchstaben RD (früher GR) bestimmt, bei Drehen gegen den Uhrzeigersinn mit den Buchstaben LG (früher GL).

Der Ausblaswinkel wird in ° (Grad) angegeben und zeigt die Stellung der Ausblasöffnung.

Die untenstehende Tabelle zeigt die Winkel, in denen die Ventilatorgehäuse lieferbar sind. Bitte beachten Sie, dass nur bei kleinen Gebläsen die Ausblasposition noch nachträglich geändert werden kann.

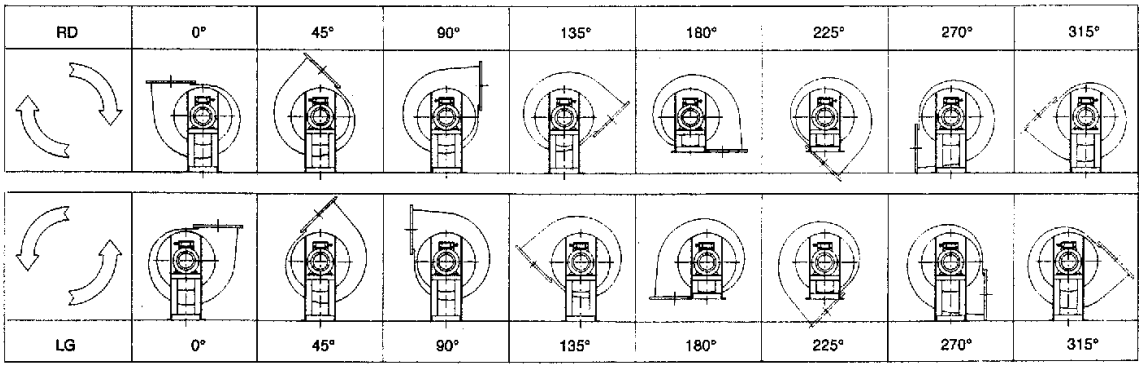

Motorlagen:

Bei keilriemengetriebenen Ventilatoren können Sie die Position des Motors mit Hilfe der untenstehenden Tabelle bestimmen. Bei Ausführung esec 9 (Motor seitlich am Lagerbock montieret) sind nur die Positionen „Z“ und „W“ lieferbar, bei Ausführung esec 12 (Motor am Grundrahmen montiert) können Sie unter allen vier Möglichkeiten wählen.

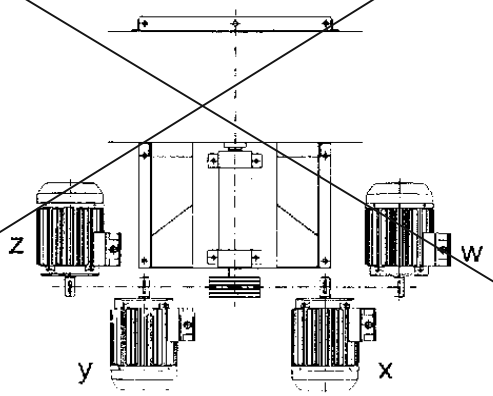

GTG Gebläsetechnik Ges. m. b. H.
Perfektastraße 79
A-1230 Wien
Firmenbuchnr. FN 279638h
Telefon: + 43 1 603 58 19
Telefax: + 43 1 600 77 19
e-mail: gtg@gtg.at
DVR-Nr.: 1013947
Bank: RLB NÖ- Wien
Konto: 6.610.802
UID-Nr.: ATU 626 31 655
Steuer-Nr.: 092/1842

Die approbierte gedruckte Originalversion dieser Diplomarbeit ist an der TU Wien Bibliothek verfügbar
The approved original version of this thesis is available in print at TU Wien Bibliothek.
TU Bibliothek WIEN Your knowledge hub

TU Wien

Variante 3

Ventilator RS 1120 RI – 90 kW

Die approbierte gedruckte Originalversion dieser Diplomarbeit ist an der TU Wien Bibliothek verfügbar
The approved original version of this thesis is available in print at TU Wien Bibliothek.
TU Bibliothek WIEN Your knowledge hub

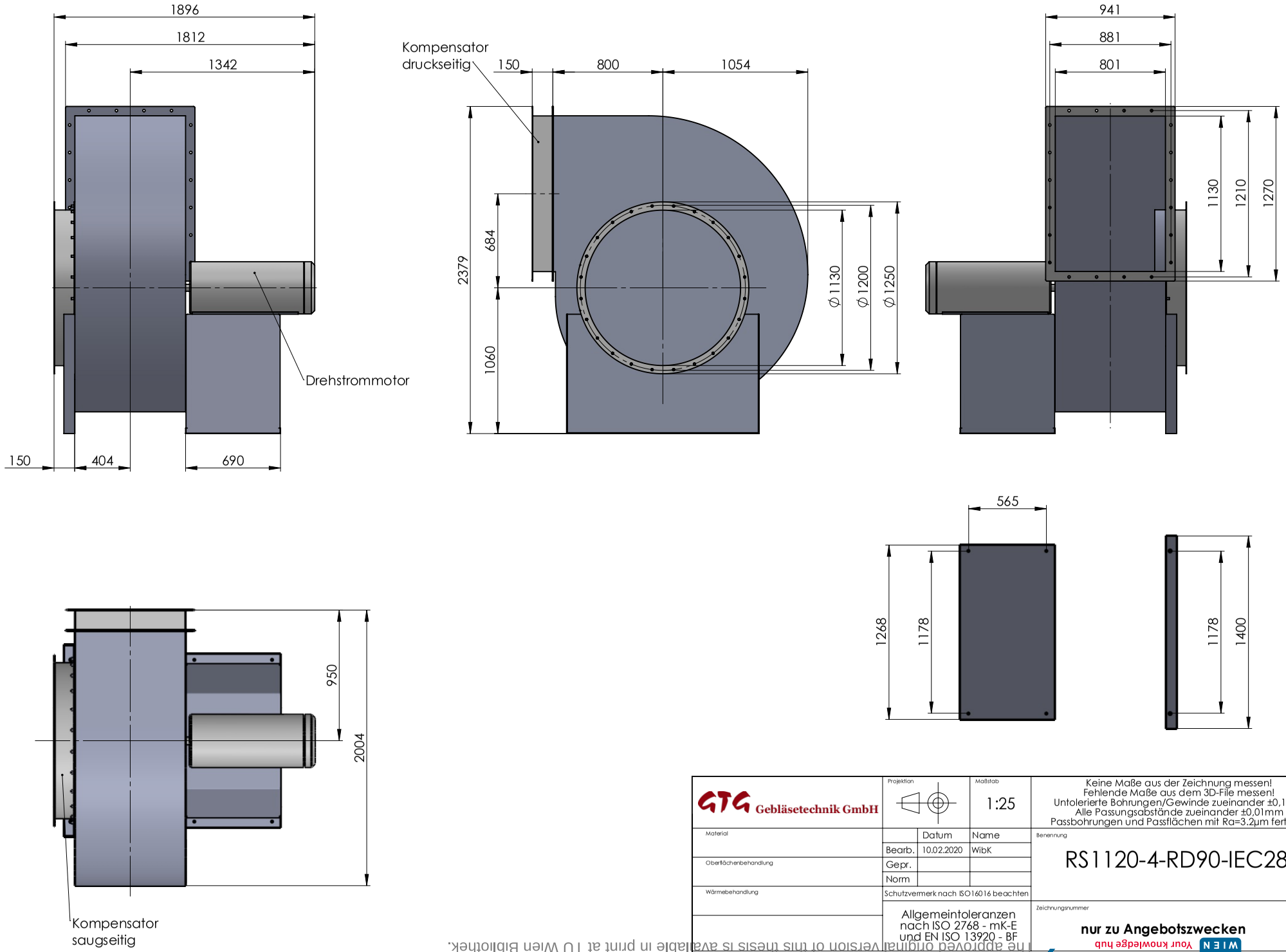
1896
1812
1342
150
404
690
Drehstrommotor
Kompensator
druckseitig
150
800
1054
2379
684
1060
Ø1130
Ø1200
Ø1250
941
881
801
1130
1210
1270
565
1268
1178
1178
1400
950
2004
Kompensator
saugseitig
GTG Gebläsetechnik GmbH
Projektion
Maßstab
1:25
Keine Maße aus der Zeichnung messen!
Fehlende Maße aus dem 3D-File messen!
Untolerierte Bohrungen/Gewinde zueinander ±0,1mm
Alle Passungsabstände zueinander ±0,01mm
Passbohrungen und Passflächen mit Ra=3.2µm fertigen
Material
Datum
Name
Bearb.
10.02.2020
WibK
Benennung
RS1120-4-RD90-IEC280
Oberflächenbehandlung
Gepr.
Norm
Wärmebehandlung
Schutzvermerk nach ISO16016 beachten
Allgemeintoleranzen
nach ISO 2768 - mK-E
und EN ISO 13920 - BF
Zeichnungsnummer
nur zu Angebotszwecken
Blatt
1 - 1
A3
GTG-Gebläsetechnik Ges.m.b.H. - A-1230 Wien - Perfektastr.
Die approbierte gedruckte Originalversion dieser Diplomarbeit ist an der TU Wien Bibliothek verfügbar
The approved original version of this thesis is available in print at TU Wien Bibliothek.
TU Bibliothek
WIEN
Your knowledge hub

GTG Gebläsetechnik GmbH

www.gtg.at

Projekt :	Variante 3	Datum :	03.08.2021
Ventilatortype :	**RS 1120**	Drehzahl :	**1318 1/min**

Auslegungsdaten :

Luftmenge :	70000	m³/h	Fördermedium :	alle	
	1166.67	m³/min	Temperatur Ansaugöffnung :	20	°C
	19.444	m³/s	Temperatur Ausblasöffnung :	23	°C
	63415	Nm³/h	Seehöhe :	200	m
Massestrom :	22.77	kg/s	Barometrischer Druck :	989.46	mbar
Luftgeschwindigkeit Ansaugöffnung :	19.39	m/s	Stat. Druck saugseitig :	963.46	mbar
Luftgeschwindigkeit Ausblasöffnung :	21.49	m/s	Feuchtigkeit :	50	%
			Dichte :	1.17076	kg/m³
			Normdichte :	1.29233	kg/Nm³

bei 1.2 kg/m³ :			bei 1.171 kg/m³ :		
Gesamtdruck :	2972.43	Pa	Gesamtdruck :	2900	Pa
	303.11	mmWS		295.72	mmWS
	29.73	mbar		29	mbar
Stat. Druck :	2695.53	Pa	Statischer Druck :	2629.85	Pa
	274.87	mmWS		268.17	mmWS
	26.96	mbar		26.3	mbar
Stat. Druck saugseitig :	-2439.38	Pa	Stat. Druck saugseitig :	-2379.94	Pa
Stat. Druck druckseitig :	30.6	Pa	Stat. Druck druckseitig :	29.85	Pa
Dynam. Druck saugseitig :	225.56	Pa	Dynam. Druck saugseitig :	220.06	Pa
Dynam. Druck druckseitig :	276.9	Pa	Dynam. Druck druckseitig :	270.16	Pa
Leistung an der Welle :	70.65	kW	Leistung an der Welle :	68.92	kW

Mechanische Daten :

Wirkungsgrad :	81.82	%
Ansaugöffnung i. L. :	1130	Ø mm
Laufradgewicht :	178.04	kg
Ausblasöffnung i. L- :	1130 x 801	mm
Laufrad GD² :	134	kg x m²
Laufraddurchmesser :	1120	Ø mm
Umfangsgeschwindigkeit:	77.3	m/s
Ventilatordrehzahl :	1318	1/min
Klasse :	III	

Elektrische Daten :

Motorleistung :	90	kW :
Motordrehzahl :	1485	1/min
Nennstrom :	157	A
Spannung :	400	V
Frequenz :	50	Hz
Anlaufzeit bei offener Klappe :	7.74	s
Anlaufzeit bei geschlossener Klappe :	8.65	s

Schalldaten :

LwA 0 :	97	
LwA 1 :	106	
LwA 2 :	115	
LpA 0 :	86	1 m
LpA 1 :	95	1 m
LpA 2 :	104	1 m
LpA 0 :	66	10 m
LpA 1 :	75	10 m
LpA 2 :	84	10 m

LpA 0 und LwA 0: Anschluss saug-und druckseitig
LpA 1 und LwA 1: Anschluss saug-oder druckseitig
LpA 2 und LwA 2: Saug-und druckseitig kein Anschluss

Die approbierte gedruckte Originalversion dieser Diplomarbeit ist an der TU Wien Bibliothek verfügbar.
The approved original version of this thesis is available in print at TU Wien Bibliothek.
TU Bibliothek WIEN Your knowledge hub

GTG Gebläsetechnik GmbH

www.gtg.at

Projekt :	Variante 3	Datum :	03.08.2021
Ventilatortype :	**RS 1120**	Drehzahl :	**1318 1/min**

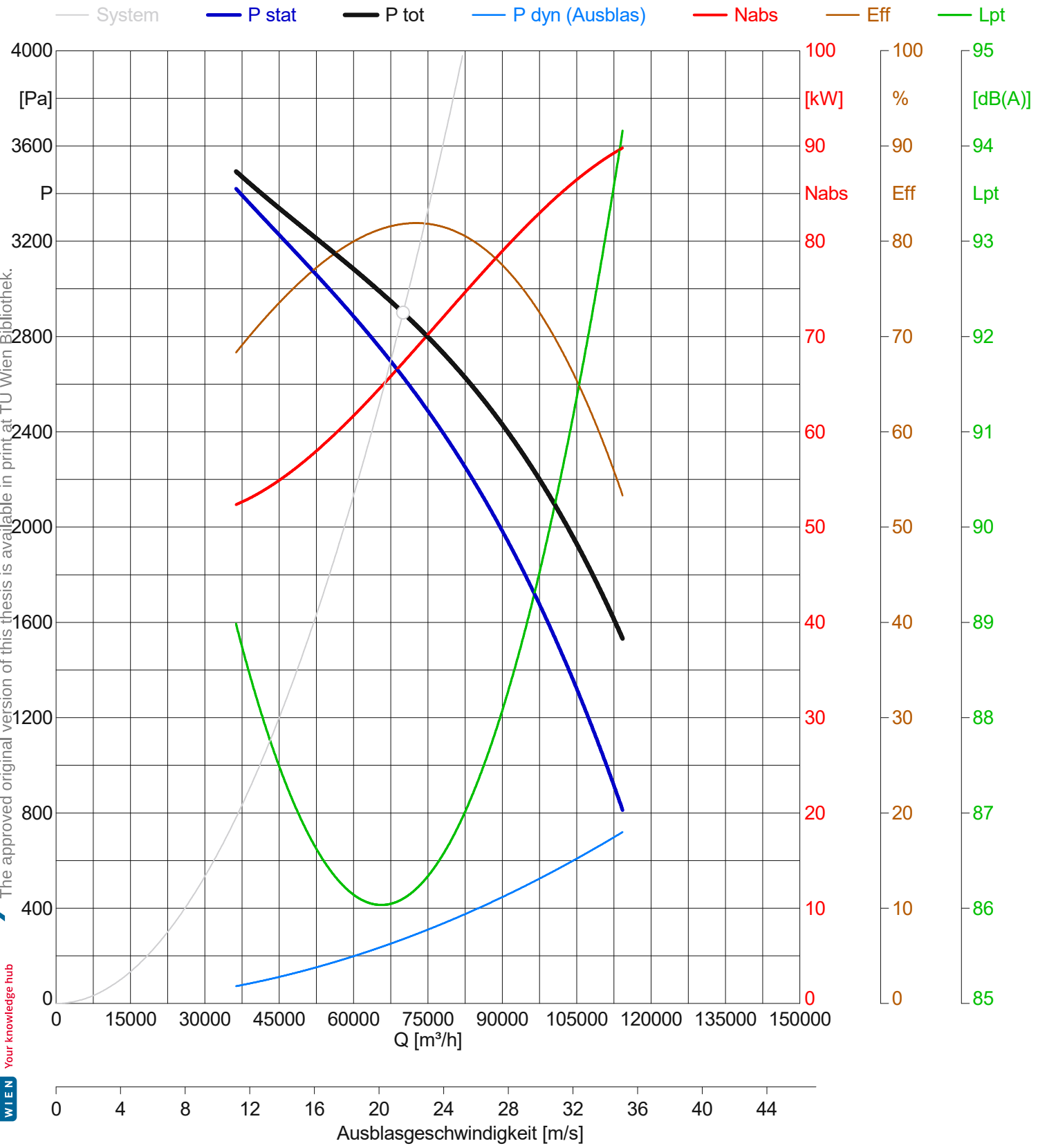

Die approbierte gedruckte Originalversion dieser Diplomarbeit ist an der TU Wien Bibliothek verfügbar
The approved original version of this thesis is available in print at TU Wien Bibliothek.
TU Bibliothek WIEN Your knowledge hub

GTG Gebläsetechnik GmbH

www.gtg.at

Projekt :	Variante 3	Datum :	03.08.2021
Ventilatortype :	**RS 1120**	Dichte :	**1.171 kg/m³**

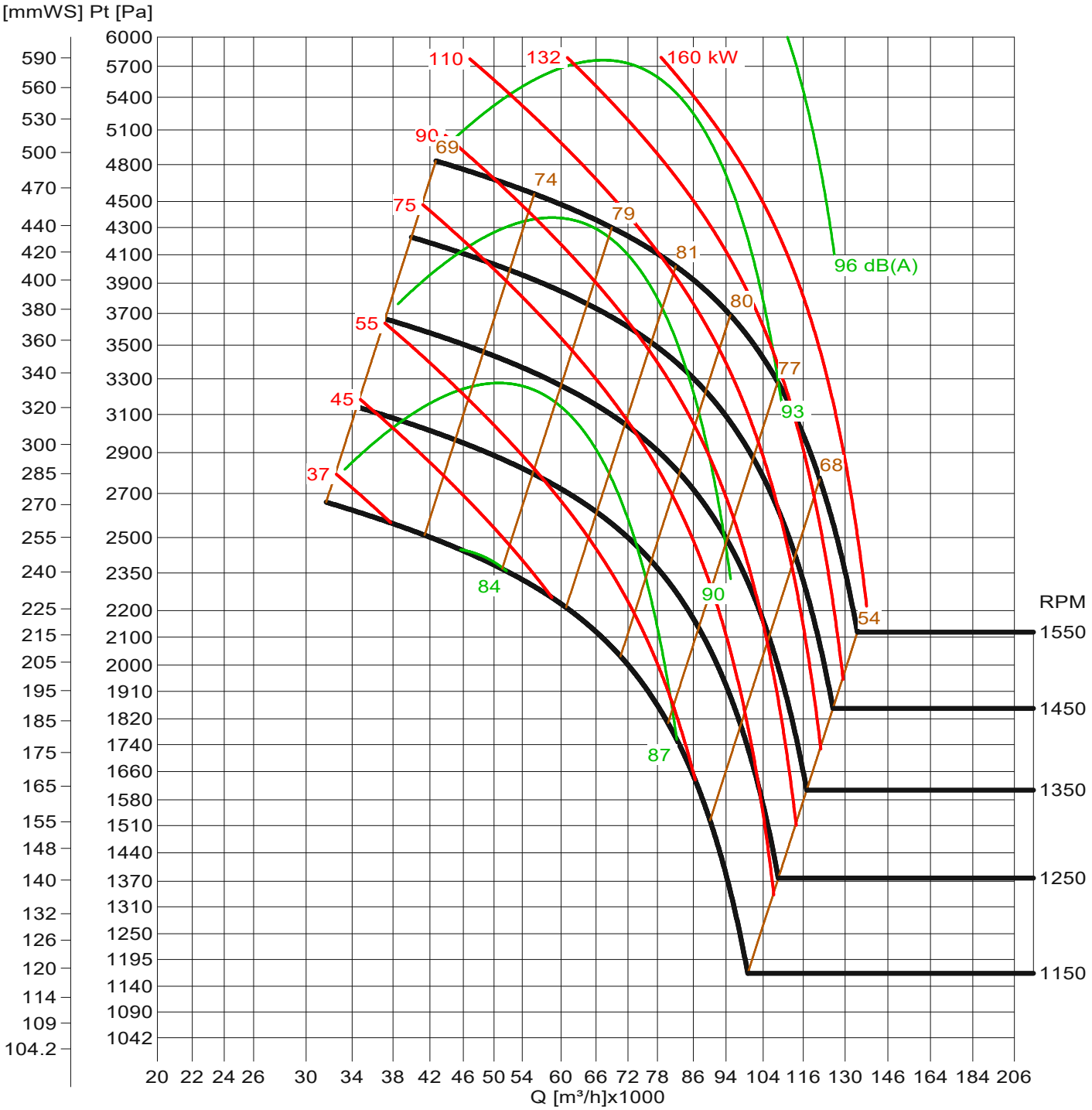

Q [m³/s]	5.9 6.5 7.4 8 8.6 9.5 10.7 12.2 14 15.5 17.6 20 22.1 25.1 28.4 32 35 38 41 45.5 51.5 58.4
v [m/s]	9 9.8 11 12.2 17 21 25 29 33 37 41 45 49 53 61
Pd [Pa]	24 28 34 40 48 56 66 78 92 112 140 174 216 268 332 412 512 634 786 974 1246 1646 2176
Pd [mmWS]	2.52 3 3.54 4.5 5.4 6.6 8.1 9.9 12 14.7 18 21 25.8 33 39 47.7 60 72 84 99 120 150 186 231

Die approbierte gedruckte Originalversion dieser Diplomarbeit ist an der TU Wien Bibliothek verfügbar
The approved original version of this thesis is available in print at TU Wien Bibliothek.
TU Bibliothek WIEN Your knowledge hub

Datenblatt für AC - DS-KL-Motoren

Motortype	ACM 280M - 4 / PHE	IM B3 / IM 1001
	Premium High Efficiency	

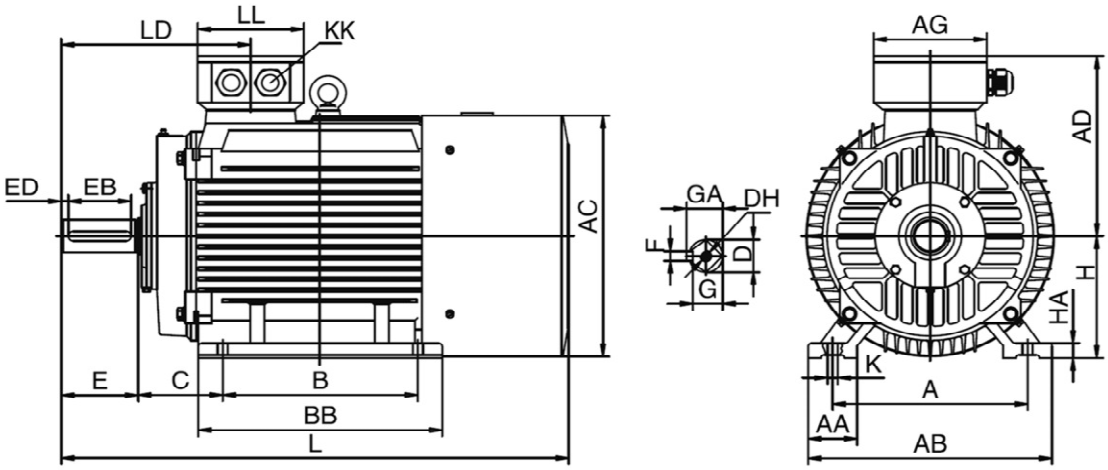

TYP	A	AA	AB	AC	AD	AG	B	BB	C	D	DH	E	EB	ED	F	G	GA	H	HA	K	KK	L	LD	LL
280M-4,6	457	85	542	547	387	248	419	536	190	75	M20X42	140	125	7,5	20	67,5	79,5	280	35	4-Ø24	2-M63X1,5	1033	355,5	218

Elektrische Daten

Motorleistung	**90,0 / 108**	KW 50 / 60 Hz
Motordrehzahl	**1486**	min-1 / 50 Hz
	1783,2	min-1 / 60 Hz
Spannung (+-5%)	**400**	V Δ / 50 Hz
	690	V Y / 50 Hz
	460	V Δ / 60 Hz
	795	V Y / 60 Hz
Motornennmoment	**578**	Nm (Mn)
Motornennstrom 50Hz	**157 / 90,9**	A (In)
Motornennstrom 60Hz	**164 / 94,7**	A (In)
Anzugsstrom	**6,7**	x In
Anlaufmoment	**2,2**	x Mn
Kippmoment	**2,3**	x Mn
Wirkungsgrad	**95,2%**	bei 100 % Last
	95,2%	bei 75 % Last
	93,3%	bei 50 % Last
IE-Klasse	**IE3**	
Leistungsfaktor	**0,87**	bei 100 % Last

Mechanische Daten

Schalldruckpegel	**65,0**	dB(A)
Trägheitsmoment	**1,48000**	Kgm²
Lager A - Seite	**6317.ZZ.C3**	
Lager B - Seite	**6317.ZZ.C3**	
nom. Lagerlebensdauer	**20000 h**	bei Fr + Fx
zulässige Radiallast (Fr)	**8541 N**	Wellenmitte
zulässige Axiallast (Fx)	**5100 N**	Zug
	6300 N	Druck
Art der Lagerung	**Festlager BS**	Standard

Explosionsschutz

Zündschutzart	**ohne**

Allgemeine Daten

Motorbaugröße	**280M**	
Bauform	**IM B3 / IM 1001**	
Gewicht	**835,0**	kg
Gehäusematerial	**Grauguß**	
Schutzart	**IP 55**	
Isolationsklasse	**F genutzt nach B**	
Tropenisolation	**nein**	
Schwingstufe	**A**	
Läufer sind	**Halbkeil gewuchtet**	
Betriebsart	**S1**	
Drehrichtung	**rechts / links**	
Kühlart / TEFC	**IC 411**	
Kabelverschraubung	**2-M63x1,5**	
Normen / Vorschriften	**IEC / DIN / ISO / VDE / EN**	
Ausführung nach	**IEC 60034 -1**	
Anstrich	**RAL 7030**	steingrau
Garantie	**12 Monate**	

Umweltbedingung

Kühlmitteltemperatur	**- 20 bis + 40**	°C
max. Aufstellhöhe	**1.000**	m über NN

Zubehör

3 eingebaute Kaltleiterfühler
.
.
.
.
.
.
.
.
.
.
.
.

Technische Änderungen und Irrtümer vorbehalten / Technical modifications reserved, errors excepted

Die approbierte gedruckte Originalversion dieser Diplomarbeit ist an der TU Wien Bibliothek verfügbar
The approved original version of this thesis is available in print at TU Wien Bibliothek.
TU Bibliothek WIEN Your knowledge hub

C.3 Quotation of the Manufactured Components

Die approbierte gedruckte Originalversion dieser Diplomarbeit ist an der TU Wien Bibliothek verfügbar
The approved original version of this thesis is available in print at TU Wien Bibliothek.
TU Bibliothek WIEN Your knowledge hub

Die approbierte gedruckte Originalversion dieser Diplomarbeit ist an der TU Wien Bibliothek verfügbar
The approved original version of this thesis is available in print at TU Wien Bibliothek.
TU Bibliothek WIEN Your knowledge hub

INNOWELD-Metallverarbeitung GmbH * Hönigsberggasse 3, 8682 Hönigsberg, AUSTRIA

Technische Universität Wien
Getreidemarkt 9/302
1060 Wien
AUSTRIA

Angebot

Belegnummer	**AN-508585**
Datum	30.07.2021
Kunden Nr.	21837
Seite	1 von 2
Ihre UID Nr.	ATU37675002

Verkauf	
Erstellt von	Martin Hirschler
Lieferzeit	nach Vereinbarung
Anfrage	Kostenvoranschlag / Herstellmöglichkeiten für Windtunnel

L

In der Zeit vom 02.08.2021 bis einschließlich 06.08.2021 haben wir Betriebsurlaub.

Wir danken für Ihre Anfrage und erlauben uns, gemäß unseren Lieferbedingungen wie folgt anzubieten:

Pos	Menge	MEH	Bezeichnung	Preis	Gesamt EUR
1	1,00	STK	Laserzuschnitt Zg.Nr.: ContractionCone S235JR gekantet/gerollt, geschweißt inkl. Beschichtung	1.937,15	1.937,15
2	1,00	STK	Laserzuschnitt Zg.Nr.: ContractionCone 1.4301 2B gekantet/gerollt, geschweißt	2.075,61	2.075,61
3	1,00	STK	Laserzuschnitt Zg.Nr.: Diffuser S235JR gekantet mit Folgebügen, geschweißt inkl. Beschichtung	4.176,85	4.176,85
4	1,00	STK	Laserzuschnitt Zg.Nr.: Diffuser 1.4301 2B gekantet mit Folgebügen, geschweißt	4.746,22	4.746,22
5	1,00	STK	Laserzuschnitt Zg.Nr.: Settling Chamber inflow S235JR gekantet mit Folgebügen, geschweißt inkl. Beschichtung	1.136,36	1.136,36
6	1,00	STK	Laserzuschnitt Zg.Nr.: Settling Chamber inflow	1.126,16	1.126,16

Die approbierte gedruckte Originalversion dieser Diplomarbeit ist an der TU Wien Bibliothek verfügbar
The approved original version of this thesis is available in print at TU Wien Bibliothek.
TU Bibliothek WIEN Your knowledge hub

Angebot

Belegnummer	**AN-508585**
Datum	30.07.2021
Kunden Nr.	21837
Seite	2 von 2
Ihre UID Nr.	ATU37675002

Verkauf
Erstellt von Martin Hirschler
Lieferzeit nach Vereinbarung
Anfrage Kostenvoranschlag / Herstellmöglichkeiten für Windtunnel

L

In der Zeit vom 02.08.2021 bis einschließlich 06.08.2021 haben wir Betriebsurlaub.

Pos	Menge	MEH	Bezeichnung	Preis	Gesamt EUR
			1.4301 2B gekantet mit Folgebügen, geschweißt		
7	1,00	STK	Laserzuschnitt Zg.Nr.: Settling Chamber Korpus S235JR gekantet, geschweißt inkl. Beschichtung	2.047,40	2.047,40
8	1,00	STK	Laserzuschnitt Zg.Nr.: Settling Chamber Korpus 1.4301 2B gekantet, geschweißt	2.059,00	2.059,00
9	2,00	STK	Rüstkosten Laser	35,00	70,00
10	2,00	STK	Rüstkosten Biegen	21,80	43,60
11	1,00	STK	Versandkosten	140,00	140,00
				Nettobetrag	**19.558,35**

- Oberfläche roh/beschichtet
- keine weitere Bearbeitung
- bei Bestellung dxf/stp/ o.ä. Dateiformat beistellen

Zahlungsbedingung	30 Tage netto
Lieferbedingungen	frei Werk Wien gegen Frachtverrechnung

Angebotsgültigkeit 2 Arbeitstage aufgrund derzeitiger starker Preissteigerung des Vormaterials - Preise nur gültig bei Gesamtabnahme.
Zuschnitttoleranzen nach DIN EN ISO 9013.
Wir hoffen, dass unser Angebot entspricht und wir Ihren Auftrag entgegen nehmen dürfen . Wir sichern prompte und zuverlässige Ausführung zu und verbleiben

mit freundlichen Grüßen

INNOWELD-Metallverarbeitung GmbH
Laser-Service-Center
A-8682 Hönigsberg

Die approbierte gedruckte Originalversion dieser Diplomarbeit ist an der TU Wien Bibliothek verfügbar
The approved original version of this thesis is available in print at TU Wien Bibliothek.

INNOWELD-Metallverarbeitung GmbH * Hönigsberggasse 3, 8682 Hönigsberg, AUSTRIA

Technische Universität Wien
Getreidemarkt 9/302
1060 Wien
AUSTRIA

Angebot

Belegnummer	**AN-508949**
Datum	30.08.2021
Kunden Nr.	21837
Seite	1 von 2
Ihre UID Nr.	ATU37675002

L

Verkauf	
Erstellt von	Martin Hirschler
Lieferzeit	nach Vereinbarung
Anfrage	Kostenvoranschlag / Herstellmöglichkeiten für Windtunnel

Wir danken für Ihre Anfrage und erlauben uns, gemäß unseren Lieferbedingungen wie folgt anzubieten:

Pos	Menge	MEH	Bezeichnung	Preis	Gesamt EUR
1	2,00	STK	Formrohrrahmen geschweißt 50x50x3mm Zg.Nr.: Rack für Settling Chamber S235JR / 3,00 mm inkl. Löcher, geschweißt, Oberfläche roh	295,00	590,00
2	1,00	STK	Formrohrrahmen geschweißt 50x50x3mm Zg.Nr.: Rack für Test Section S235JR / 3,00 mm inkl. Löcher, geschweißt, Oberfläche roh	390,00	390,00
3	1,00	STK	Laserzuschnitt Zg.Nr.: Test Section S235JR / 5,00 mm gekantet, geschweißt, inkl. Senkungen, inkl. Gewinde, inkl. Schrauben, Oberfläche roh	649,26	649,26
4	1,00	STK	Rüstkosten Laser	35,00	35,00
5	1,00	STK	Rüstkosten Biegen	21,80	21,80
6	1,00	STK	Versandkosten	120,00	120,00
				Nettobetrag	**1.806,06**

- Oberfläche roh
- keine weitere Bearbeitung
- bei Bestellung dxf/stp/ o.ä. Dateiformat beistellen

Zahlungsbedingung	30 Tage netto
Lieferbedingungen	frei Werk gegen Frachtverrechnung

Angebot

Belegnummer	**AN-508949**
Datum	30.08.2021
Kunden Nr.	21837
Seite	2 von 2
Ihre UID Nr.	ATU37675002

L

Verkauf	
Erstellt von	Martin Hirschler
Lieferzeit	nach Vereinbarung
Anfrage	Kostenvoranschlag / Herstellmöglichkeiten für Windtunnel

Pos	Menge	MEH	Bezeichnung	Preis	Gesamt	EUR

Angebotsgültigkeit 2 Arbeitstage aufgrund derzeitiger starker Preissteigerung des Vormaterials - Preise nur gültig bei Gesamtabnahme.
Zuschnitttoleranzen nach DIN EN ISO 9013.
Wir hoffen, dass unser Angebot entspricht und wir Ihren Auftrag entgegen nehmen dürfen . Wir sichern prompte und zuverlässige Ausführung zu und verbleiben

mit freundlichen Grüßen

INNOWELD-Metallverarbeitung GmbH
Laser-Service-Center
A-8682 Hönigsberg

Die approbierte gedruckte Originalversion dieser Diplomarbeit ist an der TU Wien Bibliothek verfügbar
The approved original version of this thesis is available in print at TU Wien Bibliothek.
TU Bibliothek WIEN Your knowledge hub

C.4 Quotation of the Prefabricated Components

Die approbierte gedruckte Originalversion dieser Diplomarbeit ist an der TU Wien Bibliothek verfügbar
The approved original version of this thesis is available in print at TU Wien Bibliothek.
TU Bibliothek WIEN Your knowledge hub

JAERA GmbH & Co. KG / Greifswalder Straße 2 / D-30880 Laatzen / Deutschland
Telefon: +49 / (0) 5102 / 9196-0 / Telefax: +49 / (0) 5102 / 9196-20
Homepage: http://www.jaera.de / E-Mail: info@jaera.de

A N G E B O T

Nr. 201.009.549

Lochbleche - Strukturbleche - Einfassprofile - Streckgitter - Wellengitter - Schweißgitter - Drahtgewebe - Bleche

Kundennr.: 151474 Firma diverse Kunde Deutschland	Ihre Referenz: bernhard.belmont@gmx.at Datum: 10.09.2021 Mitarbeiter: Mounir Benmoussa Telefon: +49 / (0) 5102 / 9196-13 E-Mail: benmoussa@jaera.de

****** Geschlossene Abnahme! ******

Pos.	Bezeichnung	Menge	Lieferzeit	Preis pro.	Preis ges.
1	Drahtgewebe aus Edelstahl 1.4301 Rollenware Maschenweite : 0,8 mm Drahtstärke : 0,22 mm Breite : 1300 mm Gewicht / lfdm.: 0,6 kg // Durchlass: 61,5 %	1 lfdm.	aus freibl. Vorrat	133,00 €	133,00 €
2	Drahtgewebe aus 1.4301 Rollenware Maschenweite : 1,4 mm Drahtstärke : 0,25 mm Breite : 1000 mm Gewicht / lfdm.: 0,48 kg // Durchlass: 72 %	1 lfdm.	aus freibl. Vorrat	118,00 €	118,00 €

Zahlungsbedingung: nach Vereinbarung
Lieferbedingung: frei Haus

Unsere Preise basieren auf den derzeit gültigen Vormaterialpreisen. Bei eventuell auftretenden Änderungen behalten wir uns eine Überarbeitung vor. Die genannten Preise verstehen sich netto, zzgl. Verpackung, Maut und der gesetzl. Mehrwertsteuer. Wir liefern ausschließlich zu unseren beigefügten Allgemeinen Geschäftsbedingungen.

Wir bitten um Ihren Auftrag.
Mit freundlichen Grüßen

Preisgültigkeit dieses Angebotes: 1 Tag!

Unsere Öffnungszeiten:
Büro: Mo. - Do. 7.15 - 16.30 Uhr / Fr. 7.15 - 14.15 Uhr
Lager: Mo. - Do. 6.45 - 15.45 Uhr / Fr. 6.45 - 13.15 Uhr

JAERA Radtke und Jänisch GmbH + Co. KG., Sitz: Laatzen, Amtsgericht Hannover, HRA 25525
Persönlich haftende Gesellschafterin: Jänisch u. Radtke Beteiligungs-GmbH, Sitz: Laatzen
Amtsgericht Hannover, HRB 56001, Geschäftsführer: Oliver Jänisch, Michael Radtke
Steuernummer: 23/201/29337; USt-IdNr. DE181956828

Die approbierte gedruckte Originalversion dieser Diplomarbeit ist an der TU Wien Bibliothek verfügbar
The approved original version of this thesis is available in print at TU Wien Bibliothek.
TU Bibliothek WIEN Your knowledge hub

Die approbierte gedruckte Originalversion dieser Diplomarbeit ist an der TU Wien Bibliothek verfügbar
The approved original version of this thesis is available in print at TU Wien Bibliothek.

schöftner technik GmbH

www.lbt-schoeftner.at

LBT Schöftner Technik GmbH · Brunnern 5 · A-4622 Eggendorf i. Tr.

Bernhard Kunitzky

LBT Schöftner Technik GmbH
Brunnern 5
A-4622 Eggendorf im Traunkreis

Tel.: +43-7221-72659
Fax: +43-7221-72659-44
E-Mail: office@lbt-schoeftner.at

Lieferadresse:
Bernhard Kunitzky

Rechnungsadresse:
Bernhard Kunitzky

Angebot Nr.: A2104200

Datum: 13.09.2021

Art. Nr.	Beschreibung	Menge	Einzelpreis	Steuern	Betrag
	Aluminium Honeycomb Core - expandiert Werkstoff: Alu 3000, 50µ, mikro-perforiert Zellgröße: ø6,35mm, 54kg/m³ Abmessungen (expandiert): 2500×1250mm Dicke/Höhe: 35mm	2 Stk.	203,0000	USt 20%	406,00 €
	Zuschnitt auf 1740×870	1,00	0,0000		0,00 €
	Verpackung	1,00	45,0000	USt 20%	45,00 €

Zahlungsbedingungen:
Vorauskasse

Netto:	**451,00 €**
Steuern:	**90,20 €**
Gesamt:	**541,20 €**

Toleranz Dicke: +-0,2mm

Da es sich bei dem angebotenen Produkt um eine auftragsbezogene Maßanfertigung handelt ist ein Rücktritt bzw. Widerruf nach Fern- und Auswärtsgeschäftegesetz nach Produktionsbeginn nicht möglich.

Ab Werk A-4622 Eggendorf im Traunkreis. Selbstabholung möglich.

Art.Nr.	Art.-Bild	Artikel		Menge		Preis	Gesamt
0000068501		DIN 933 6kt-Schraube mit Gewinde bis Kopf, 8.8, blank 10X20		Stück	70	39,40 € pro 100 Stück	27,58 €
0000068521		DIN 933 6kt-Schraube mit Gewinde bis Kopf, 8.8, blank 10X70		Stück	10	80,25 € pro 100 Stück	8,03 €
0000070017		DIN 934 Sechskantmutter, .8, blank M10X1,25		Stück	80	38,20 € pro 100 Stück	30,56 €
0000222133		DIN 125 Unterlegscheibe, Stahl, blank A10,5 200HV		Stück	160	10,45 € pro 100 Stück	16,72 €
0000031953		DIN 464 Rändelschraube hohe Form, 5.8, blank 5X20		Stück	100	64,48 € pro 100 Stück	64,48 €

Summe	147,37 €
Porto/Verpackung (Paketdienst)	7,50 €
Liefersumme	154,87 €
Gutschein	-4,42 €
zzgl. gesetzliche MwSt.	30,09 €
Gesamtsumme inkl. MwSt.	180,53 €

Die approbierte gedruckte Originalversion dieser Diplomarbeit ist an der TU Wien Bibliothek verfügbar
The approved original version of this thesis is available in print at TU Wien Bibliothek.
TU Bibliothek Your knowledge hub WIEN

Zahlart/Versandkosten

Die Bestellung folgt in mehreren Schritten:

Sofern Sie Neukunde sind, müssen Sie sich zunächst auf der folgenden Seite registrieren.
Nachdem Sie Ihre Angaben kontrolliert und ggf. korrigiert haben, werden Sie durch den Bezahlprozess geleitet. Bitte akzeptieren Sie unsere AGB und unsere Datenschutz-Bedingungen im Bestellprozess.
Sie schließen den Bestellprozess mit Klick auf „Zahlungspflichtig bestellen“ ab.
Unmittelbar danach erhalten Sie von uns per E-Mail eine automatisch generierte Bestellbestätigung. Die Bestellbestätigung stellt noch keine Annahme der Bestellung im Rechtssinne dar, sondern dient Ihrer Information.

Versandkostenfrei ab 150,00 €

Die approbierte gedruckte Originalversion dieser Diplomarbeit ist an der TU Wien Bibliothek verfügbar
The approved original version of this thesis is available in print at TU Wien Bibliothek.
TU Bibliothek Your knowledge hub WIEN

4 Stück Lenkrollen GD-40S Leveling Caster aus Nylon, f...

43 Sternebewertungen

Gebraucht - Wie neu

34 68 €

In den Einkaufswagen

Kostenlose Lieferung: **Morgen**
Bestellung innerhalb 1 Std. und 39 Min. Siehe Details.

2 weitere Optionen
sortiert nach Preis + Lieferung: aufsteigend

Filter

Neu

81 59 €

Sparen Sie 20€ beim Kauf von 200€ ausgewählten Artikeln. Weitere Artikel

In den Einkaufswagen

Kostenlose Lieferung: **Morgen**
Bestellung innerhalb 10 Stdn. und 39 Min. Siehe Details.

Die approbierte gedruckte Originalversion dieser Diplomarbeit ist an der TU Wien Bibliothek verfügbar
The approved original version of this thesis is available in print at TU Wien Bibliothek.
TU Bibliothek WIEN Your knowledge hub

Roulettes de Nivellement

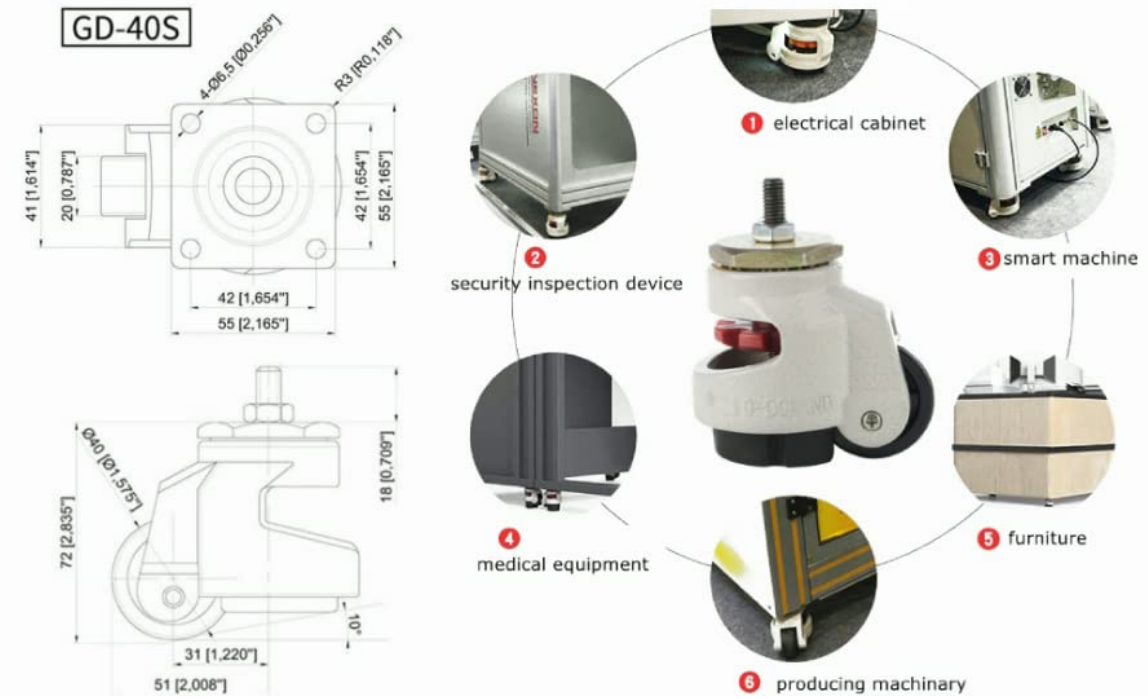

Flache Oberseite

Stärken Sie die Niettechnologie,
um die Installation fester zu machen

Einstellbarer Gang

Niveauregulierung, stoßfest,
kein Rütteln, lange Lebensdauer

Spezifikation

Material: MC Nylon

Halterung: Aluminiumlegierung

Tragfähigkeit: 50 kg / Stück

Gesamtlast: 150 kg / Stück

Temperatur: -15 ° ---- 70 °

Einbauhöhe: 72MM

Die approbierte gedruckte Originalversion dieser Diplomarbeit ist an der TU Wien Bibliothek verfügbar
The approved original version of this thesis is available in print at TU Wien Bibliothek.
TU Bibliothek Your knowledge hub WIEN

TU Bibliothek
WIEN Your knowledge hub
Die approbierte gedruckte Originalversion dieser Diplomarbeit ist an der TU Wien Bibliothek verfügbar
The approved original version of this thesis is available in print at TU Wien Bibliothek.

Produktinformation

j.posamentir Ges.m.b.H. Stahlgroßhandel

Zentrale :
1230 Wien, Siebenhirtenstraße 15
☎ 01 / 869 47 71 – 0
🖷 01 / 869 06 64
info.zentrale@posamentir.at

www.posamentir.at

Filiale :
1160 Wien, Koppstraße 7
☎ 01 / 492 09 29 – 0
🖷 01 / 492 08 54 33
info.stadtlager@posamentir.at

T-STAHL, U-STAHL

JULI 2008

T-STAHL hochseitig, rundkantig nach DIN 1024

für das Bundesgebiet Österreich

Die nachstehenden Staffelpreise verstehen sich je Dimension und Bezugsmengen in EURO per 100 kg - in aufpreisfreien Normallängen - ohne Schneidekostenzuschlag, welcher gegebenenfalls zusätzlich zur Berechnung gelangt.

Abmessung mm	
20-20-3	398,50
25-25-3,5	214,10
30-30-4	197,20
35-35-4,5	197,20
40-40-5	184,40
45-45-5,5	237,30
50-50-6	175,70
60-60-7	175,70
70-70-8	230,60
80-80-9	194,60
100-100-11	190,00
120-120-13	310,80

U-STAHL nach DIN 1026 S235JRG2

Abmessung mm	
40-20-5	181,20
40-35-5	181,20
50-25-5	181,20
50-38-5	178,70
60-30-6	178,70
65-42-5,5	178,70

Inhaltsverzeichnis

Die approbierte gedruckte Originalversion dieser Diplomarbeit ist an der TU Wien Bibliothek verfügbar
The approved original version of this thesis is available in print at TU Wien Bibliothek.
TU Bibliothek WIEN Your knowledge hub

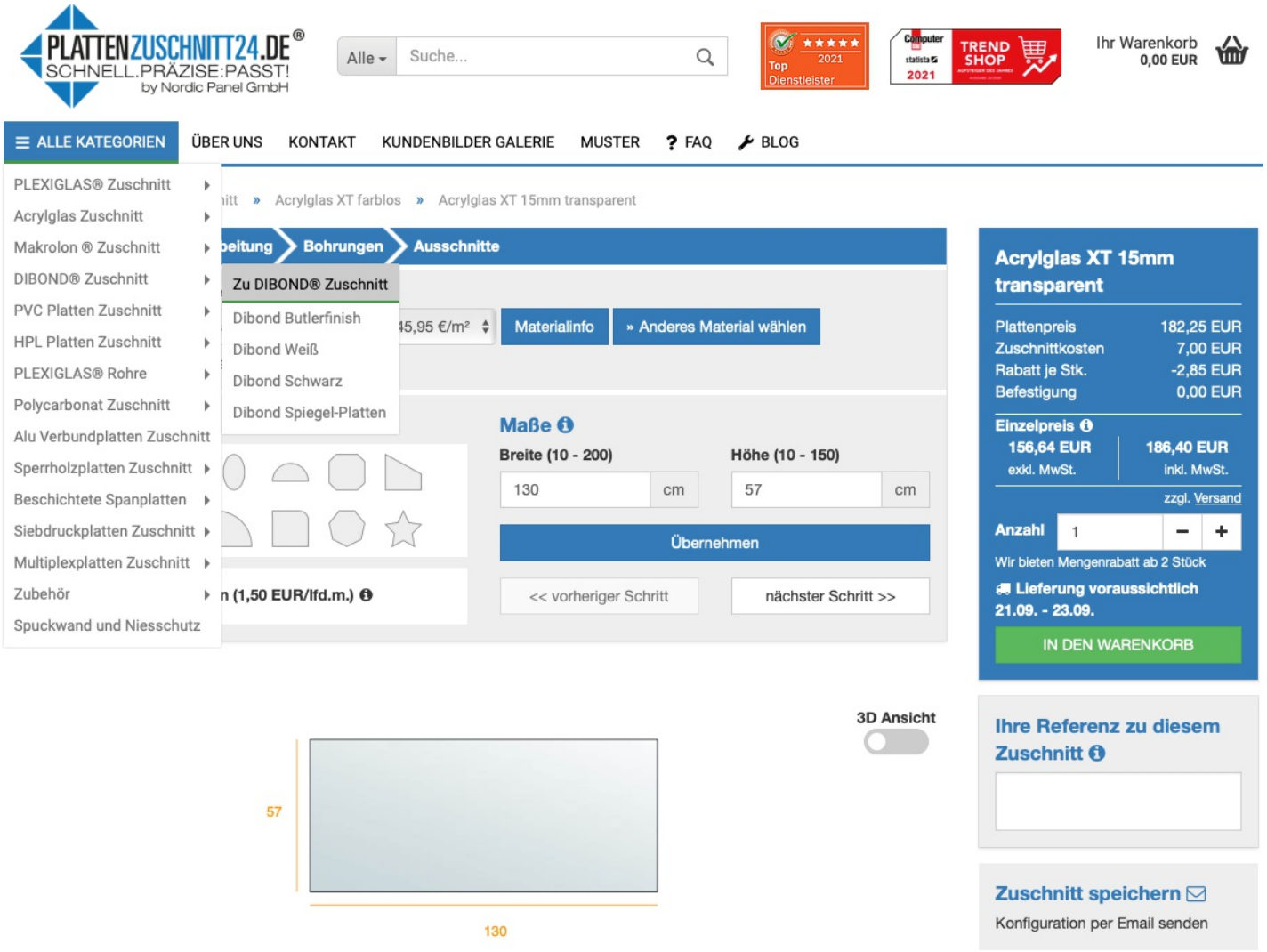

Die approbierte gedruckte Originalversion dieser Diplomarbeit ist an der TU Wien Bibliothek verfügbar
The approved original version of this thesis is available in print at TU Wien Bibliothek.
TU Bibliothek WIEN Your knowledge hub

Die approbierte gedruckte Originalversion dieser Diplomarbeit ist an der TU Wien Bibliothek verfügbar
The approved original version of this thesis is available in print at TU Wien Bibliothek.

PLATTENZUSCHNITT24.DE®
SCHNELL.PRÄZISE:PASST!
by Nordic Panel GmbH

Alle | Suche...

Top Dienstleister 2021 | Computer statista 2021 TREND SHOP | Ihr Warenkorb 0,00 EUR

ALLE KATEGORIEN | ÜBER UNS | KONTAKT | KUNDENBILDER GALERIE | MUSTER | FAQ | BLOG

Startseite » Acrylglas Zuschnitt » Acrylglas XT farblos » Acrylglas XT 15mm transparent

Zuschnitt | Kantenbearbeitung | Bohrungen | Ausschnitte

Ihre aktuelle Auswahl

Acrylglas XT 15mm transparent - 245,95 €/m² | Materialinfo | » Anderes Material wählen

Videoanleitung

Formen

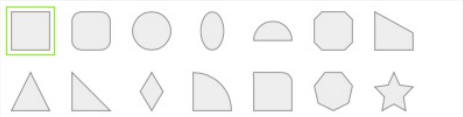

entgratet - empfohlen (1,50 EUR/lfd.m.)

Maße

Breite (10 - 200): 128 cm

Höhe (10 - 150): 66 cm

Übernehmen

<< vorheriger Schritt | nächster Schritt >>

Acrylglas XT 15mm transparent

Plattenpreis	207,78 EUR
Zuschnittkosten	7,00 EUR
Rabatt je Stk.	-2,85 EUR
Befestigung	0,00 EUR

Einzelpreis

178,09 EUR exkl. MwSt. | 211,93 EUR inkl. MwSt.

zzgl. Versand

Anzahl: 1 − +

Wir bieten Mengenrabatt ab 2 Stück

Lieferung voraussichtlich 21.09. - 23.09.

IN DEN WARENKORB

3D Ansicht

Ihre Referenz zu diesem Zuschnitt

Zuschnitt speichern

Konfiguration per Email senden

Die approbierte gedruckte Originalversion dieser Diplomarbeit ist an der TU Wien Bibliothek verfügbar
The approved original version of this thesis is available in print at TU Wien Bibliothek.

PLATTENZUSCHNITT24.DE®
SCHNELL.PRÄZISE:PASST!
by Nordic Panel GmbH

Alle | Suche...

Top Dienstleister 2021 | Computer statista 2021 | TREND SHOP

Ihr Warenkorb
0,00 EUR

ALLE KATEGORIEN | ÜBER UNS | KONTAKT | KUNDENBILDER GALERIE | MUSTER | FAQ | BLOG

Startseite » Acrylglas Zuschnitt » Acrylglas XT farblos » Acrylglas XT 15mm transparent

Zuschnitt | Kantenbearbeitung | Bohrungen | Ausschnitte

Ihre aktuelle Auswahl

Acrylglas XT 15mm transparent - 245,95 €/m² | Materialinfo | » Anderes Material wählen

Videoanleitung

Formen

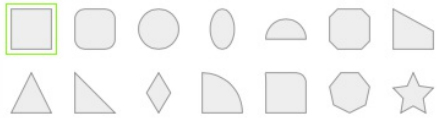

☐ entgratet - empfohlen (1,50 EUR/lfd.m.)

Maße

Breite (10 - 200): 130 cm

Höhe (10 - 150): 58.5 cm

Übernehmen

<< vorheriger Schritt | nächster Schritt >>

3D Ansicht

Acrylglas XT 15mm transparent

Plattenpreis	187,04 EUR
Zuschnittkosten	7,00 EUR
Rabatt je Stk.	-2,85 EUR
Befestigung	0,00 EUR

Einzelpreis

160,66 EUR exkl. MwSt.	191,19 EUR inkl. MwSt.

zzgl. Versand

Anzahl: 1 − +

Wir bieten Mengenrabatt ab 2 Stück

Lieferung voraussichtlich 21.09. - 23.09.

IN DEN WARENKORB

Ihre Referenz zu diesem Zuschnitt

Zuschnitt speichern

Konfiguration per Email senden